Geochimica et Cosmochimica Acta

JOURNAL OF THE GEOCHEMICAL SOCIETY

Editors : L. H. AHRENS, *Capetown*. C. W. CORRENS, *Göttingen*. E. INGERSON, *Washington*. S. R. NOCKOLDS, *Cambridge*. F. A. PANETH, *Mainz*. H. C. UREY, *Chicago*. JOHN VERHOOGEN, *Berkeley, Calif.* A. P. VINOGRADOV, *Moscow*. L. R. WAGER, *Oxford*. F. E. WICKMAN, *Stockholm*.

CONTENTS VOLUME 13, NO. 4 1958

T. C. HOERING and H. E. MOORE: The isotopic composition of the nitrogen in natural gases and associated crude oils 225
WALTER NICHIPORUK: Variations in the content of nickel, gallium, germanium, cobalt, copper and chromium in the kamacite and taenite phases of iron meteorites 233
G. W. REED, H. HAMAGUCHI and ANTHONY TURKEVICH: The uranium contents of iron meteorites 248
FRANK CUTTITTA and JESSE J. WARR, JR.: Retention of lead during oxidative ashing of selected naturally occurring carbonaceous substances 256
ELAINE G. MURRAY and JOHN A. S. ADAMS: Thorium, uranium and potassium in some sandstones 260
JOHN A. S. ADAMS, JASPER E. RICHARDSON and CHARLES C. TEMPLETON: Determinations of thorium and uranium in sedimentary rocks by two independent methods 270
PAUL E. DAMON and J. LAURENCE KULP: Inert gases and the evolution of the atmosphere . 280
S. R. TAYLOR and K. S. HEIER: Alkali elements in potash feldspar from the pre-Cambrian of Southern Norway 293
A. E. RINGWOOD: The constitution of the mantle—I. Thermodynamics of the olivine-spinel transition 303
CHARLES D. KEELING: The concentration and isotopic abundances of atmospheric carbon dioxide in rural areas 322
HAROLD C. UREY: Comments on two papers by John F. Lovering concerning a typical parent meteorite body 325
Geochemical Note:
G-1–*W*-1 values—spectrochemical determination using an internal standard 339
Report of Meeting 341
Book Reviews:
"Irradiation Colours and Luminescence. Contribution to Mineral Physics" by KARL PRZIBRAM (reviewed by M. WENZEL) 342
"New Research Methods in Hydrology" Edited by Harmon Craig (reviewed by EARL INGERSON) 342
"Introduction à l'étude des roches métamorphiques et des gîtes métallifères" by PIERRE LAFFITTE (reviewed by E. RAGUIN) 343

PERGAMON PRESS LONDON • NEW YORK • PARIS • LOS ANGELES

GEOCHIMICA ET COSMOCHIMICA ACTA

EDITORS

PROF. L. H. AHRENS *Department of Chemistry, University of Capetown, Rondebosch, Cape Province, South Africa*
PROF. C. W. CORRENS *Sedimentpetrographisches Institut der Universität, Lotzestr.* 13, *Göttingen, Germany*
DR. E. INGERSON *Geochemistry and Petrology Branch, U.S. Geological Survey, Washington* 25, *D.C., U.S.A.*
DR. S. R. NOCKOLDS *Department of Mineralogy and Petrology, The University, Cambridge, England*
PROF. F. A. PANETH, F.R.S. *Max-Planck-Institut für Chemie, Mainz, Saarstrasse* 23, *Germany*
PROF. H. C. UREY, For. Mem. R. S. *The Enrico Fermi Institute for Nuclear Studies, University of Chicago, Illinois, U.S.A.*
DR. JOHN VERHOOGEN *Department of Geology, University of California, Berkeley, California, U.S.A.*
PROF. A. P. VINOGRADOV *Vernatsky Institute, Moscow, U.S.S.R.*
PROF. L. R. WAGER, F.R.S. *Department of Geology and Mineralogy, The University, Oxford, England*
PROF. F. E. WICKMAN *Naturhistoriska Riksmuseets, Mineralogiska Avdelning, Stockholm* 50, *Sweden*

EDITORIAL ADVISORY BOARD

EUROPE

T. BARTH, *Oslo*
L. CAPDECOMME, *Toulouse*
E. J. CONWAY, *Dublin*
P ESKOLA, *Helsinki*
P GALLITELLI, *Modena*
A. HADDING, *Lund*
O. HAHN, *Göttingen*
H. W. HARVEY, *Plymouth*
F. HEIDE, *Jena*
A. HOLMES, *Edinburgh*
W. Q. KENNEDY, *Leeds*
PH. H. KUENEN, *Gröningen*
S. LANDERGREN, *Stockholm*
F. MACHATSCHKI, *Vienna*
A. MUIR, *Harpenden*
J. ORCEL, *Paris*
E. RAGUIN, *Paris*
K. RANKAMA, *Helsinki*
E. REINHARD, *Basle*
TH. G. SAHAMA, *Helsinki*
C. E. TILLEY, *Cambridge*
T. VOGT, *Trondheim*
W. WAHL, *Helsinki*

AMERICAN CONTINENT

A. F. BUDDINGTON, *Princeton*
D. GUIMARAES, *Belo Horizonte*
G. E. HUTCHINSON, *New Haven*
B. H. MASON, *New York*
F. WHIPPLE, *Cambridge*
R. WILDT, *New Haven*

FAR EAST

T. WATANABE, *Tokyo*

Publishing Offices: Pergamon Press Ltd., 4 & 5 Fitzroy Square, London W.1 (EUSton 4455)

Four issues per volume, three volumes per year

Subscription *per annum* (including postage) (A) £16. 10s. (U.S.A. $46.50); (B) For individual subscribers who certify that the Journal is for their private use, £10. 10s. (U.S.A. $30.00). Members of the Geochemical Society, or non-members who occasionally publish papers in the Journal, £3. 10s. (U.S.A. $10.00) *per annum.*

Payment must be made in advance

Back numbers, £7 (U.S.A. $19.60) per volume

Copyright © 1958 Pergamon Press Ltd.

PERGAMON PRESS LTD.

4 & 5 FITZROY SQUARE, LONDON W.1 122 EAST 55TH STREET, NEW YORK 22, N.Y

PRINTED IN NORTHERN IRELAND AT THE UNIVERSITIES PRESS, BELFAST

Geochimica et Cosmochimica Acta, 1958, Vol. 13, pp. 225 to 232. Pergamon Press Ltd., London

The isotopic composition of the nitrogen in natural gases and associated crude oils

T. C. Hoering and H. E. Moore
Department of Chemistry, University of Arkansas, Fayetteville, Arkansas

(*Received* 18 *July* 1957)

Abstract—Measurement of the $^{15}N/^{14}N$ ratio of the nitrogen from a number of samples of natural gas and crude oil show that wide variations exist. A systematic variation in the $^{15}N/^{14}N$ ratio exists across a natural gas field. Experiments on the flow of nitrogen through porous sandstone indicate that two processes could account for the fractionation of the nitrogen isotopes in natural gas, namely effusive flow and surface diffusion.

Introduction

Previous work performed in this laboratory (Hoering, 1955) has shown that there are variations in the $^{15}N/^{14}N$ ratio of the nitrogen in natural gas. The present work was undertaken to extend these measurements and to determine the cause of this isotope fractionation.

The possibility that processes of diffusion could cause natural variations in stable isotope abundances has been suggested (Rankama, 1954). Ingerson (1953) has suggested that migration of gases in petroleum deposits may be accompanied by isotope fractionation. He ascribes the observed fractionation of the sulphur isotopes (Thode, 1949) in waters near oil wells as being due to migration.

Smith and Hudson (1951) have reported that there are no large variations in the $^{15}N/^{14}N$ ratio in coal and crude oils. Their mass spectrometer was not capable of measuring precisely the small variations that are to be expected in natural chemical fractionation.

In this work, the isotopic composition of the nitrogen in natural gas and crude oil has been measured. Experiments on the fractionation of the nitrogen isotopes during flow through porous sandstone are described.

Experimental

The samples of natural gas were carefully collected at the individual wells and care was taken to prevent contamination by atmospheric N_2 or other nitrogen compounds. The samples were collected in aviators' oxygen tanks which were swept free of air by flowing natural gas through them for long periods.

Nitrogen was separated from natural gas by condensing the gases in a large cold trap cooled with liquid nitrogen. The non-condensables consisted of N_2, the inert gases and some methane. The non-condensed gases were cycled with an automatic Toeppler pump for several hours over Cu–CuO at 700°C and through a cold trap. In this time, all hydrocarbons and carbon monoxide were burned to carbon dioxide and water and frozen out in the cold trap. In a few cases, separation from helium was necessary. This was accomplished by quantitatively absorbing the N_2 on animal charcoal at liquid-nitrogen temperatures and pumping off the

helium. It was shown that this separation could be carried out without fractionation of the nitrogen isotopes. A qualitative analysis of the inert fractions of several natural gases showed them to consist of N_2 with a trace of argon. No attempt was made to analyse the natural gases quantitatively for nitrogen.

The nitrogen from crude oil was isolated by Kjeldahl digestion, using mercury as the catalyst (Lake, 1952). Three or more determinations of the nitrogen content were made until analytical checks were obtained. The ammonia isolated by the Kjeldahl digestion was oxidized to nitrogen gas by sodium hypobromite and the nitrogen purified as previously described (Hoering, 1955).

The $^{15}N/^{14}N$ ratio of the purified N_2 was determined, relative to atmospheric nitrogen, in a mass spectrometer designed for the measurement of small differences in isotope content (Dole, 1952; McKinney *et al.*, 1950). Samples of our atmospheric nitrogen standard were compared with the Bureau of Standards Isotope Reference Standard and found to be identical. The standard atmospheric nitrogen was isolated by passing air repeatedly over cleaned copper turnings at 700°C and then through a cold trap cooled with liquid nitrogen.

The nitrogen isotope content of the natural gases and crude oil and other data are presented in Table 1. The nitrogen isotope content is expressed in parts per thousand (per mil) difference in the $^{15}N/^{14}N$ ratio between the sample and atmospheric nitrogen;

$$\delta^{15}N = \frac{(^{15}N/^{14}N)_{sample} - (^{15}N/^{14}N)_{standard}}{(^{15}N/^{14}N)_{standard}} \times 1000 \qquad (1)$$

The result of each isotopic analysis is estimated to have a precision of ± 0.3/mil.

It is interesting to note that in samples taken from the same well, the $\delta^{15}N$ in the natural gas is lower than in the crude oil. From the data in Table 1, it is evident that the N_2 in natural gas displays wide variations in the $^{15}N/^{14}N$ ratio. The samples from Franklin County, Arkansas, represent gas taken from several wells in the same formation distributed over an area of about 35 square miles. In this field, there is no crude oil associated with the natural gas. The $^{15}N/^{14}N$ ratio shows a regular trend across the dimensions of the field. Fig. 1 gives a plot of the relative positions of the wells in this field with the observed isotopic compositions.

The data in Table 1 suggest the possibility of fractionation of nitrogen isotopes by flow and migration through porous structures. To check this hypothesis, a core of Torpedo sandstone, mounted in Lucite plastic, was obtained. The mounted core was 18 in. in length, 2 in. in diameter and had a high permeability.

Two sets of experiments were run. In the first, flow of nitrogen through the dry core was studied. In the second, flow through the core when saturated with petroleum ether was studied. The experiments were performed in the apparatus shown in Fig. 2. The mounted core was swept free of air with carbon dioxide. A sample of tank nitrogen was introduced into the core and swept through with CO_2 at a rate of 2 ml/min. The CO_2 was absorbed in the KOH in the nitrometer and the N_2 collected in 2 ml cuts in the evacuated bulbs. The nitrogen gas was purified as previously described and an isotopic analysis made on it. The results of these experiments are shown in Tables 2 and 3. Since the nitrogen isotope content of tank nitrogen is different from that of atmospheric N_2 and varies from

Table 1. Data on nitrogen isotopes in crude oil and natural gas

State	County	Formation	$\delta^{15}N$ in gas	$\delta^{15}N$ in crude oil
Oklahoma	Caddo	Rowe Sand	−2·1	+3·9
	Grady	Lower Simpson	−4·1	+3·4
	Garvin	Hart	−9·7	—
	Caddo	Medrano	−2·1	+5·3
	Oklahoma	Bartlesville	−6·4	+3·4
	Grady	Upper Simpson	−3·3	+4·3
	Caddo	Marchand	−5·5	+6·7
	Oklahoma	Hunton Lime	−10·5	—
	Caddo	Marchand	−3·5	+3·8
Mississippi	Adams	Wilcox	−8·9	—
	Adams	Wilcox	−8·5	—
	Adams	Wilcox	—	+1·0
	Adams	Wilcox	—	+2·0
	Yazoo	Stevens	−8·2	+1·7
	Yazoo	Tuscaloosa	−7·5	+2·0
	Adams	Wilcox	—	+1·8
	Adams	Wilcox	—	+2·0
	Jones	Bailey Sand	−8·4	+4·3
	Jones	Bailey Sand	—	+4·0
	Jones	Bailey Sand	—	+6·3
Texas	Brazoria	Manvel-Miocene	−7·7	+3·9
	Brazoria	Oligocene	−3·8	+2·9
	Harris	Vicksburg	−9·2	+2·1
	Liberty	Yegua	−8·4	+2·6
	Anderson	Rodessa	−8·2	—
	Anderson	Woodbine	−6·2	+1·9
	Anderson	Sub-clarksville	−9·3	+1·2
	Brazoria	Huston Farms	−5·9	—
	Brazoria	Banfield Zone	−4·0	—
	Brazoria	Alibel	−6·0	+5·5
Arkansas	Washington	Sylamore	+2·7	—
	Franklin	Sells Sands	+11·9	—
	Franklin	Sells Sands	+7·1	—
	Franklin	Sells Sands	+14·4	—
	Franklin	Sells Sands	+13·4	—
	Franklin	Sells Sands	+4·8	—
	Franklin	Sells Sands	+11·0	—
	Franklin	Sells Sands	+2·6	—
	Franklin	Sells Sands	+1·3	—

tank to tank, all results are normalized to the case where the starting N_2 had $\delta^{15}N$ equal to zero.

The data in Tables 2 and 3 can be used to calculate a kinetic isotope effect for the process of the flow of N_2 through porous sandstone as follows. Consider the uni-directional processes

$$^{14}N^{14}N_{(in)} \longrightarrow {}^{14}N^{14}N_{(out)} \quad (2)$$

$$^{14}N^{15}N_{(in)} \longrightarrow {}^{14}N^{15}N_{(out)} \quad (3)$$

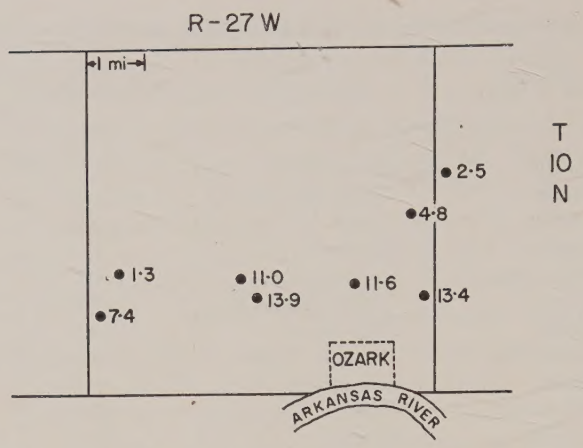

Fig. 1. Observed $\delta^{15}N$ of the N^2 in natural gases from the White Oak Gas Field, Franklin County, Arkansas.

Table 2. Fractionation of nitrogen isotopes during flow through dry Torpedo sandstone

Cut no.	f	$\delta^{15}N$	β
1	0·143	−4·6	1·0054
2	0·286	+0·7	1·0002
3	0·429	+3·0	1·0003
4	0·572	+3·2	0·9992
5	0·715	+1·8	0·9983
6	0·858	+0·5	0·9975
7	1·000	−4·8	—

Table 3. Fractionation of nitrogen isotopes during flow through Torpedo sandstone saturated with petroleum ether

Cut no.	f	$\delta^{15}N$	β
1	0·200	−5·1	1·0056
2	0·400	−3·5	1·0056
3	0·600	−1·7	1·0055
4	0·800	+0·6	1·0060
5	1·000	+7·7	—

In the increment of time dt, the fractional increase of the lighter molecule coming through the process will be, in general, different than for the heavier molecule by a factor β, the kinetic isotope effect.

$$\frac{d(^{14}N^{14}N)}{(^{14}N^{14}N)} = \beta \frac{d(^{14}N^{15}N)}{(^{14}N^{15}N)} \tag{4}$$

This equation can be integrated and put in the convenient form:

$$\beta = \frac{\ln (1 - f)}{\ln (1 - fr/r_0)} \tag{5}$$

where f is the fraction of the total nitrogen put through the process, β is the kinetic isotope effect, r is the ratio $^{15}N/^{14}N$ in the fraction f put through and r_0 is the ratio $^{15}N/^{14}N$ in the starting material. The data in Tables 2 and 3 were treated

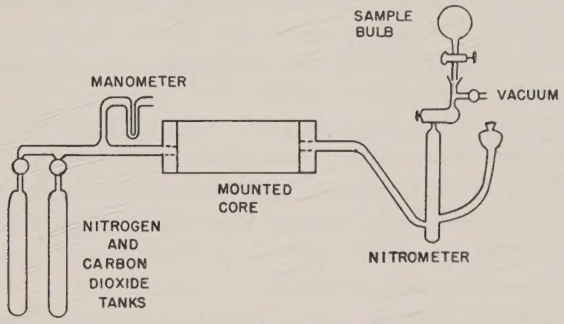

Fig. 2. Apparatus for measuring the fractionation of the nitrogen isotopes during flow through porous sandstone.

this way and the values of β obtained are tabulated. These values of β are to be compared with the value expected for free molecular flow, 1·0177 (the ratio of the square root of the masses of the isotopic nitrogen molecules).

The fact that a constant value for β is not obtained for the data in Table 2 indicates that there is more than one method by which fractionation occurs during the flow of nitrogen through porous sandstone. Two methods that seemed more probable were effusive flow and an interaction at the surface. To eliminate the surface effect, the sandstone core was saturated with petroleum ether and the experiment was repeated. These results, shown in Table 3, give a constant value for β. This indicates that only one method of isotope fractionation is operative.

The following experiment was performed to measure the isotope fractionation during the adsorbtion of N_2 on the surface of powdered sandstone. A sample of powdered Torpedo sandstone, weighing 100 g, was placed in a bulb attached to the vacuum system and thoroughly outgassed. The bulb was then cooled to −187°C and a 10 ml sample of tank N_2 was introduced. The pressure of the system was 4 mm Hg. After equilibrium was established between the gas and adsorbed phase, the gas was pumped off with a Toepler pump and purified. The bulb was gently heated with a burner to drive off the adsorbed N_2 and the sample treated as before. Isotopic analysis showed that the N_2 adsorbed had $\delta^{15}N = +0{\cdot}8$/mil, while the

N_2 in the gas phase had $\delta^{15}N = -4{\cdot}7$/mil. The heavier isotope is preferentially adsorbed on the surface of sandstone.

The isotope effect in the solution of N_2 gas in distilled water and in crude oil was measured. The fractionation factor for the reaction

$$^{14}N^{14}N_{(gas)} + {}^{14}N^{15}N_{(solution)} = {}^{14}N^{15}N_{(gas)} + {}^{14}N^{14}N_{(solution)}$$

was $1{\cdot}0000 \pm 0{\cdot}0004$ at room temperature.

Discussion

The data in Table 1 show that large variations in the isotopic composition of the N_2 in natural gas exist and Fig. 1 shows that a systematic trend in the $\delta^{15}N$ can exist across a gas field. Laboratory experiments on the flow of N_2 through sandstone indicate possible mechanisms for this isotope fractionation.

One of the factors that govern the ability of various types of flow to cause isotope separation is the relationship between the mean free path of the gas molecules and the size of the pores and capillaries of the porous substance. The flow of gases through porous substances has been discussed by several authors (Barrer, 1941; Carman, 1956).

Molecular flow occurs when the mean free path is much greater than the dimensions of the pores. This type of flow is characterized by the relationship that the rate of flow is inversely proportional to the square root of the ratio of the masses of the molecules. Viscous and turbulent flow occur when the mean free path is much less than the dimensions of the pores. The rate of flow by these last two types is not mass dependent and is not separative.

Another type of flow through porous substances which may result in isotope separation is surface diffusion (Haul 1954a, b; Trawick and Berman 1957). This effect occurs during flow through material with a very high surface area. The theory and mechanism of this type of flow and a discussion of the relative importance of surface and gas phase transport of gases in fine tubes and pores has been given by Sears (1954) and by Hill (1956). They conclude that the amount of surface transport becomes about equal to the amount of gas transport when the pores have dimensions of the order of several hundred ångström units. These discussions are not directly applicable to the present experiment, as they are derived for lower pressures.

The data of Table 3 (sandstone covered with a hydrocarbon) indicate that at atmospheric pressure, separative flow can take place. The difference between the measured isotope effect and that calculated for molecular flow indicates that both molecular (separative) and viscous (non-separative) flow are occurring. The data of Table 2 indicate that these two types of flow plus a flow involving the interaction with the surface is occurring simultaneously.

The laboratory experiments do not, of course, duplicate the conditions found in gas wells, but merely show possible processes that could account for the observed isotope fractionation in natural gas. At the high pressure found in the gas wells, the mean free path becomes small and isotope fractionation by molecular flow becomes less likely, unless the pore sizes of the associated rocks are very small. An interaction of N_2 gas with surfaces at atmospheric pressure to produce isotope

fractionation is somewhat surprising. This effect may become important at the high pressures of gas wells.

The possibility that thermal diffusion could cause the observed isotope fractionation is not treated in this work.

These experiments show possible mechanisms for isotope separation, but they give no information on the time factor involved. Several possibilities exist. If the migration of gas through a field is slow throughout geological time and all parts of the field are not in equilibrium, the isotope fractionation could define the direction of this migration. If the migration were rapid and equilibrium in the field were rapidly established, the observed fractionation could be due to momentary disturbances of the equilibrium and the subsequent flow through the porous structure. The trend of the observed isotope fractionation in the White Oak Field, Franklin Co., Arkansas, could then be due to the non-homogeneous structure of the reservoir rock across the field. A possible test of these ideas would be a study of the pattern of isotope fractionation as a function of the production rate in the wells of this field.

The origin of the N_2 in natural gas is not known, but several sources are possible. As the ratio of nitrogen to argon in natural gas is much higher than in the atmosphere, it is unlikely that it represents air trapped in the sedimentary material that formed the source of the natural gas. It may have originated from the decomposition of the nitrogenous compounds in crude oil or sedimentary material. This is suggested from the observed fact that the nitrogen in natural gas is "lighter" than the nitrogen in the accompanying crude oil. In general, the molecules with the lighter isotope would decompose more readily, enriching the gas phase in ^{14}N relative to the remaining oil. The N_2 in natural gas may have come from the outgassing of the surrounding rocks. It has been found in this laboratory that the $\delta^{15}N$ of the nitrogen in igneous rocks falls in the narrow range of $+3$ to $+5$/mil (Scalan, 1957).

Acknowledgements—This work was supported by Contract AT-(40)-1-1313 with the U.S. Atomic Energy Commission. The assistance of the following companies who supplied samples of natural gas and crude oil is acknowledged: The Phillips Petroleum Co., The Sohio Oil Company, The Texas Company, The Arkansas-Western Gas Co. The assistance of Dr. B. Nagy of the Cities Service Research and Development Co. in obtaining the mounted core is gratefully acknowledged.

References

Barrer R. M. (1941) *Diffusion in and through Solids.* Cambridge University Press.
Carman P. C. (1956) *Flow of Gas through Porous Media.* Butterworths, London.
Dole M. (1952) *Chem. Rev.* **51,** 263.
Haul R. A. (1954a) *Naturwissenschaften* **41,** 255; (1954b) *Z. Phys. Chem.* **1,** 153.
Hill T. L. (1956) *J. Chem. Phys.* **25,** 730.
Hoering T. C. (1955) *Science* **122,** 3182.
Ingerson E. (1953) *Bull. Geol. Soc. Amer.* **64,** 301.
Lake G. R. (1952) *Analyt. Chem.* **24,** 1806.
McKinney C. R., McCrea J. M., Epstein S., Allen H. A. and Urey H. C. (1950) *Rev. Sci. Instrum.* **21,** 724.

Rankama K. (1954) *Isotope Geology*. McGraw-Hill, New York.
Scalan R. S. (1957) Ph.D. Thesis, University of Arkansas.
Sears G. W. (1954) *J. Chem. Phys.* **22,** 1252.
Smith P. V. and Hudson B. E. (1951) *Science* **113,** 577.
Thode H. G. (1949) *Canad. J. Res.* B **27,** 361.
Trawick W. G. and Berman A. S. (1957) *J. Chem. Phys.* **26,** 709.

Geochimica et Cosmochimica Acta, 1958, Vol. 13, pp. 233 to 247. Pergamon Press Ltd., London

Variations in the content of nickel, gallium, germanium, cobalt, copper and chromium in the kamacite and taenite phases of iron meteorites*

Walter Nichiporuk
Division of Geological Sciences, California Institute of Technology, Pasadena, California

(*Received* 27 *September* 1957)

Abstract—The nickel content of kamacite in hexahedrites and octahedrites has been found to vary within 3·3–5·8 per cent. The average of 4·7 per cent of all nickel values is lower than the heretofore reported figure of 5·5–6·0 per cent.

In the light of the iron–nickel phase diagram the low nickel values in kamacite appear to point to the possible existence in taenite at its boundary with kamacite of nickel values which are considerably lower than the over-all values 31–54 per cent found in six different taenites.

The concentrations of gallium, germanium and copper are much greater in the taenite than in the kamacite phase. The larger proportion of cobalt, however, exists in the kamacite phase. All these elements are concentrated in their preferred phases to a degree which is higher than that observed for nickel.

The relative contribution of taenite to the over-all concentrations is invariably greater than the contribution of kamacite in the case of gallium, germanium and copper, quite negligible in the case of cobalt and nearly the same as that of kamacite in the case of nickel.

Correlations are observed between the nickel content of taenite, its surface inclusions of foreign phases, and the thin parallel lines which traverse the two larger surfaces of the taenite plates.

1. Introduction

Compared with the over-all composition of iron meteorites (Goldberg *et al.*, 1951; Lovering *et al.*, 1957) the composition of their two metallic phases, the kamacite (low-nickel α-iron) and taenite (high-nickel γ-iron) are known only poorly.

In view of this, a programme has been undertaken aimed at separating the two phases in a form suitable for the determination of both major and minor constituents and analysing the phases for a select group of elements, notably nickel, cobalt, gallium, germanium and copper.

Nickel and cobalt, and to a much lesser extent copper, have been determined during the last century in several samples of kamacite and taenite.

In the data compiled by Farrington (1915) the nickel content of kamacite varies from 5·26 to 6·81 per cent and the cobalt content varies from 0·25 to 0·77 per cent. In the taenite phase, the nickel content varied from 13·0 to 48·0 per cent and the cobalt content from 0·02 to 2·10 per cent.

Later, Pfann (1917) found that the taenite phase of the San Cristobal iron contained 26·4 per cent nickel. Smith and Young (1939) reported that the taenite phase of the Butler iron contains 50–54 per cent nickel.

2. Analytical Methods

Isolation of kamacite and taenite

In most octahedral irons the kamacite and taenite are firmly joined along their

* This research was carried out under U.S. Atomic Energy Commission Contract AT (11-1)-208.

planes of contact. Only in rare instances resulting from surface oxidation, a segregation takes place along these planes. An example of such segregation is furnished by the Welland iron from which Davison (1891) was able to pick out mechanically both kamacite and taenite. In most cases, however, chemical methods of isolation must be used. In these methods, a partial dissolution of the taenite surface cannot be completely avoided. As a result a small portion of taenite at the immediate boundary with kamacite is always lost and only the remaining taenite can be analysed.

In this investigation, advantage was taken of the greater solubility in dilute acids of kamacite than of taenite, as well as of the fact that in samples of octahedral irons, the proportion of the total surface area of taenite which is exposed on a polished surface is negligible in comparison with the total surface area of kamacite. Therefore, the solution of a small portion of an inclusion-free sample of an iron meteorite obtained with a sufficiently dilute acid may be regarded as containing primarily the low-nickel (kamacite) phase.

Three rectangularly shaped bars, varying in weight from 3 to 30 g were cut from each of the six selected octahedrites and two hexahedrites, and polished but not etched. Precautions were taken to avoid discernable fissures and surface inclusions of troilite, cohenite and schreibersite. Microscopic examination of each unetched bar showed no evidence of intrusions of oxides into the phase boundaries. The upper limit of the total amount of surface inclusions of minor phases was estimated at 1–2 per cent.

Each bar was treated at room temperature with 50 ml of 0·0075 N H_2SO_4. The acid was renewed three times a day for a time ranging from 243 to 377 hr. The volumes of the resulting solutions were adjusted to 250 ml, two-fifths of which was used in the trace elements analysis and three-fifths in the nickel analysis.

In order to isolate the taenite phase, the octahedrites were treated at room temperature with 0·05 N H_2SO_4 for an average of 40 days. The taenite plates were removed as soon as they became loose enough to be detached or broken off with forceps. Following a thorough mechanical cleaning, the plates were stored in absolute alcohol. The residues were discarded.

Determination of nickel

The dilute sulphuric acid fractions of kamacite and nitric acid solutions of the taenite plates were analysed for nickel.

Nickel was also determined on pieces of the original untreated meteorites.

A modification of the gravimetric method of Henderson (1941) was used. In this modification, aqua regia is substituted for chlorine gas and ammonium acetate for ammonium hydroxide as the oxidizing and precipitating agents respectively. It has been found that these substitutions are especially advantageous in the analyses of kamacite where cobalt to nickel ratio is higher than is normally encountered in the analyses of iron meteorites. This high ratio tends to increase the co-precipitation hazards if the unmodified method is used.

The accuracy of the modified method based on the analysis of a synthetic sample with a known content of nickel is about 4 per cent.

Spectrographic procedure

The apparatus, the spectral lines, the internal standards and the usual precautions required by the trace elements analysis were the same as those described by Lovering *et al.* (1957). However, in order to take into account the possible effects of the chemical differences between kamacite and taenite and of the chemical isolation methods, the spectrographic standards and the graphite and the sodium carbonate-in-quartz dilution ratios were modified.

The matrix for the analysis of kamacite contained 95 per cent iron and 5 per cent nickel and that for taenite contained 62 per cent iron and 38 per cent nickel. Both matrices were prepared as nitric acid solutions containing the indicated proportions of iron and nickel and the appropriate ranges of the trace elements concentrations. Inasmuch as the kamacite phase was isolated as sulphuric acid solution, the synthetic kamacite matrix was converted into iron–nickel sulphate prior to its ignition at 600°C.

The dilution ratios were adjusted so as to take into account the large differences between the concentrations of the elements studied in kamacite and taenite.

The standard deviations of the results were evaluated and compared with those observed in the analyses of the complete samples of iron meteorites (see Lovering *et al.*, 1957). There are apparently sources of errors in the procedures involving the chemical isolation as well as the analyses of the individual phases. The results for gallium and germanium appear to be reproducible to within 15 per cent (s.d.), while those for chromium and copper are reproducible to within 25 per cent in kamacite and 20 per cent in taenite. The results for cobalt are the most reproducible, with standard deviations being less than 15 per cent.

3. Results

Nickel content of kamacite and taenite

The nickel results are collected in Table 1. Each value for both the kamacite and taenite is an average of three determinations and includes in addition the mean deviation from that average.

Examining Table 1, we note that in the hexahedrites studied there is a difference of 0·8 per cent between the nickel content of the complete hexahedrites and the dilute acid fractions. Later in this paper (Table 4) it will be shown that a similar difference exists in the concentrations of all the trace elements studied. Both of these differences lie outside of the respective experimental errors. They are further supported by the frequent occurrence on the surface of the hexahedrite bars of light, relatively unetched areas localized in the immediate vicinity of rhabdite needles, in addition to dark areas which are obviously more attacked by the acid (see Fig. 1(a) for the Coahuila hexahedrite). The proportion of the light areas is approximately 30 per cent and they are more or less symmetrically distributed around the rhabdite needles. In view of this, it appears obvious that in order to account for the difference of 0·8 per cent nickel we must assume that the unetched, light areas have a nickel content which is higher than that found in the dilute acid fractions.

In connection with this assumption, Henderson (1957) points out that in

several cases he found that the kamacite around schreibersite is lower in nickel than kamacite remote from it. On this basis he expects the same relationship to also hold for rhabdite needles which are surrounded by kamacite. The fact that

Table 1. Nickel content of kamacite and taenite and the thickness of taenite plates

	Meteorite	Class	Average thickness of taenite in mm	No. of plates measured	Content of nickel in per cent		
					Over-all	Kamacite (dilute acid fr.)	Taenite
1	Coahuila	H			5·65 ± 0·06	4·78 ± 0·08	
2	Coya Norte	H			5·63 ± 0·05	4·80 ± 0·00	
	Canyon Diablo (taenite sample isolated by E. P. HENDERSON)						46·0 ± 1·5
3	Canyon Diablo (fragment A)	Og	0·12 ± 0·04	58	6·98 ± 0·01	3·32 ± 0·01	46·4 ± 1·2
	Canyon Diablo (fragment B)		0·24 ± 0·06	107	7·30 ± 0·03		53·7 ± 0·2
4	Mount Tabby (?)	Og	0·14 ± 0·04	67	6·82 ± 0·11	4·09 ± 0·06 (acid frct.1) 5·26 ± 0·21 (acid frct.2)	35·1 ± 0·8
5	Henbury (fragment A sample 1)	Om	0·38 ± 0·11	82	7·94 ± 0·01	4·91 ± 0·03	33·4 ± 0·1
	Henbury (fragment A sample 2)					5·26 ± 0·21	31·1 ± 1·1
6	Toluca	Om	0·20 ± 0·06	103	8·25 ± 0·02	4·00 ± 0·14	47·0 ± 2·0
7	Bristol	Of	0·08 ± 0·02	98	8·32 ± 0·14	5·84 ± 0·25	32·3 ± 0·4
8	Duchesne	Of	0·20 ± 0·08	115	9·63 ± 0·02	4·32 ± 0·01	30·8 ± 0·4
						aver. 4·66%	aver. 39·6%

the results of this study indicate a reverse relationship may mean that nickel in rhabdite in the Coya Norte and Coahuila hexahedrites was above a critical range of its stability. Reheating of these meteorites may have caused movement of the excess nickel from rhabdite back into the adjacent kamacite, thus accounting for the observed light areas being richer in nickel than the dark areas. The sharp contours of the rhabdite needles as seen on Fig. 1(a) appear to suggest that this process probably occurred at a temperature considerably lower than 800°C.

Fig. 1(a). Coahuila hexahedrite after 250 hr of continuous treatment with the 0·0075 N H_2SO_4. The average nickel content of the samples drilled out of three bars is 5·65 ± 0·06 per cent. The average nickel content of dilute acid fractions collected from the bars is 4·78 ± 0·08 per cent. Light, relatively unetched areas are nearly symmetrically distributed around the rhabdite needles. ×3.

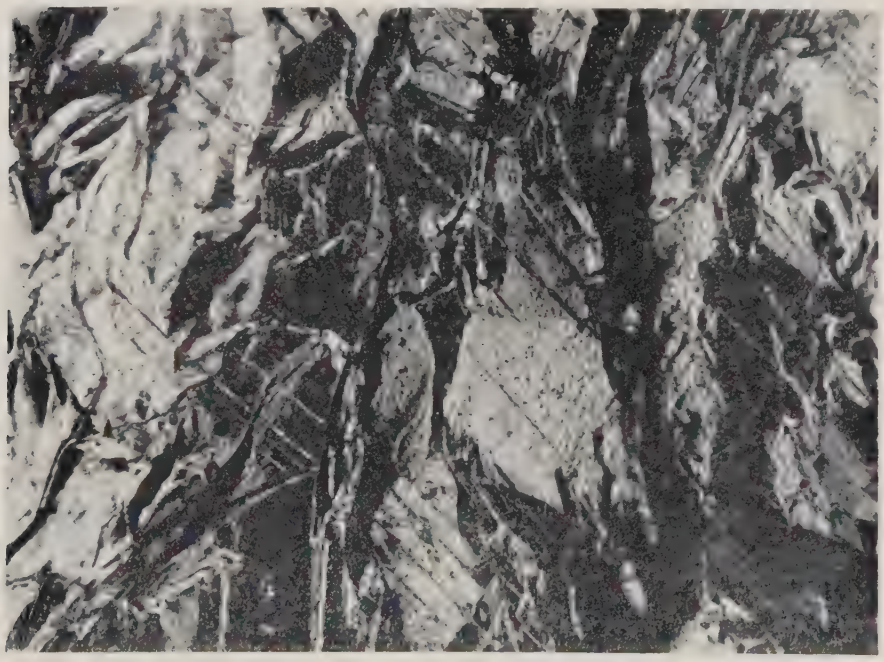

Fig. 1(b). Parallel lies on taenite plates from the Duchesne fine octahedrite. ×70.

Experiments have shown (Perry, 1944) that in the neighbourhood of this temperature phosphide begins to diffuse into its surroundings. Rhabdites thus become rounded bodies or may disappear entirely, leaving only sites of phosphide enrichment.

There is no direct evidence that the observed nickel differences may be due to the presence in the hexahedrites of the traces of the high-nickel phase (taenite) which did not dissolve in the dilute acid.

By analogy with the hexahedrites, it is possible that the kamacite in the octahedrites is also inhomogeneous and that the over-all nickel content of that kamacite is somewhat higher than that indicated by the nickel contents of the dilute acid fractions. None the less, most of the old (nineteenth century) values ranging between 5·5 and 6·9 per cent nickel for kamacite isolated from octahedrites are too high, the reason being that such kamacite is invariably contaminated with phosphide or taenite, or both. Yavnel' (1951a) estimates that the rhabditic phosphide which cannot be removed from kamacite prior to its analysis amounts to 1 per cent. Accepting for the composition of this phosphide the formula Fe_2NiP, he believes that the nickel content of "pure" kamacite should be lower than that of the kamacite containing the non-removable phosphide by about 0·25 per cent. Consequently, the nickel concentration in the "pure" kamacite of the Sikhote–Alin meteorite is about 5 per cent instead of 5·27 per cent, as found by averaging a large number of values obtained in the analyses of the phosphide-containing samples.

Taking into account all present nickel values for kamacite, it is seen that the range of their variations is 3·3–5·8 per cent, with an average of 4·7 per cent.

Accepting these nickel contents, we note that they are appreciably lower than the nickel values of 5·3–6·0 per cent indicated for the kamacite phase by Perry (1944), Henderson (1953), Uhlig (1954) and Yavnel' (1951, 1954).

These lower nickel values for kamacite and the over-all nickel values for taenite (Table 1) are difficult to reconcile with the iron–nickel phase diagram as worked out by Owen and Liu (1949) and corrected by Uhlig (1954) for the effects of high pressure. The data of the original diagram for atmospheric pressure are summarized in Table 2. It is noticed, for example, that the Canyon Diablo low nickel kamacite containing 3·3 per cent nickel is a high temperature phase (600–700°C), whereas taenite from the same meteorite containing 46·4 per cent is a low temperature phase (about 350°C).

Uhlig (1957) suggests that the low nickel values for kamacite, if correct, would perhaps indicate that the nickel content of taenite at its boundary with kamacite is much lower than the average nickel values of 31–54 per cent shown in Table 1. For example, the iron–nickel diagram shows that an iron–nickel alloy containing 3·7 per cent nickel (close to 3·3 per cent found in the kamacite of the Canyon Diablo meteorite) is in an equilibrium with an alloy containing 17·3 per cent nickel. Secondary heat treatment of iron meteorites could have led to an equilibrium condition between a low nickel kamacite and taenite only within that region which is immediately adjacent to the phase boundary rather than through the entire extent of the taenite phase.

The nickel values in taenite at its boundary with kamacite and their relation

to the over-all as well as the interior values are not well known. The data obtained by SMITH and YOUNG (1939), PERRY (1944), DALTON (1950, 1951), and UHLIG (1954), using various indirect methods of studying taenite in the polished sections

Table 2. Phase equilibria in iron-nickel system according to OWEN and LIU (1949)

Temp. (°C)	Ni content, atomic percentage	
	α-phase boundary (kamacite)	γ-phase boundary (taenite)
800	1·2	3·8
700	2·5	9·4
600	3·7	17·3
550	4·4	22·2
500	5·0	27·5
450	5·7	34·3
400	6·3	41·5
350	6·9	48·5
300	7·5	56·0

from its edge to centre, are only qualitative and for the most part conflicting; they indicate a nickel content at the edges of taenite which is both low and high relative to the content in the interior.

In this study an attempt has been made to determine quantitatively the variations of nickel content in taenite. The experiment consisted of progressive withdrawal at room temperature of dissolved fractions of variable weight (each 5–30 per cent of initial weight of the sample) from taenite samples comprised of a large number of plates using 0·3 normal sulphuric acid. The solutions were then analysed for total dissolved material and for nickel.

The nickel contents of the fractions collected from four different taenites are assembled in Table 3. The table also includes the average nickel content of each series of fractions, the over-all nickel content of each of the four taenites as shown in Table 1 and the total weight of each taenite sample prior to its fractional dissolution.

The results show that the nickel content of taenite is variable, the first fraction of each taenite sample containing lower concentrations of the element than either the complete sample or its last fraction. The intermediate fractions possess nickel contents which are both low and high relative to the first fraction.

The factor affecting the nickel values for the first fraction is the loss of the outermost surface layer of taenite in the process of its isolation. The effect of this loss is such that the nickel values for the first fraction of all four taenite samples studied represent the nickel content of taenite, not at its immediate boundary with kamacite, but probably at some appreciable and very likely variable distance from that boundary.

Table 3. Variations in the nickel content of taenite

Meteorites	Class	Start. weight in mg of total sample	Nickel content of consecutive fractions (per cent)														Average of all fractions	Ni in the complete sample (Table 1)
			1	2	3	4	5	6	7	8	9	10	11	12	13	14		
Canyon Diablo*	Og	59·3	40·3	50·0	43·3	57·7	47·2	48·5	49·4	58·6	52·2						49·7	46·0
Henbury	Om	115·5	30·3	29·8	29·4	33·7	31·5	34·6	30·2	34·6	28·5	30·8	40·9				32·2	31·1
Toluca	Om	101·1	35·7	39·4	42·5	42·5	46·0	47·8	48·7	50·7	42·6	50·9	53·7	53·8	55·9	38·2	46·3	47·0
Bristol	Of	118·9	29·0	26·9	32·9	27·9	40·0	29·3	46·7	27·6	24·9	35·3	32·5	37·2			32·5	32·2

* Canyon Diablo taenite used for fractional dissolution was that isolated by E. P. HENDERSON

Likewise, the lack of precise information concerning the uniformity of thickness of the last and the intermediate layers dissolved off each taenite plate introduces considerable uncertainty into the nickel values for the last and the intermediate fractions of each taenite sample.

Accurate studies of the composition of taenite should, therefore, aim at obtaining a taenite sample having an unaltered boundary surface as well as developing method which will permit to achieve a uniform dissolution of small increments of such sample from its surface toward the interior.

Physical characteristics of taenite in relation to its content of nickel

The roughly estimated plate area of the great majority of the isolated taenite plates varied from about 2 to 35 mm^2. Since most of them were fragments rather than integral plates as seen in the more or less continuous structural patterns of the octahedral irons, no great significance should be attached to these dimensions.

Some 400 plates from the six octahedrites studied were examined under binoculars ($\times 72$). It was observed that aside from the usual metallic lustre and the profusion of ridges, grooves and depressions, the most prominent characteristics of the taenite plates are their surface inclusions, the thin parallel lines traversing the two larger surfaces and the variable thickness.

The surface inclusions of foreign phases occur as bulky bodies having a random distribution or as well defined geometrical figures, among which most outstanding and abundant are rhombs, squares, rectangles and longer or shorter rods. The rods frequently terminate in sharp points on one or both of their ends. Of all the geometrical forms observed, the elongated rods display the largest degree of preferred orientation. Often two or more rods traverse the plate at nearly the same angle. A very similar observation was made by Yavnel' (1951) on the rhabdite inclusions in the kamacite fields of the Sikhote-Alin meteorite. He noticed that needles and elongated rectangles had a definite orientation, whereas all other crystalline forms of rhabdite were scattered over the kamacite field in a completely random fashion.

A considerable number of inclusions are not level with the surrounding surface but project distinctly above it. This may very likely be due to some taenite surface having been dissolved off during the process of isolation.

Chemically, the inclusions have been classified into those which reduced copper out of the copper sulphate solution, and those which did not. The inclusions were approximately equally distributed among these two groups. It was observed that no particular crystalline form of the inclusions had a tendency to reduce copper preferentially. According to Perry (1944), cohenite precipitates copper from solution, whereas schreibersite does not. Henderson (1957) states that both of these phases precipitate copper.

Perhaps the most prominent trend in all inclusions is the decrease of their abundance on going from taenites with high content of nickel (46–54 per cent) to those in which the content of nickel is lower (30–35 per cent). At the latter level, the inclusions are rare.

The thin parallel lines (see Fig. 1b) are very rare, faint, widely spaced, interrupted in their course and visible mostly only on one side of the plates in

taenites having high contents of nickel (46–54 per cent). As one proceeds toward lower contents of nickel the abundance of these lines as well as their continuity appears to increase noticeably. At the same time they tend to occur on both sides of the plates. It should be added that even on the level of their greatest abundance, the lines in the taenite plates are a great deal less abundant than the Neumann lines in hexahedrites (see, for example, PERRY, 1944, Fig. 1).

When subjected to the action of the dilute acid until their nearly complete dissolution, several plates from the Bristol meteorite retained their lines, although their intensity seemed to have decreased in the process.

PERRY (1944) states that very fine slip lines which can be produced in artificial irons by slight movement along gliding planes disappear on etching, while Neumann lines persist.

UHLIG (1957) and HENDERSON (1957) concur in their independent conclusions based on examination of the Fig. 1(b) that the observed lines are not the Neumann lines such as occur in kamacite. UHLIG states that the appearance of Neumann lines in the face-centred cubic lattice which is the structure of taenite, is highly unusual. According to HENDERSON, the described lines represent a trace of the Neumann lines on the taenite, but actually they are not Neumann lines in the taenite. When examined in polished sections, the exposed cross-sections of taenite do not show Neumann lines.

Lines similar to those described for the taenite plates have been reported by HENDERSON and MONNIG (1956) for rhabdite inclusions in the Richland, Texas, hexahedrite. These lines, the authors suspect, are deformations that occurred when the Neumann lines formed in kamacite. The rhabdite being firmly held within the kamacite was deformed by the compressional wave, but was not broken or displaced. In octahedrites, the taenite may have been deformed in a similar fashion, giving rise to the observed lines on the taenite plates.

The average thickness of the taenite in the octahedrites studied was evaluated statistically by measuring thickness of more than 600 individual plates with a micrometer. The relatively small size of the plates permitted measurements of their thickness over their entire surface area. Since only the isolated plates were measured, no correction was needed for the orientation of the taenite plates, which is an important factor in all thickness measurements involving taenite in the etched sections of iron meteorites. Therefore, the errors involved result largely from the surface relief and from the action of the acid. The extent to which these opposing tendencies cancel each other is not known.

The results of the measurements are shown in Table 1, columns 4 and 5, and the frequency distribution of the thickness in Fig. 2. In each case the average thickness includes the absolute value of the mean deviation. It is striking that the lower limit of thickness is 0·04 mm for all taenite plates measured and the mean deviation with the exception of the Duchesne taenite is nearly constant (approximately 30 per cent). It is observed that no correlation exists between the average thickness and either the structure or the nickel content of the taenite.

Table 1 also shows that the taenite plates from the fragments A and B of the Canyon Diablo meteorite have different thicknesses. The nickel content of both the complete samples of those fragments and the taenites isolated from them are also different.

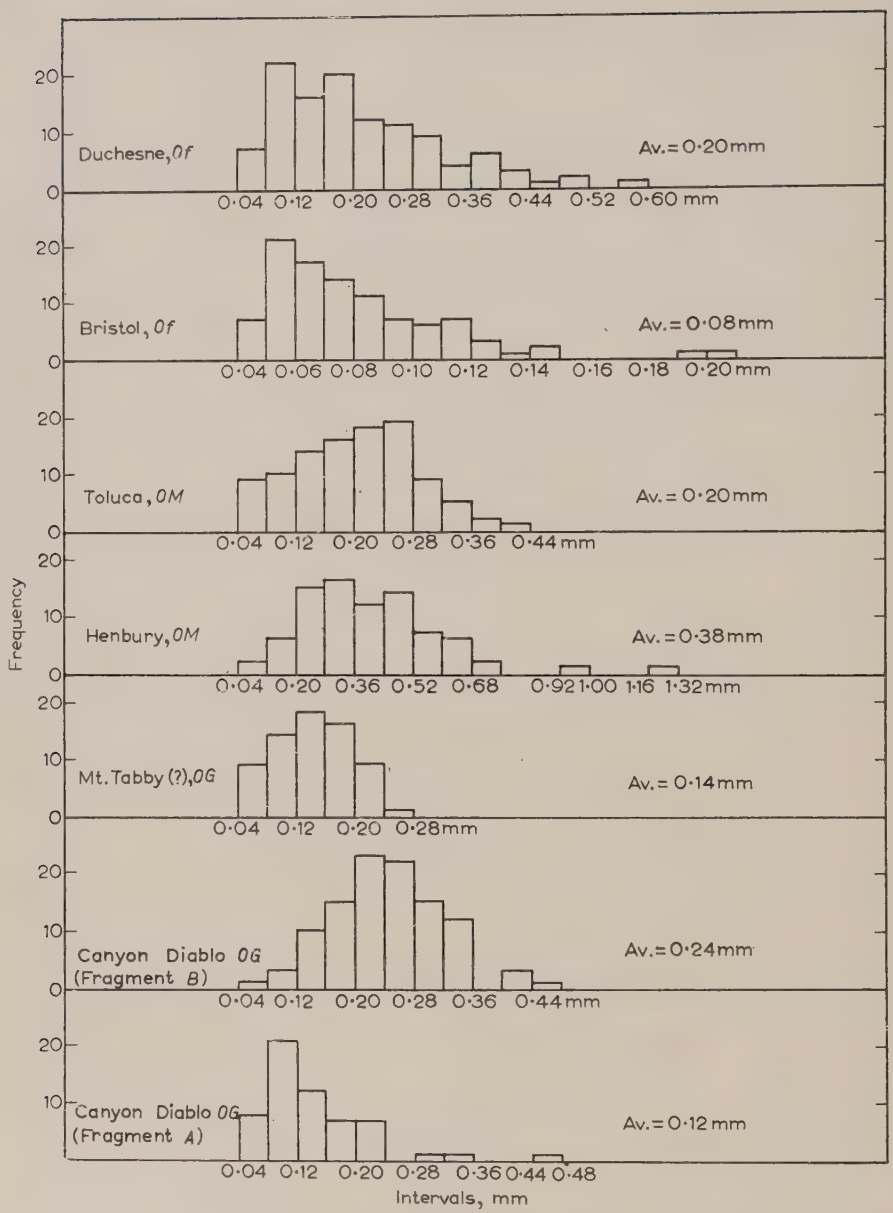

Fig. 2. Frequency distribution of the thickness of taenite plates.

Distribution of gallium, germanium, copper, cobalt and chromium in kamacite and taenite in relation to nickel distribution

The results on the distribution of the elements studied in kamacite and taenite are presented in Table 4. The symbols *c*, *k* and *t* designate the over-all content of the elements in the original meteorites and in the kamacite and taenite phases respectively. The over-all contents of the elements studied with exception of

Table 4. Kamacite–taenite distribution of gallium, germanium, cobalt, copper and chromium in relation to the distribution of nickel

Meteorite	Ga–Ge group	Ni (per cent)			Ga (p.p.m.)			Ge (p.p.m.)			Co (p.p.m.)			Cu (p.p.m.)			Cr (p.p.m.)		
		c	*k*	*t*	*c*	*k*	*t*	*c*	*k*	*t*	*c*	*k*	*t*	*c*	*k*	*t*	*c*	*k*	*t*
Coahuila, H.	II	5·65	4·78		54	30		152	43		4500	4600		122	43		44	13	
Coya Norte, H	II	5·63	4·80		56	37		144	63		5100	4500		123	39		48	17	
Canyon Diablo Og, fragment A	I	6·98	3·32	46·4	74	26	525	283	23	2200	4900	5200	440	157	23	2600	7	6	36
Canyon Diablo Og, fragment B		7·30		53·7			505			1050			590			2500			17
Mt. Tabby (?), Og	II	6·82	4·09	35·1	50	22	250	202	19	1400	5100	4800	740	125	14	1300	44	10	200
Henbury, Om		7·94	4·91	33·4	60	38	210	209	60	700	4900	6100	1470	186	51	1500	15	15	28
Toluca, Om	II	8·25	4·00	47·0	61	19	290	170	28	950	4500	5100	600	125	17	1900	5	3	24
Bristol, Of	IV	8·32	5·84	32·3	2	<1	2	<1	<1	7	4400	4100	1100	333	37	1250	111	44	300
Duchesne, Of	IV	9·63	4·32	30·8	2·2	<1	7·5	<1	<1	3	3800	4300	1460	127	27	950	10	7	6

nickel are those determined by LOVERING *et al.* (1957). The roman numerals in the second column indicate the gallium–germanium families of iron meteorites observed by these same authors.

It is seen that in most cases the cobalt content of kamacite is higher than is the over-all content. The discrepancy is largely due to the errors in the cobalt determination and does not affect the principal trends in the distribution of this element. Examination of Table 4 shows that in the meteorites studied the greater proportion of the total cobalt exists in the kamacite than in the taenite phase.* At the same time the degree of its concentration in that phase is higher than the corresponding degree observed for nickel. As a result of this trend, the kamacite phase as represented by the dilute acid fractions of both hexahedrites and octahedrites accounts for 60–90 per cent of the total content of cobalt.

Unlike cobalt, the elements gallium, germanium, copper and chromium are present to a considerably larger extent in the taenite (high nickel phase) than in the kamacite phase.

In the hexahedrites, this tendency is manifested indirectly by the fact that with the exception of gallium, the proportions of the other trace elements which exist in the low-nickel fraction (4·8 per cent Ni) of the hexahedrites are less than 50 per cent.

From this it is apparent that the elements gallium, germanium, copper and chromium are, like the element nickel, higher in concentration in the light, acid-resisting areas of the hexahedrites than in their acid-soluble fractions.

It is possible that the kamacite in the octahedrites is similar to the hexahedrites in having the acid-resistant areas. This would tend to make the reported concentrations of gallium, germanium, copper and chromium in the kamacite somewhat lower than the actual values. However, the analytical results are certainly influenced to some degree by limited solution of taenite, which would tend to offset this effect. No observations of the acid-resistant areas were made in the etched kamacite in the octahedrites.

Compared with the taenite from other octahedrites, the Henbury taenite contains the smallest concentration of gallium, germanium and copper. This may be connected with the fact that the lamellae of this taenite are thickest relative to the lamellae (see Table 1) of all other taenites which have been measured.

Further examination of Table 4 shows that there is no dependence of the distribution of the elements gallium and germanium between kamacite and taenite on the gallium–germanium groups of iron meteorites as observed by LOVERING *et al.* (1957). In view of this the phase distribution of these elements, unlike their over-all concentrations, is probably not a distinctive feature among the iron meteorites.

4. RELATIVE PROPORTIONS OF KAMACITE AND TAENITE

The over-all concentrations of the elements as determined in this study and assembled in Table 4 are used to calculate the proportions of kamacite and taenite in the octahedrites listed.

* *Note added in proof*: A. A. YAVNEL' (private communication) of the Committee on Meteorites, U.S.S.R. points out that the predominant concentration of cobalt in kamacite can be explained with the aid of the diagram of the three component system Fe–Ni–Co for sufficiently low temperatures. He illustrates this point using a non-rigorous isothermal projection of the diagram.

We have the relationships,

$$K + T = 1 \tag{1}$$

$$k \,.\, K + t \,.\, T = c \tag{2}$$

where K and T are the proportions of kamacite and taenite respectively: and k, t, c, in this order are the contents of a given element in kamacite, taenite and the complete sample of an octahedrite.

Solved for T, equations (1) and (2) yield:

$$T = \frac{c - k}{t - k} \tag{3}$$

Using the Canyon Diablo meteorite as an illustration where the c, k and t values for germanium are 283, 23 and 2200 p.p.m. respectively, we have:

$$T = \frac{283 - 23}{2200 - 23} = 0{\cdot}12 = 12{\cdot}0 \text{ per cent}$$

The calculated T values for the six octahedrites rounded off to the nearest 0·5 per cent are assembled in Table 5. The absolute phase concentrations t and k of the elements (Table 4) multiplied by the observed proportions T and K of the taenite and kamacite phase, are designated by t_1 and k_1, respectively.

The germanium data for kamacite and the complete samples of the Bristol and Duchesne meteorites indicate only the upper concentration limits of the element and have, therefore, not been used in the calculations. In the case of gallium in kamacite of these same meteorites, a value of 0·6 p.p.m. has been assumed instead of the less than 1 p.p.m.

It is seen from Table 4 that because the concentrations of cobalt are higher in the kamacite than in the taenite phase, the denominator $(t - k)$ in the equation (3) is negative, and therefore the proportions of taenite obtained on the basis of this element are also negative. For this reason, the cobalt data have not been included in Table 5.

Aside from cobalt, it is observed that the proportions of taenite in the individual octahedrites calculated using the concentrations of the remaining elements vary widely depending on the element, with copper yielding the lowest values. The differences by as much as a factor of 2 between the smallest and the largest values of the proportions are quite common for all elements.

The proportions of taenite in various octahedrites calculated on the basis of the same element tend to increase, although not entirely uniformly, from coarse to fine octahedrites. This is in a qualitative agreement with the metallographic observation of the polished and etched specimens.

The absolute concentrations of the elements in taenite shown in Table 4 when multiplied by the proportions of taenite give the relative contributions of taenite to the over-all composition of the investigated octahedrites. These contributions are shown as the decimal fractions in the columns t_1 in Table 5. It is evident that the relative contribution of taenite is consistently greater and apparently independent of the structure of the meteorites in the case of gallium (with the

Table 5. Relative contributions of taenite and kamacite to the over-all concentrations of nickel, gallium, germanium, copper and chromium

Meteorite	Ni			Ga			Ge			Cu			Cr		
	T	k_1	t_1	T	k_1	t_1	T	k_1	t_1	T	k_1	t_1	T	k_1	t_1
Canyon Diablo, Og	8·5	3·04	3·94 (0·56)	9·5	24	50 (0·68)	12·0	20	265 (0·94)	5·0	22	130 (0·82)	5·0	6	2 (0·29)
Mt. Tabby (?), Og	9·0	3·72	3·16 (0·46)	12·5	19	31 (0·62)	13·0	17	182 (0·90)	8·5	13	111 (0·89)	17·5	8	35 (0·80)
Henbury, Om	10·5	4·35	3·51 (0·44)	13·0	33	27 (0·45)	23·0	46	161 (0·77)	9·5	46	143 (0·77)			
Toluca, Om	10·0	3·60	4·70 (0·57)	15·5	16	45 (0·74)	15·5	24	147 (0·86)	6·0	16	114 (0·91)	9·5	3	2 (0·40)
Bristol, Of	9·5	5·25	3·07 (0·37)	13·0	<0·5	1·6 (0·75)				24·5	28	306 (0·92)	26·0	33	78 (0·70)
Duchesne, Of	20·0	3·46	6·16 (0·64)	24·0	<0·5	1·8 (0·75)				11·0	24	105 (0·83)			

exception of the Henbury meteorite), germanium and copper. In the case of nickel and chromium, the corresponding contribution is considerably smaller and shows fluctuations within the range 37–64 and 30–70 per cent, respectively.

Acknowledgements—The writer wishes to thank Professors Harrison Brown and L. T. Silver of the California Institute of Technology, Dr. E. P. Henderson of the U.S. National Museum, and Professor H. H. Uhlig of the Massachusetts Institute of Technology, for their suggestions after critical reading of the manuscript.

Thanks are also due to Professors G. Bergmann and F. S. Buffington of the California Institute of Technology for informative discussions in the early stages of this work.

I am greatly indebted to the members of the geochemistry group at the California Institute of Technology for their numerous suggestions pertaining to the various phases of this problem, especially to Prof. L. T. Silver and Dr. M. Gruenenfelder for their generous help in the microscopic examination of the meteorite samples and the taenite plates; and to Mr. A. Chodos, the director of our spectrographic laboratory, who gave much of his time helping to adapt the previously devised (see Lovering *et al.*, 1957) spectrographic methods to this study. Mr. F. Wilde of the Institute's Glass Shop performed cutting of the iron meteorites into bars of the desired shape.

Gratitude is extended to the following individuals and institutions for their generous gifts of samples used in this study: Dr. E. P. Henderson of the U.S. National Museum for the gift of a sample of the Canyon Diablo taenite; Prof. C. Frondel of Harvard University for the gift of a slice of the Coahuila hexahedrite; and the Geological Museum of the University of Utah for the gift of a slice of the Mount Tabby (?) coarse octahedrite.

References

Dalton F. (1950) *J. R. Astr. Soc. Canad.* **44,** 185–195.
Dalton F. (1951) *J. R. Astr. Soc. Canad.* **45,** 162–166.
Davison J. M. (1891) *Amer. J. Sci.* **42,** 64–66.
Farrington O. C. (1915) *Meteorites* pp. 130–135. Chicago.
Goldberg E., Uchiyama A. and Brown H. (1951) *Geochim. et Cosmochim. Acta* **2,** 1–25.
Henderson E. P. (1941) *Amer. J. Sci.* **239,** 372.
Henderson E. P. (1953) *Amer. Mineral.* **38,** 1025–1039.
Henderson E. P. and Monnig O. E. (1956) *Meteoritics* **1,** No. 4, 459–469.
Henderson E. P. (1957) Private communication.
Lovering J., Nichiporuk W., Chodos A. and Brown H. (1957) *Geochim. et Cosmochim. Acta* **11,** 263–278.
Owen E. A. and Liu Y. H. (1949) *J. Iron St. Inst.* **163,** 132–137.
Perry S. H. (1944) *The Metallography of Meteoric Iron.* United States Printing Office, Washington, D.C.
Pfann E. (1917) *Z. Metallog.* **2,** 65.
Smith S. W. J. and Young J. (1939) *Nature, Lond.* **143,** 384–385.
Uhlig H. H. (1954) *Geochim. et Cosmochim. Acta* **6,** 282–301.
Uhlig H. H. (1957) Private communication.
Yavnel' A. A. (1951) *Izv. Akad. Nauk Kaz. SSR* (*ser. astronom. i fiz.*) **4,** 46–73.
Yavnel' A. A. (1951a) *Izv. Akad. Nauk Kaz. SSR* (*ser. astronom. i fiz.*) **5,** 32–56.
Yavnel' A. A. (1954) *Meteoritika* **II,** 107–116.

Geochimica et Cosmochimica Acta, 1958, Vol. 13, pp. 248 to 255. Pergamon Press Ltd., London

The uranium contents of iron meteorites*

G. W. Reed, H. Hamaguchi† and Anthony Turkevich

Argonne National Laboratory, Lemont, Illinois, and Enrico Fermi Institute for Nuclear Studies, University of Chicago, Chicago, Illinois

(*Received* 22 *October* 1957)

Abstract—Seven iron meteorites and the iron phase of one pallasite have been examined for uranium content by neutron activation. The results are at the limit of detection by this method under the conditions used, but indicate a variable uranium content in the range 10^{-12} to 10^{-10} g/g. This agrees with the limits set by Reed and Turkevich (1955) in preliminary results of the application of neutron activation to this problem, and is more than a factor of 10 lower than previous determinations by other methods.

Introduction

In 1955, Reed and Turkevich reported the first results of the determination of uranium in iron meteorites using neutron activation. These gave only limits (half of them less than 5×10^{-10} g/g) for two iron meteorites (Tamarugal and Thunda), but these limits were considerably lower than previous work (Dalton, Golden, Martin, Mercer and Thomson, 1953; Dalton, Paneth, Reasbeck, Thomson and Mayne, 1953; Dalton and Thomson, 1954; Deutsch, Houtermans and Picciotto, 1956; Davis, 1950). More recently Starik and Shats (1956) have reported uranium contents for four iron meteorites to be 2×10^{-8} g/g, thus much higher than the limits reported by Reed and Turkevich.

It is the purpose of this paper to report the results of further neutron activation analyses for uranium in iron meteorites. The sensitivity of the method has been increased by more than an order of magnitude and a variety of iron meteorites have been examined. The results indicate a uranium content that may be variable but is below 3×10^{-10} g/g. Thus the neutron activation method continues to give results much lower than other methods.

Experimental

The neutron activation technique for determining the uranium content of a sample has already been sufficiently described (Smales, 1952; Mahlman and Leddicote, 1955). The application of the method to meteorites can be found in the paper by Hamaguchi, Reed and Turkevich (1957) on the uranium content of stone meteorites. The special advantages of the method for the problem at hand are the high sensitivity, the possibility of getting independent results by analysis for both ^{239}Np and a fission product (e.g. ^{140}Ba) and the relative freedom from contamination.

In this work essentially the same procedure was used as is described in detail in the report of Hamaguchi, Reed and Turkevich (1957). Approximately 1 g samples were exposed to neutrons concurrently with monitors containing small

* Based on work performed under the auspices of the U.S. Atomic Energy Commission.

† Now at Tokyo University of Education, Tokyo, Japan.

known amounts of uranium. After an irradiation the surface (a few per cent) of the samples was dissolved and discarded (to avoid possible surface contamination). The rest of the sample was then analysed radiochemically for both ^{239}Np and ^{140}Ba—^{140}La. By comparison with similar analyses on the monitor, the uranium content of the meteorite samples could be established.

Three types of monitors were used. In one, a solution containing the same principal metallic constituents as iron meteorites, together with a known added amount of uranium, was evaporated in a quartz vial. In the second, a hole was drilled into a small piece of iron meteorite and a solution containing a known amount of uranium was evaporated in it. Finally, a piece of iron–nickel alloy was prepared containing uranium. Samples from various parts of this iron alloy were analysed to establish the uranium content and the homogeneity. The uranium content of all the monitors was of the order of 1 μg/g. They appeared to be equally satisfactory. A few tests with the monitors checked our expectation that neither neutron absorption by the other constituents nor self-absorption by the uranium at the μg/g level was serious.

The irradiations were carried out primarily in the "Thimble" of the Argonne heavy-water reactor (CP-5). Two irradiations were performed at the Atomic Energy Commission MTR reactor at Arco, Idaho. In both places the increased sensitivity from the higher-neutron flux is complicated by the importance of resonance activation of ^{238}U. It is not quite clear how completely this can be simulated in the monitor, so that the results of the ^{239}Np method must be assigned errors of the order of 30 per cent.

The chemistry used was very much the same as previously (Hamaguchi, Reed and Turkevich, 1957). After dissolution of the sample in HCl in the presence of ^{237}Np tracer and the barium carrier, the neptunium and barium were isolated. The main modifications were frequent use of mono-octyl phosphate to extract Np(IV) away from iron (Peppard, Maier, Mason and Moline, 1957), and the introduction into the neptunium procedure of basic carbonate scavengings and specific gold precipitations to ensure the removal of the radioactivity induced in this element. In almost all cases the barium sample isolated was milked for ^{140}La several days after separation of the barium.

The small samples dissolved almost completely upon digestion with HCl. Very small occasional residues were brought into solution with aqua regia and combined with the main solution. The first steps of the procedures always involved an oxidation of the Np to a higher valent state and then reduction to a state where it would either extract in mono-octyl phosphate(IV) or be carried by LaF_3(III or IV).

The radiochemical purification procedures were more exhaustive than in the work of Reed and Turkevich (1955), and as a result the recoveries of neptunium were still only fair (5–40 per cent). These, however, were measured by the ^{237}Np recovered. The yields of the barium averaged 50 per cent and were measured by the weight of barium carrier recovered. In both cases, however, the samples were radiochemically cleaner than in the earlier work. Finally, much of the counting was done using an anti-coincidence shielded proportional counter with a background of only approximately 1·2 counts/min. Together with the higher neutron fluxes

used, these improvements led to an increase of almost a factor of 100 in sensitivity in the best runs over that achieved by Reed and Turkevich (1955).

Nine different meteorites were examined in this work. Most of them were obtained from Prof. H. C. Urey. The small samples used were sawed off from large pieces, making efforts to select the most homogeneous appearing regions. Seven of the samples studied were typical iron meteorites; one was the metal phase of a pallasite (Brenham). In this case the metal portion was separated, taking care not to include any silicate. Finally, the small metal portion of a chondrite (Holbrook) was separated mechanically and magnetically, washed and then irradiated to get information on the uranium content of the metal phase of chondrites. This chondrite as a whole had been found to have a uranium content of 10^{-8} g/g in the work of Hamaguchi, Reed and Turkevich (1957).

Results

Twenty-five samples of these meteorites were irradiated at various times. In general, both ^{239}Np and ^{140}Ba were separated radiochemically and their radioactivity measured. Due to variations in the neutron flux used, the times of irradiation and decay, the chemical recovery and the occasional small amounts of contaminating radioactivity, the sensitivity achieved for a given sample varied widely. We have classed our results into two groups. In one, the radioactivity isolated could, with reasonable certainty, be assigned to the sought-after species—^{239}Np and ^{140}Ba or ^{140}La—by virtue of its decay period and/or the absorption characteristics of its radiations. In these cases the uranium content of the meteorite was calculated directly by comparison with the monitor.

The second group of results yielded only limits to the amounts of sought-after radioactive species present in the isolated sample. This arose primarily because the amount of radioactivity was so small that its identification could not be positively established. Except in a few cases, we were not able to characterize with sufficient confidence a decay curve starting initially with less than 1 count/min. In addition, in some samples, the small amount of radioactivity isolated did not decay properly, but this could not be established soon enough to warrant chemical re-purification. In both of these cases limits to the uranium content were calculated on the assignment of the maximum amount of radioactivity, consistent with the measurements, to the appropriate radioactive species (^{239}Np or ^{140}Ba—^{140}La).

The results are presented in Table 1. The first column identifies the meteorite studied. The second column indicates the number of samples of each meteorite irradiated. From each sample two determinations were made, one from the ^{239}Np isolated, and one from the isolation of the fission-product mass 140 chain. The third and fourth columns of the table give the number of determinations which resulted only in limits to the uranium content of the meteorite and the range of these limits. The fifth and sixth columns give, respectively, the number of determinations that lead to values for the uranium content of the meteorites, and the range in which these values lie.

It is seen that somewhat less than half of the determinations gave rise to

Table 1. Uranium content of iron meteorites (Units of 10^{-11} g/g)

Meteorite	Number of samples irradiated	Number of determinations leading only to limit	Range of limits	Number of determinations leading to values	Range of values
Tamarugal†	5	4*	8–60	5	0·3–3·5
Carbo	6	7	1·6–50	5	0·3–7·0
Thunda†	5	7	5–20	3	0·5–32
Canyon Diablo	2	2	2–5	2	0·5–1·4
Arispe	1	2	4–20		
Coahuila	1	2	16–20		
Henbury	1	2	0·7–6		
Brenham (Fe phase)	4	5	1·2–28	3	0·5–12

* One sample of ^{140}Ba for Tamarugal had an apparent uranium content of 200×10^{-11}. We consider this to have been accidental contamination. The corresponding neptunium result was $3{\cdot}3 \times 10^{-11}$.

† The data reported by Reed and Turkevich (1955) are not included in this compilation.

positive results—the rest yielded only limits. About two-thirds of the numbers came from the neptunium analyses. The table indicates that the uranium contents deduced for a given meteorite varied often by a factor of 10. This variation is supported by the fact that many of the limits obtained (column 4) were lower than some of the values obtained (column 6).

Confronted with this type of data and appreciating the extreme limits to which we are pushing the technique, we have considered seriously the possibility that even the cases leading to definite results were examples of contamination. Unfortunately, there were only a few cases where both ^{239}Np and ^{140}Ba—^{140}La yielded definite values—not enough to support each other in the establishment of the uranium present, certainly not enough to seriously test the assumption of the terrestrial isotopic composition of the uranium in the meteorite. The individual positive results do stand up to the usual test of radiochemical purity, and we therefore accept them as measures of the uranium present.

Our conclusion is that the data indicate the frequent presence of uranium in iron meteorites, variable in amount, but in the range 10^{-12}–10^{-10} g/g. The amount of variation is indicated in Fig. 1, which illustrates the frequency distribution of all the positive results on a logarithmic abundance scale. Eighty per cent of the values lie in a flat distribution below 10^{-10} g/g.

Two of the results merit special mention. In one sample of Tamarugal the ^{140}Ba isolated indicated a uranium content of 200×10^{-11} g/g. The radioactivity was definitely ^{140}Ba, and yet the corresponding ^{239}Np result showed a uranium content of $3{\cdot}3 \times 10^{-11}$. We consider that the safest interpretation of this one case is severe radioactive contamination.

The experiment on the separated metal portion of a chondrite (Holbrook) gave the following results: It was found that some 90 per cent of the sample after irradiation was soluble in HCl. This and the residue—which was dissolved

by peroxide fusion—were analysed separately for ^{239}Np and ^{140}Ba. The acid-soluble (or leachable) part indicated a uranium content of 10^{-9} g/g from the fission product analysis and only 3×10^{-10} g/g from the ^{239}Np analysis. Only limits of 3 and 1×10^{-10} g/g could be set for the contribution of the acid-insoluble part.

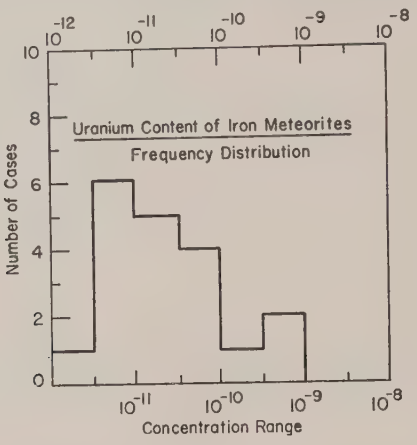

Fig. 1. Variation in uranium contents of iron meteorites.

These results appear to be most consistent with the idea that the small amount of silicate present had about the usual amount (10^{-8} g/g) of uranium. After irradiation, the barium is found primarily in the acid-soluble part either as a result of leaching or due to the fission products recoiling out of the silicate phase during irradiation. Both processes are less probable for neptunium.

Discussion

The results reported here on the uranium content of iron meteorites as measured by neutron activation indicate a variable uranium content primarily in the range 10^{-12}–10^{-10} g/g. They are thus consistent with the limits obtained by Reed and Turkevich (1955) as first results of the application of this technique; they are factors of 10 to 1000 lower than any previously published values, including the recent results ($\sim 10^{-8}$ g/g) reported by Starik and Shats (1956) for the uranium content of four iron meteorites.

In trying to understand the discrepancy, we might consider that the higher uranium contents found in other work are just more extreme examples of the variability found in our samples. Another possibility is that the results are very sensitive to sample size (other workers have, in general, had to use much larger samples) and that in such the probability of inclusions contributing would be appreciable.

However, the situation appears more serious. The neutron activation method gives only 10^{-8} g/g for chondrites (Hamaguchi, Reed and Turkevich, 1957). In addition to being a factor of 10 lower than, for example, the result of Starik and Shats (1956) for chondrites, it is clear that no inclusions of such material can raise the uranium content of primarily metallic substances to 10^{-8} g/g (a typical value claimed by other workers for uranium in iron meteorites).

The particularly strong point of the neutron activation method is the fact that the samples can be irradiated before they are dissolved or treated in any manner. Thus contamination by the minute amounts of uranium in reagents, or by dust, is minimized. The blanks run by other workers to check on such contamination are reported by them to contribute only 10–20 per cent to their results (Starik and Shats, 1956; Dalton *et al.*, 1953); however, they are an order of magnitude higher than what we claim are the uranium contents of iron meteorites.

Accepting our results, some consequences as regards currently interesting problems can be pointed out. First, the results establish the extent to which the uranium in iron meteorites can contribute to the helium found therein. All of the iron meteorites investigated here have had their helium contents determined, in most cases in two independent investigations. In many cases the isotopic composition of the helium found has also been established. The results are presented in Table 2. This gives for each meteorite (column 1) the helium content in cm^3 at STP $\times 10^{+6}$/g (column 2), the isotopic composition (column 3), and the investigating group (column 4). There is moderate agreement in the various determinations on a given meteorite. Except for Brenham, the values range from 10^{-7} to 3×10^{-5} cm^3. Since even 10^{-10} g of normal uranium and an assumed Th/U ratio of 3·6 could have produced only 10^{-7} cm^3 in $4{\cdot}5 \times 10^9$ years, it would appear as if most of the helium found, except possibly in the case of Coahuila, arises from a non-radiogenic source. This is the conclusion reached already by many authors (Bauer, 1947; Begemann, Geiss and Hess, 1957)* on the basis of the high He^3/He^4 ratios (column 4), although Canyon Diablo appears anomalous.

If our results on the uranium content of iron meteorites are typical, then this conclusion would apply to all helium contents of iron meteorites greater than 10^{-7} cm^3 STP/g (groups I and II of Dalton *et al.*, 1953). There are meteorites known, however (group III of Dalton *et al.*, 1953), that have helium contents less than 10^{-7} cm^3 STP/g. The iron phase of Brenham (see Table 2) is an example. The amount of helium is too small to establish the isotopic composition. Such meteorites must either have a uranium content in the lower part of our distribution or be younger than the others. In addition, they must not have been exposed to the same non-radiogenic helium-producing processes as meteorites in groups I and II.

It is likewise clear that radioactive heating in the core of a planet such as the earth cannot be important if it has the same chemical composition as iron meteorites. The concentration of other radioactive elements such as potassium or thorium can hardly be expected to be significant if uranium is as low as indicated here. Likewise, transuranics with their chemical properties so similar to those of uranium and rare earths should not have been significantly concentrated in the metal phases of matter at early times. Thus, if radioactive heating was ever important after the separation of matter into metallic and non-metallic phases, it would appear, on the basis of long-lived radioactive isotopes known today, to have been confined to the non-metallic phase.

The problem of the chemical separation of the elements into metal and silicate phases merits comment. Urey (1955) has made calculations on the

* For other references see G. W. Reed and Anthony Turkevich (1957) *Nature, Lond.* **180,** 594.

theoretically expected distribution coefficient for uranium between the silicate and iron phases of meteorites. These were based on the assumption of no solubility of uranium in metallic iron and led to a distribution coefficient (U in silicate/U in iron) of many orders of magnitude. Taking our results for chondrites as 10^{-8} g/g, a "distribution coefficient" of greater than 100 is indicated for uranium going

Table 2. Amounts and isotopic composition of helium in iron meteorites

Meteorite	He content observed cm^3 STP $\times 10^6$/g	$\frac{[He^3]}{[He^4]}$	Reference
Tamarugal	4		Arrol *et al.* (1942)
	24	0·31	Dalton *et al.* (1953)
Carbo	22		Mayne, Reasbeck and Paneth (1952)
	17–23	0·29	Chackett *et al.* (1953)
Thunda	28		Arrol *et al.* (1942)
	31		Chackett *et al.* (1953)
Canyon Diablo	1		Arrol *et al.* (1942)
	0·4	0·11	Gentner and Zähringer (1957)
Arispe	7		Arrol *et al.* (1942)
	5·3	0·27	Dalton *et al.* (1953)
Coahuila	0·2		Arrol *et al.* (1942)
	0·08		Chackett *et al.* (1953)
	0·2	0·23	Dalton *et al.* (1953)
Henbury	5		Arrol *et al.* (1942)
	0·9	0·25	Dalton *et al.* (1953)
	10	0·22	Gentner and Zähringer (1957)
Brenham (iron phase)	0·02		Reasbeck and Mayne (1955)

into the silicate as contrasted with the metal phase. Such a distribution may actually be an upper limit and the true value may lie between this and Urey's estimate. Our actual results, however, indicate that the segregation of uranium is not as extreme as that of other electropositive elements. Thus we find that the ^{140}Ba, when found, was significantly less contaminated with the products of neutron interaction with the barium present in iron meteorites than in the case of the chondrites (Hamaguchi, Reed and Turkevich, 1957). We estimate the barium content of iron meteorites to be less than 3×10^{-9} g/g, and thus the "distribution coefficient" of barium to be greater than 1000. In addition, this observation argues against the uranium actually present being in the form of silicate inclusions. The same conclusion was reached by Reasbeck and Mayne

(1955). It speaks more for either other types of inclusions or else perhaps uranium–iron compounds or carbides that might have a limited solubility in the metal phase. The low barium content also makes unimportant the contribution of double-neutron captures on ^{138}Ba to the ^{140}Ba that we attribute to fission.

In conclusion, we should like to acknowledge our debt to Prof. H. C. Urey for originally suggesting this investigation and for supplying the samples. We should like, also, to thank Prof. Nathan Sugarman for many discussions on problems connected with neutron activation, and Dr. Irving J. Russell for suggestions related to radiochemical procedures.

References

Arrol W. J., Jacobi R. B. and Paneth F. A. (1942) *Nature, Lond.* **149,** 235.
Bauer C. A. (1947) *Phys. Rev.* **72,** 354.
Begemann F., Geiss J. and Hess D. C. (1957) *Phys. Rev.* **107,** 540.
Chackett K. F., Reasbeck P. and Wilson E. J. (1953) *Geochim. et Cosmochim. Acta* **3,** 261.
Dalton J. C. and Thomson S. J. (1954) *Geochim. et Cosmochim. Acta* **5,** 74.
Dalton J. C., Golden J., Martin G. R., Mercer E. R. and Thomson S. J. (1953) *Geochim. et Cosmochim. Acta* **3,** 272.
Dalton J. C., Paneth F. A., Reasbeck P., Thomson S. J. and Mayne K. I. (1953) *Nature, Lond.* **172,** 1168.
Davis G. L. (1950) *Amer. J. Sci.* **248,** 107.
Deutsch S., Houtermans F. G. and Picciotto E. E. (1956) *Geochim. et Cosmochim. Acta* **10,** 166.
Gentner W. and Zähringer F. (1957) *Geochim. et Cosmochim. Acta* **11,** 60.
Hamaguchi H., Reed G. W. and Turkevich A. (1957) *Geochim. et Cosmochim. Acta* **12,** 337.
Mahlman H. A. and Leddicote G. W. (1955) *Analyt. Chem.* **27,** 823.
Mayne K. I., Reasbeck P. and Paneth F. A. (1952) *Geochim. et Cosmochim. Acta* **2,** 300.
Peppard D. F., Maier J. L., Mason G. W. and Moline, S. W. (1957) *The Isolation of Np as a Mono-octyl Phosphoric Acid Complex by Liquid-Liqiud Extraction.* Talk presented at the American Nuclear Society Meeting, Pittsburgh.
Reasbeck P. and Mayne K. I. (1955) *Nature, Lond.* **176,** 186.
Reed G. W. and Turkevich A. (1955) *Nature, Lond.* **176,** 794.
Smales A. A. (1952) *Analyst* **77,** 778.
Starik I. E. and Shats M. M. (1956) *Dokl. Akad. Nauk SSSR* **2,** 20.
Urey, H. C. (1955) *Nature, Lond.* **175,** 321.

Geochimica et Cosmochimica Acta, 1958, Vol. 13, pp. 256 to 259. Pergamon Press Ltd., London

Retention of lead during oxidative ashing of selected naturally occurring carbonaceous substances*

Frank Cuttitta and Jesse J. Warr, Jr.
U.S. Geological Survey, Washington 25, D.C.

(*Received* 10 *September* 1957)

Abstract—The amount of lead retained in the ash of lead-bearing carbonaceous material is essentially independent of the method of ashing. Samples containing lead in the range of 0·00*X* to 0·*X* per cent were ashed by ignition in a high-oxygen atmosphere and were also wet-ashed. The lead in the ash was determined colorimetrically. Results were the same by both methods, but the time required is 3 to 10 times less for the dry-ashing method.

Introduction

The determination of geologic age by the lead–uranium or lead–lead methods is based on a knowledge of the $^{206}Pb/^{238}U$, $^{207}Pb/^{235}U$, and $^{207}Pb/^{206}Pb$ ratios. Errors in the chemical analyses for lead and uranium introduce uncertainties in the computed age. In the quantitative isolation of milligram and submilligram amounts of lead from large amounts of mineral sample, special care must be exercised to prevent loss of lead.

The isolation or the determination of lead in carbonaceous substances generally includes an oxidative ashing step. Previous experience indicates that lead may be lost by volatilization of elemental lead resulting from reduction by the large organic content of the ores during the ashing process (Vogel, 1951). As there are few or no data regarding the loss of lead from carbonaceous substances during ashing, it was considered necessary to investigate the effects of oxidative ashing on the lead associated with selected uranium-bearing carbonaceous substances. To do this, comparison was made of the lead contents determined by dry ashing in a high-oxygen atmosphere, and by wet-ashing techniques (Kahane, 1934; Smith, 1934, 1953; Smith and Sullivan, 1935) that would preclude loss of lead through volatilization.

The samples selected for this study were chosen from a series submitted for age determinations. Among the substances are coals, "asphaltites", woody extracts, and uraninites with admixed organic material. Data for samples containing lead in the range of 0·00*X* to 0·*X* per cent, determined by both wet and dry techniques, are summarized in Table 1.

Experimental Methods

Dry ashing (*direct combustion in high-oxygen atmosphere*)

Samples weighing about 0·2 g were placed in a porcelain boat in a tubular furnace. The furnace temperature was gradually raised to 550°–600°C and maintained there until all visible evidences of organic matter were gone. Then the temperature was slowly raised to 800°C and the heating was continued until

* Publication authorized by the Director, U.S. Geological Survey.

Table 1. Results of lead determinations

Sample no.	Nature of material	Lead (per cent)		Calculated age (millions of years)	
		Dry ashing	Wet ashing	Dry ashing	Wet ashing
GS/146/55	Carbonaceous sandstone	0·024 0·026	0·023 0·022	185	175
GS/147/55	Carbonaceous sandstone	0·0066	0·006 0·006	180	170
GS/151/55	Carbonaceous uranium-vanadium ore	0·009	0·008 0·008	150	130
GS/180/55	Carbonaceous uranium ore	0·069 0·066	0·061 0·062	150	140
GS/182/55	Carbonaceous sandstone	0·13 0·13	0·11	85	75
GS/375/55	Carbonaceous sandstone	0·080	0·082 0·083	185	190
GS/417/55	Carbonaceous pellets	0·062 0·061	0·061	1700	1650
GS/424/55	Carbonaceous pellets	0·078 0·079	0·083 0·083	*	*
GS/445/55	Admixture of carbonaceous material with coffinite	0·020	0·018 0·018	*	*
GS/446/55	Admixture of carbonaceous material with coffinite	0·079	0·091	*	*

* Mass spectrometric data not available.

the sample reached constant weight. Length of time for attaining constant weight depends upon the actual carbon content, the kind of organic constituents, and the nature of the sample being ignited. The quartz combustion tube was continually swept free of combustion products by a mixture 1 part air and 2 parts oxygen at the rate of 5 ml/min (5 lb/in^2 pressure). The cooled residue was quantitatively transferred to a platinum dish and dissolved with HF : HNO_3 (1 : 3 to 1 : 4 v/v). The amount of acids used varied with the ash content of the ignited

samples. However, in all cases an identical reagent blank was carried through the procedure. The HF and HNO_3 were made lead-free by distillation in platinum and in glass, respectively. The lead content was determined colorimetrically with dithizone, as described by Sandell (1950).

Wet ashing

Samples of the carbonaceous material weighing about 0·2 g were treated in a 100 ml volumetric flask with 10 ml of 70–72 per cent $HClO_4$, 5 ml concentrated H_2SO_4, and 20 ml concentrated HNO_3 (all redistilled, lead-free reagents). The samples were digested at 125°–150°C on an electric hot-plate with condensation of vapours occurring about halfway up the neck of the flask. Decomposition required from several hours to several days for completion; digestion was stopped when the liquid became clear yellow in colour. After cooling, the solution was transferred to a 100 ml platinum dish with 1 + 1 HNO_3 solution. Ten millilitres of distilled HF was added to the solution, the digestion was continued, and the temperature was gradually raised until heavy fumes appeared in the dish. Fuming was continued to incipient dryness.

Sufficient 1 + 2 HNO_3 was added to dissolve the salts. The solution was transferred to a volumetric flask and made up to volume. The final acidity was made to 1 + 4 HNO_3. The lead content was then determined colorimetrically with dithizone as described by Sandell (1950).

Analysis of Data

To determine if a difference exists between results of the two methods of ashing, the t test for the difference between two means was used (Dixon and Massey, 1951). The t value of 0·71 which was obtained is not significant when compared to the table value of $t = 2{\cdot}04$ for 30 degrees of freedom at the 95 per cent confidence level.

The ages calculated using these lead data were compared by pairing the observations and taking differences (Youden, 1951). The average difference between the ages was not significantly different from zero at the 95 per cent confidence level.

Conclusions

There is no significant difference in the lead content of the samples determined either by the dry- or wet-ashing techniques. The time involved in the wet-ashing procedure was from three to ten times greater than that required in the dry-ashing procedure. When oxidative dry ashing of lead-bearing carbonaceous materials containing 0·00X to 0·X per cent lead is carried out in a high-oxygen atmosphere, no significant loss of lead takes place.

Acknowledgement—This work is part of a programme being conducted by the U.S. Geological Survey on behalf of the Division of Research of the U.S. Atomic Energy Commission.

References

Dixon W. J. and Massey F. J., Jr. (1951) *Introduction to Statistical Analysis* p. 102. McGraw-Hill, New York.

Kahane E. (1934) *L'action de l'Acide Perchlorique sur les Matières Organiques et ses Applications a Chimie Analytique*, Pt. 1. *Généralités*, Pt. 2. *Applications*, Hermann et Cie, Paris.

Sandell E. B. (1950) *Colorimetric Determination of Traces of Metals* (2nd Ed.) p. 392. Interscience, New York.

Smith G. F. (1934) Mixed perchloric and sulfuric acids. I. Simultaneous oxidizing and reducing properties of hot concentrated perchloric acid. *Industr. Engng. Chem.* (*Anal.*) **6,** 229–230.

Smith G. F. (1953) The wet ashing of organic matter employing hot concentrated perchloric acid. The liquid fire reaction: *Analyt. Chim. Acta* **8,** No. 4, 397–421.

Smith G. F. and Sullivan V. R. (1935) The determination of chromium in chrome tanned leather. Nitric, perchloric, and sulfuric acids as oxidant for organic matter and chromium. *Amer. Leather Chem. Ass. J.* **30,** 442–453.

Vogel A. I. (1951) *A Text Book of Quantitative Inorganic Analysis, Theory and Practice* (2nd Ed.) p. 420. Longmans, Green, London.

Youden W. J. (1951) *Statistical Methods for Chemists* p. 28. Wiley, New York.

Geochimica et Cosmochimica Acta, 1958, Vol. 13, pp. 260 to 269. Pergamon Press Ltd., London

Thorium, uranium and potassium in some sandstones

Elaine G. Murray and John A. S. Adams

(*Received* 24 *September* 1957)

Abstract—Thorium, uranium, and potassium concentrations have been determined in nineteen sands and sandstones by γ-ray spectrometry, fluorometric uranium analysis, and α-counting. The samples were selected so that both common and extreme thorium and uranium ratios would be represented.

The average and nearly uniform values found in orthoquartzitic, clay-free sands were potassium (as metal) 0·64 $\pm$ 0·04 per cent; thorium 1·7 $\pm$ 0·1 p.p.m.; and uranium 0·45 $\pm$ 0·05 p.p.m., giving a Th/U ratio of 3·8 $\pm$ 0·8. The Th/U ratio found is very near to that of average igneous rocks and may represent an independent determination of the average crustal Th/U ratio. Heavy mineral separations on some of the ordinary sands indicate that very little of the thorium, uranium, and potassium in a common sand is associated with the heavy detrital grains. Neglecting a very minor feldspar content, the radioactivity of the common sandstones studied is contained almost entirely in the quartz, where it appears to be largely related to microscopic and submicroscopic inclusions. The heavy detrital minerals do not begin to affect the Th/U ratio or concentration ratios until they occur in large quantities as in placer sands. Within experimental error, the modern beach sands studied were in radioactive equilibrium.

These preliminary data provide some independent and experimental comparisons for the average thorium and uranium content of sandstones calculated from geochemical balances. The data are also helpful in constructing models of the changes in thorium and uranium ratios that might be observed in moving from a beach line through shallow water sediments to deep-water sediments.

Introduction

Recent papers by Baranov, Ronov and Kunashova (1956) and by Adams and Weaver (1957) have provided much information about the thorium and uranium concentrations in shales and carbonate rocks. The published data, however, on sandstones are extremely limited. Adams and Weaver (1957) attempted to calculate average thorium and uranium concentrations for sandstones by means of geochemical balances. The investigation reported upon here was undertaken to explore the analytical and sampling problems involved in making an experimental verification of the sandstone values calculated from geochemical balances.

Summary of Sampling and Laboratory Procedures

The samples listed in Table 1 are of three main types: (1) a suite of samples representing the full range of modern environments on the convenient and well studied Galveston Island beach (Bullard, 1942; Shepard and Moore, 1955); (2) several individual orthoquartzites having approximately the same bulk composition as the Galveston samples; (3) three placer sand samples containing commercial or nearly commercial concentrations of heavy detrital minerals enriched in thorium and uranium.

The Galveston samples were collected along a line perpendicular to the shore line at the extreme northern end of the island in order to sample the various environments on the beach. Samples were taken at a depth of about 1 ft from the intertidal zone, the high-tide strand line, the beach ridge, and from the seaward edge of the dunes on both the Gulf and Bay side of the island. One deeper sample was taken at a depth of 18 in. from the sand over which the present beach is prograding. The other individual sands were either purchased or given for this study.

Handling and treatment of all the samples were minimized until the thorium and uranium determinations had been made. The Galveston samples were dried overnight at 90°C. Several of the lightly cemented individual samples were disaggregated by gentle grinding. Care was taken in the grinding not to break any of the individual detrital grains.

Thorium, uranium, and potassium were determined for all of the samples by means of γ-ray spectrometry before proceeding with any other work (see Table 1). This method has been described in detail by Adams, Richardson and Templeton (1957). Following the initial γ-ray determinations, the Galveston samples were sieved to remove the bulk of the shell debris they contained. Most of this shell material was retained on a 60-mesh sieve, whereas all of the sand passed an 80-mesh sieve. More than half of the samples sieved were reanalysed on the γ-ray spectrometer. The results of this reanalysis (see Table 1) indicate that the shell material had no detectable effect on the determinations. This conclusion was confirmed by fluorometric uranium determinations on the shell fractions, which showed that the uranium content of the shell material was essentially the same as that found in the original sample. All the fluorometric uranium determinations in this study were made according to the procedures described by Adams and Maeck (1954).

Heavy mineral separations were made on the following: seven of the Galveston samples, the Berea grit, and the Ottawa, Berkshire, and Gallup sands. Because about 1 kg was required for the γ-ray determinations, standard separatory techniques were impractical. The separations were made by placing batches of 100–200 g of sample in a large evaporating dish which was partially filled with bromoform. After standing about 15 min, the "light" fraction was ladled into another evaporating dish, where the procedure was repeated. After the second separation the "light" fraction was transferred to a Buchner funnel, where the bromoform was removed by suction and washing with acetone. After the "heavy" fraction was concentrated, a final separation was made in a separatory funnel. This procedure has been described more fully by Hutton (1950) and by Larsen, Keevil and Harrison (1952). The efficiency of the above procedure was tested against a procedure in which the sample was centrifuged in bromoform in batches of about 40 g. It was found that the evaporating-dish procedure separated about 85 per cent of the "heavy" mineral weight recovered by centrifugation. The "light" sand fraction of more than half of the samples from which the "heavy" minerals were separated were again measured on the gamma-ray spectrometer (see Table 1).

Fluorometric uranium determinations and α-activity counts were made on several of the separates and the Th/U ratio calculated from these data (see Table 1). The Th/U ratios so calculated agree well with those determined by γ-ray spectrometry and establish that the samples are in radioactive equilibrium to within experimental error (Adams, Richardson and Templeton, 1957).

Grain counts were made of the heavy mineral separates and the minerals were identified (Tables 2 and 3). The results of the grain counts of the Galveston suite showed little difference from those reported by Bullard (1942). Thus the Galveston suite is remarkably uniform over the range of environments studied.

The Ottawa and Berkshire sand samples were devoid of any recoverable heavy-mineral suite. A few grains of quartz cemented with iron oxide were all that settled in the bromoform.

Discussion of Results

The data in Table 1 are particularly noteworthy for the rather uniform and low thorium and uranium concentrations found in the ordinary orthoquartzites studied. Excluding the three placer-sand samples, the average thorium is 1·7 ± 0·1 p.p.m., the average uranium is 0·45 ± 0·05 p.p.m., and the average Th/U ratio is 3·8 ± 0·8. All of the uranium and thorium values are well within a factor of three of these average values; all the Th/U ratios are within a factor of 2 of the average. It is believed that this uniformity is due to: (1) the fact that each kilogram of orthoquartzite sample is a rather well-mixed and representative sample of average terrestrial quartz; and (2) the thorium and uranium in these common orthoquartzites is contained almost entirely in this average quartz with the heavy detrital grains like zircon and monazite making only a very minor contribution. The evidence for the minor contribution of minerals like zircon and monazite to the total thorium and uranium in a common orthoquartzite is

Table 1. Summary of data

Sample no.	Formation or locality	Fluorometric uranium (p.p.m.)		α-counts/hr* (sand)†	Th/U by $\alpha cph/U_f$ (sand)†
		Sands†	Shells		
EM-1	Galveston Island	0·4	0·33	13 ± 6	3·9 ± 0·8
EM-2	Galveston Island	0·35	0·46		
EM-3	Galveston Island	0·37	0·41		
EM-4	Galveston Island	0·29	0·30		
EM-5	Galveston Island	0·23	0·23		
EM-6	Galveston Island	0·41	0·20		
EM-7	Galveston Island	0·32	0·29		
EM-8	Galveston Island	0·36	0·23	18 ± 4·5	4·9 ± 1·0
EM-9	Galveston Island	0·29	0·12		
EM-10	Galveston Island	0·26	0·14		
EM-11	Ottawa (St. Peter)	0·18		7 ± 1	4·4 ± 1·0
EM-12	Berkshire (Cheshire)	0·19			
EM-13	Berea	0·55			
EM-14	Roubidoux	0·37		8·3 ± 1·5	2·0 ± 0·4
EM-15	St. Peter	0·35		8·4 ± 1·5	5·9 ± 1·2
EM-16	Placer Co., Calif.				
EM-17	Florida beach				
EM-18	Gallup				
EM-19	Ottawa (finely ground)	0·38			

* All α-counts are given in terms of α-counts/hr per 20·2 cm².
† After shells removed by sieving and heavy minerals removed with bromoform.

Table 1—(*continued*)—Summary of data

Sample no.	γ-ray Spectrometry*											
	Total sample				Shells removed				Shells and heavy minerals removed			
	Th/U	p.p.m. Th	p.p.m. U	%K	Th/U	p.p.m. Th	p.p.m. U	%K	Th/U	p.p.m. Th	p.p.m. U	%K
EM–1	3·8 ± 0·3	2·0 ± 0·1	0·5 ± 0·03	1·0 ± 0·1	4·4 ± 0·7	1·9 ± 0·1	0·43 ± 0·06	1·08 ± 0·04	3·9 ± 0·6	1·8 ± 0·1	0·46 ± 0·06	0·98 ± 0·04
EM-2	5·2 ± 0·7	2·2 ± 0·1	0·4 ± 0·05	1·1 ± 0·04	3·5 ± 0·3	2·1 ± 0·1	0·60 ± 0·05	1·1 ± 0·04	4·2 ± 0·5	1·9 ± 0·1	0·45 ± 0·05	1·05 ± 0·04
EM-3	3·1 ± 0·3	2·0 ± 0·1	0·64 ± 0·05	1·0 ± 0·04	3·6 ± 0·4	2·0 ± 0·1	0·55 ± 0·06	1·1 ± 0·04	4·0 ± 0·4	1·9 ± 0·1	0·48 ± 0·04	1·1 ± 0·04
EM-4	3·8 ± 0·4	1·8 ± 0·1	0·48 ± 0·05	1·0 ± 0·04	4·5 ± 0·6	2·1 ± 0·1	0·47 ± 0·06	1·0 ± 0·04	3·4 ± 0·3	1·9 ± 0·1	0·56 ± 0·04	0·95 ± 0·04
EM-5	3·0 ± 0·3	1·8 ± 0·1	0·61 ± 0·05	1·0 ± 0·04	3·8 ± 0·4	2·1 ± 0·1	0·56 ± 0·05	0·92 ± 0·03	4·3 ± 0·8	1·6 ± 0·1	0·37 ± 0·06	0·94 ± 0·04
EM-6	3·1 ± 0·4	1·6 ± 0·1	0·52 ± 0·06	1·0 ± 0·04					4·2 ± 0·6	1·8 ± 0·1	0·43 ± 0·06	1·01 ± 0·04
EM-7	2·6 ± 0·2	1·5 ± 0·1	0·58 ± 0·04	0·77 ± 0·03								
EM-8	4·7 ± 0·6	2·0 ± 0·1	0·43 ± 0·05	0·87 ± 0·03								
EM-9	6·5 ± 1·1	2·0 ± 0·1	0·31 ± 0·05	0·84 ± 0·03	5·4 ± 0·8	2·0 ± 0·1	0·37 ± 0·05	0·85 ± 0·03				
EM-10	3·7 ± 0·4	1·9 ± 0 1	0·52 ± 0·05	0·86 ± 0·03								
EM-11	5·4 ± 1·6	0·81 ± 0·09	0·15 ± 0·04	0·01 ± 0·01								
EM-12	4·0 ± 3·5	0·8 ± 0·1	0·2 ± 0·1	0·01 ± 0·01								
EM-13	3·6 ± 0·4	4·0 ± 0·2	1·1 ± 0·1	0·57 ± 0·03								
EM-14	1·8 ± 0·3	0·67 ± 0·1	0·38 ± 0·02	0·08 ± 0·01								
EM-15	5·8 ± 1·9	0·93 ± 0·1	0·16 ± 0·05	0·08 ± 0·1								
EM-16	0·86 ± 0·05	24·6 ± 1·1	28·5 ± 0·8	0·55 ± 0·17								
EM-17	2·1 ± 0·1	159·8 ± 2·9	74·6 ± 1·6	0·5 ± 0·3								
EM-18	7·3 ± 0·3	362 ± 6	50 ± 2	1·7 ± 0·4								
EM-19	4·4 ± 0·9	1·2 ± 0·1	0·27 ± 0·05	0·02 ± 0·01								

* Error estimates are based on counting statistics alone.

Table 2. Mineral percentages in heavy mineral in separates from the Galveston Island sands

Mineral	Sample number						
	1	2	3	4	5	6	7
Apatite	1	2	1	–	tr	2	1
Augite	3	1	4	2	5	4	6
Basaltic hornblende	8	10	9	9	11	10	7
Biotite	–	tr	1	1	1	1	2
Enstatite	3	1	1	1	1	tr	4
Epidote	9	11	10	7	9	8	9
Garnet	3	5	5	2	6	8	3
Hornblende	15	15	19	15	16	8	16
Hypersthene	3	6	3	2	5	–	3
Kyanite	–	2	tr	–	–	1	–
Limonite	–	–	1	–	–	–	–
Monazite	1	3	5	8	3	6	6
Opaque black	30	26	26	34	34	32	30
Rutile	1	tr	1	1	tr	tr	–
Staurolite	tr	5	2	tr	–	4	–
Titanite	4	tr	2	tr	tr	–	2
Tourmaline	4	7	3	10	5	3	7
Zircon	15	6	7	8	4	13	4
Zoisite	–	1	–	–	–	–	–

Table 3. Mineral percentages in heavy mineral separates

Mineral	Florida	Gallup		Berea
		125 μ	<125 μ	
Anatase			3	
Andalusite	tr			
Apatite				1
Brookite			14	
Epidote	1			
Garnet	4	5	2	
Ilmenite	44	88	65	
Monazite	10		7	6
Opaque		1		54
Rutile	17		1	
Tourmaline	1			8
Zircon	13	6	8	31

as follows: (a) there was no detectable change in the thorium and uranium concentration after the heavy minerals had been separated from the quartz (see Table 1); (b) after removal of the heavy minerals, very small sub-samples of 1 g for the fluorometric uranium determination and about 0·2 g for the α-activity measurement showed no variation in thorium and uranium content from the

bulk sample (see Table 1); (c) the heavy minerals separated constituted less than 1 per cent by weight of the total sample, the average being 0·23 per cent; (d) of these heavy minerals, the minerals known to contain unusually high amounts of thorium and uranium were only a minor constituent (see Tables 2 and 3); (e) the available evidence (Merlin *et al.*, 1957) indicates that the few per cent of feldspar in some of the samples are not likely to have markedly more thorium and uranium than the quartz; (f) in sands where the contribution of heavy detrital minerals is known to be important, namely the placer sands like those discussed below, the Th/U ratio varies widely due to differences in the relative contributions of low Th/U ratio minerals like zircon and high Th/U ratio minerals like monazite.

Granted that the average Th/U ratio of the common orthoquartzites studied is really the average Th/U ratio of common quartz, it is interesting to note that this average ratio of 3·8 ± 0·8 is very similar to the average Th/U ratio of 3 to 4 found in igneous rocks (Evans and Goodman, 1941; Senftle and Keevil, 1947). It is quite possible that the Th/U ratio determinations reported in this paper represent an independent confirmation of the over-all crustal Th/U ratio indicated by average igneous rocks. This possibility is suggested by: (1) the autoradiographic evidence of Coppens (1950) and Merlin *et al.* (1957) that much of the radioactivity in igneous quartz is contained in inclusions; (2) the crystal chemical consideration that the valences and sizes of thorium and uranium are such that it is unlikely that they would be contained in quartz by isomorphic substitution. Thus it is quite possible that the thorium and uranium accidently included in quartz from a wide variety of sources would represent a good random sampling of the relative average crustal abundance of thorium and uranium, namely a Th/U ratio of 3 to 4. Of course, quartz that was from a single or extremely differentiated source, e.g. a pegmatite, might have a very uncommon Th/U ratio. The orthoquartzites, however, are well-mixed samples of quartz from many sources, and they do show a Th/U ratio very close to the overall crustal average.

The three placer-sand samples listed in Table 1 indicate some of the range in Th/U ratios that may be found in sands where most of the thorium and uranium is contained in the heavy-mineral suite. The concentrate from the Florida beach sand placer has a thorium content of 160 ± 2·9 p.p.m. and a uranium content of 74 ± 1·9 p.p.m. This gives a Th/U ratio of 2·1 ± 0·1, which is about half of the ratio found in the orthoquartzites studied. Although thorium is strongly concentrated in this sample, uranium is concentrated even more. Because monazite and zircon are the major carriers of thorium and uranium in this sample, it is believed that the Th/U ratio found in the sample is a result of the relative amounts of these two minerals. The relative amounts of thorium and uranium to be expected in these two minerals are indicated by some values drawn from the literature and presented in Table 4. Taking the average values in Table 4, the Th/U ratio found in the Florida sample could be explained by having the high thorium, high Th/U ratio of the monazite somewhat overcompensated by much more abundant low Th/U ratio zircon. The effect of zircon is clearer in the zircon sand from Placer Co., California. This sand has a thorium content of 24 ± 1·1 p.p.m. and a uranium content of 28·5 ± 0·8 p.p.m. giving a Th/U ratio of 0·86 ± 0·05. Zircon is by far the dominant carrier of thorium and uranium in this sample and

the Th/U ratio is in very good agreement with the zircon values quoted in Table 4. By contrast, the Th/U ratio of 7·3 ± 0·3 found in the Gallup sandstone is largely due to monazite. An autoradiograph of a thin section of this sample showed that the greater part of the α-radioactivity was from monazite grains,

Table 4. Thorium, uranium and Th/U in zircon and monazite

	p.p.m. U	p.p.m. Th	Th/U	
Zircon	1433	673	0·46	average of 21[a]
	1060	177	0·17	average of 5[b]
			0·2–0·6	range in granites[c]
Monazite	2054	76550	37·3	average of 20[d]
	6800	164500	24·2	1[e]
	2286	75275	32·9	average of 4[f]

[a] Webber, Hurley and Fairbairn (1956)
[b] Faul, (1954)
[c] Hurley and Fairbairn (1955)
[d] Holmes (1948)
[e] Holmes, Leland, Nier and Smales (1949)
[f] Tilton and Nicolaysen (1957)

the zircons being markedly less important. Some of the activity is also associated with the silt and clay size fractions of the Gallup sandstone. Allen (1956) and Chenoweth (1956) have studied the radioactivity of the Gallup formation, and our sample was provided through the courtesy of Allen.

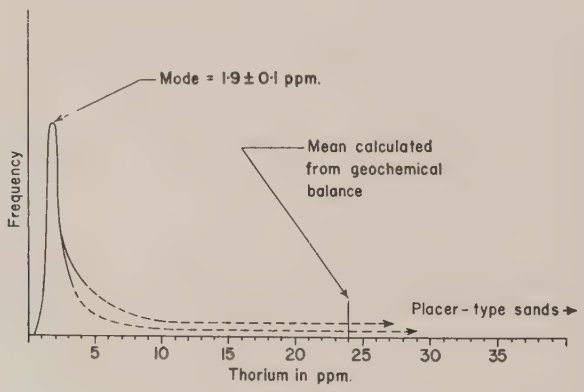

Fig. 1. Schematic frequency diagrams of thorium in sandstones.

The data discussed above indicate that it will be very difficult to determine the average thorium and uranium content of sandstones by the analysis of individual sand samples, because it will be difficult to know what statistical weight to give the common orthoquartzites and what statistical weight to give the relatively uncommon, but high thorium and uranium placer sands. The difficulty is shown schematically in the frequency curve for thorium in Fig. 1, where the average

thorium content of the common orthoquartzites studied is indicated as the mode or most frequent value and where two possible curves for the asymmetrical effect of the placer sands are dashed in. Assuming that both dashed curves extend equally far to the right, the upper dashed curve will indicate a higher average or mean value than the lower. In either case the mean value will be somewhere to

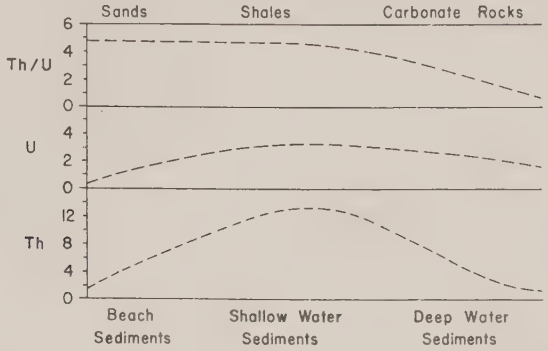

Fig. 2. Schematic diagram of Th, U and Th/U variation across an ideal basin of sedimentation.

the right of the mode. It will take a large number of determinations on carefully sampled sandstones to determine the shape of this very asymmetrical frequency curve. The theoretical mean thorium content of 24 $\pm$ 7 for sandstones calculated from a geochemical balance by Adams and Weaver (1957) is also shown in Fig. 1. The calculation of this theoretical mean is subject to a number of errors, particularly regarding the relative amounts of shale, limestone, graywacke, and orthoquartzites. At present it can only be concluded that the mean thorium content of sandstones can only be estimated to an order of magnitude, namely between about 2 and 24 p.p.m. Similar difficulties affect any estimate of the mean uranium content.

Using the scanty data then available, several previous authors (Beers and Goodman, 1944; Koczy, 1949a) have suggested relationships between the Th/U of sedimentary rocks and the position of those rocks in a sedimentary basin. Koczy (1949a), following Pettersson and others, suggested that, since thorium is relatively insoluble, most thorium enters the ocean in detrital minerals that accumulate in sandstones in a near-shore environment. Koczy (1949b) also suggested several near-shore chemical mechanisms for the fixation of any thorium that might be in solution. The results of this study, together with the work of Adams and Weaver (1957), do not confirm a high concentration of thorium in the near-shore sands and sediments. Instead, the maximum thorium content is found in shales in the general case, which is schematically given in Fig, 2. Fig. 2 also shows the variation of uranium and the Th/U ratio as a function of distance from shore in the ideal case. The scales along the ordinate are based upon over-all averages from this study and Adams and Weaver (1957). Mixtures of sandy shales or shaley limestones would be expected to have intermediate values in many cases; Adams and Weaver (1957) showed how the amount of shale in limestone could be estimated by the amount of thorium present. In actual basins,

wide deviations may be expected, but only in cases where the sand is of a placer type will the thorium concentration be highest near the shore.

Conclusions

The principal conclusions of this study are:

(1) The thorium and uranium in many common orthoquartzites are contained almost entirely in the quartz grains; the heavy detrital minerals, like zircon and monazite, play very minor roles, except in placer sands.

(2) The quartz grains in the orthoquartzites had an average and rather uniform concentration of 1·7 $\pm$ 0·1 p.p.m. thorium and 0·45 $\pm$ 0·05 p.p.m. uranium, giving an average Th/U ratio of 3·8 $\pm$ 0·8.

(3) The average Th/U of 3·8 $\pm$ 0·8 in the common orthoquartzites studied may represent an independent determination of the overall crustal Th/U ratio.

(4) It is very difficult to estimate the average thorium and uranium content of sandstones, because the importance of placer sands is difficult to assess.

(5) The data presented here indicate that in many sedimentary basins the near-shore sand sediments are depleted in thorium and uranium relative to deeper-water shales.

Acknowledgements—Thanks are due to Dr. Charles E. Weaver of the Shell Oil Company for his interest in and assistance to this project, and to Dr. John Eliot Allen of the New Mexico Bureau of Mines for providing the sample of the Gallup sandstone.

This project was supported generously through Grant C-0009 from the Robert A. Welch Foundation.

Notes added in proof: The Gallup sandstone sample described above (EM–18) was supplied by J. E. Allen and Ming-Shan Sun, and, in their recent paper about this sandstone [*J. Sed. Pet.* **27**, 265–270 (1957)], they report that the bulk of the radioactivity is in zircon instead of in monazite as reported above. The autoradiographs and the optical identification of monazite were rechecked and, in addition, a series of single crystal X-ray diffraction photographs were made to confirm the identification. We still find that in the coarser grains (over 20 μ) the monazite is much more radioactive than the zircons present and is responsible for a greater share of the total radioactivity.

Through the courtesy of F. S. Grimaldi and others at the Trace Elements Laboratory of the U.S. Geological Survey, a Galveston beach sample (EM–1) was analysed independently for thorium by a colorimetric method and for uranium by a fluorometric procedure. These independent determinations gave 1·7 p.p.m. thorium and 0·8 p.p.m. uranium, which is well within the limits of error of the values cited above.

References

Adams J. A. S. and Maeck W. J. (1954) Fluorometric and colorometric microdetermination of uranium in rocks and minerals. *Analyt. Chem.* **26**, 1635–1639.

Adams J. A. S. and Weaver C. E. (1957) Thorium to uranium ratios as indicators of sedimentary processes: an example of the concept of geochemical facies. *Bull. Amer. Ass. Pet. Geol.* To be published.

Adams J. A. S., Richardson J. E. and Templeton C. C. (1957) Determinations of thorium and uranium in sedimentary rocks by two independent methods. *Geochim. et Cosmochim. Acta.* **13,** 282–291.

Allen J. E. (1956) Titaniferous Cretaceous beach placer in McKinley County, New Mexico (abstract). *Bull. Geol. Soc. Amer.* **67,** 1789.

Baranov V. I., Ronov A. B. and Kunashova K. G. (1956) Geochemistry of thorium and uranium in clays and carbonate rocks of the Russian Platform. *Geokhim. Izd. Akad. Nauk SSSR,* No. 3, 3–8.

Beers R. F. and Goodman C. (1944) Distribution of radioactivity in ancient sediments. *Bull. Geol. Soc. Amer.* **55,** 1229–1254.

Bullard F. M. (1942) Sources of beach and river sands on Gulf Coast of Texas. *Bull. Geol. Soc. Amer.* **53,** 1021–1044.

Chenoweth W. L. (1956) Radioactive titaniferous heavy-mineral deposits in the San Juan Basin, New Mexico and Colorado (abstract). *Bull. Geol. Soc. Amer.* **67,** 1792.

Coppens R. (1950) Étude de radioactivité de quelques roches par emulsion photographique. *Bull. Soc. franc. Minér.* **73,** 217–321.

Evans R. D. and Goodman C. (1941) Radioactivity of rocks. *Bull. Geol. Soc. Amer.* **52,** 459–490.

Faul H. (Editor) (1954) *Nuclear Geology.* Wiley, New York.

Holmes A. (1948) Monazite from Bodmin Moor. *Proc. Roy. Soc. Edinb.* B **63,** pt. 2, 115–124.

Holmes A., Leland W. T., Nier A. O. and Smales A. A. (1949) The age of uraninite and monazite from the post-Delhi pegmatite of Rajputana. *Geol. Mag.* **86,** 288–302.

Hurley P. M. and Fairbairn H. W. (1955) Ratio of thorium to uranium in zircon, sphene, and apatite (abstract). *Bull. Geol. Soc. Amer.* **66,** 1578.

Hutton C. O. (1950) Studies of heavy detrital minerals. *Bull. Geol. Soc. Amer.* **61,** 635–716.

Koczy F. F. (1949a) The thorium content of the Cambrian alum shales of Sweden. *Sverig. Geol. Unders. Arsbok* **43,** No. 7.

Koczy F. F. (1949b) Thorium in sea water and marine sediments. *Geologiska Foreningens i Stockholm Forhanlingar* **71,** No. 2, 238–242.

Larsen S. S., Jr., Keevil N. B. and Harrison H. C. (1952) Method of determining the age of igneous rocks. *Bull. Geol. Soc. Amer.* **63,** 1045–1052.

Merlin O. H., Picciotto E. and Wilgain S. (1957) Étude photographique de la distribution de la radioactivité dans la granodiorite de l'Adamelle. *Geochim. et Cosmochim. Acta* **11,** 171–188.

Senftle F. E. and Keevil N. B. (1947) Thorium/uranium ratios in the theory of genesis of lead ores. *Trans. Amer. Geophys. Un.* **28,** 732.

Shepard F. P. and Moore D. G. (1955) Central Texas Coast Sedimentation: Characteristics of sedimentary environment, recent history and diagenesis. *Bull. Amer. Ass. Pet. Geol.* **39,** 1463–1593.

Tilton G. R. and Nicolaysen L. O. (1957) The use of monazites for age determinations. *Geochim. et Cosmochim. Acta* **11,** 28–40.

Webber G. R., Hurley P. M. and Fairbairn H. W. (1956) Relative ages of eastern Massachusetts granites by total lead ratios in zircons. *Amer. J. Sci.* **254,** 574–583.

Geochimica et Cosmochimica Acta, 1958, Vol. 13, pp. 270 to 279. Pergamon Press Ltd., London

Determinations of thorium and uranium in sedimentary rocks by two independent methods*

John A. S. Adams†
The Rice Institute and Shell Development Co., Houston, Texas

Jasper E. Richardson and Charles C. Templeton
Shell Development Company, Houston, Texas

(*Received* 30 *August* 1957)

Abstract—Two independent methods for the determination of uranium and thorium-to-uranium ratios are described. One method is based upon γ-ray spectral analysis; the other is based upon total α-activity and fluorometric uranium determinations. Results and errors of measurements on 4 standard samples and 18 sedimentary rocks of various types are discussed. By applying both methods to the same sample, it is possible to determine if secular radioactive equilibrium exists to within experimental error. Where secular radioactive equilibrium exists in well-homogenized samples, both methods agree to within the experimental errors. The observed thorium-to-uranium ratio in sedimentary rocks ranges from less than 0·02 to more than 20; the two methods presented are capable of measuring this ratio to well within ± 1 over most of this range.

Introduction

The determination of thorium, uranium, or thorium-to-uranium ratios in rocks and minerals is essential for understanding the geochemistry of these elements. In such problems as radioactivity dating (Faul, 1954), the heat balance of the earth (Birch, 1954), and the rate of sedimentation (Koczy, 1954), very low concentrations of thorium and uranium must be measured in many samples. Thus rapid and accurate methods for the determination of these elements in common rocks have been widely sought (Adams, 1954, 1955; Beers and Goodman, 1944; Evans and Goodman, 1941; Larsen and Phair, 1954; Hurley, 1956; Facchini *et al.*, 1956), but more sensitive methods are still needed. The two independent methods described and compared below can determine about one part per million of thorium or uranium in common rocks. Lack of secular radioactive equilibrium can also be detected by use of both methods.

α-Activity-Fluorometric Uranium Method

If we neglect very minor natural α-emitters like ^{147}Sm, the absolute α-activity of a natural rock sample is solely a function of its thorium and uranium content and the state of the radioactive equilibrium. Thus the absolute alpha activity in α-counts/hr per unit area, αcph, can be expressed as

$$\alpha cph = \alpha_{Th} + \alpha_U \qquad (1)$$

where α_{Th} is the contribution from the ^{232}Th series and α_U is the contribution from the ^{238}U and ^{235}U series. The two uranium series can be grouped into a single term because the isotopic composition has not been found to vary in nature (Rankama, 1954). At radioactive equilibrium, the relative magnitudes of α_{Th} and α_U will depend upon the thorium-to-uranium ratio and the specific activities of the decay series involved. The measured α-activities will also depend

* Publication No. 123, Shell Development Company, Exploration and Production Research Division, Houston, Texas.

† The portion of this work done at The Rice Institute was supported by Grant No. C-009 from the Robert A. Welch Foundation.

upon the energies of the α-particles emitted, the precise sites of the α-emitting nuclides in the sample, self-absorption in the sample, and instrumental characteristics.

Autoradiographic techniques (Bowie, 1954; Guilbert and Adams, 1955; and many others) demonstrate that the α-emitting nuclides in a rock may have at least three widely different distributions: (1) concentrated in high-density accessory minerals, e.g. zircons, which may constitute much less than 0.1 per cent of the rock by volume; (2) uniformly distributed, e.g. the Chattanooga shale (Bates *et al.*, 1954); (3) concentrated as a coating or "paint" on the mineral grains (see Neuerburg, 1956, for a more detailed classification of sites). These distribution and density differences may be expected to have some effect on the measured α-activity. Although the energies of the various α-particles are known, the factors just cited may make self-absorption corrections difficult (Nogami and Hurley, 1948). To determine experimentally the maximum effects of absorption, α-emitter distribution, and instrument sensitivity, the α-activity of a wide variety of rock types was measured using thick sources.

The thick-source α-activities were measured at The Rice Institute in a commercially available proportional counter (Model PC-2B, Nuclear Measurements Corp., Indianapolis, Ind.). A proportional counter was selected for this work because it has 50 per cent more sensitivity than the scintillation counters used in previous work (Adams, 1955). Powdered rock samples were placed in a 2 in. dia. planchet with a depth of $\frac{1}{8}$ in. The sample powders varied in fineness, but all passed 100-mesh silk bolting cloth. The levelled sample surface was 20·3 cm² in area. The counting chamber was continually swept with commercial argon. The positive argon pressure in the chamber prevented any influx of oxygen and other gases that would lower the instrumental sensitivity. The degassing of certain carbonaceous black shales, e.g. sample 4, sometimes took an hour or so. The α-particle signals were recorded on a conventional binary scaler. Counting was continued until several hundred counts had been recorded. The net α-counts/hr from the 20·3 cm² sample surface are given in Table 1. The background on granulated sugar was 4 α-counts/hr or less during 24 hr counts. In every case, the total-to-background ratio and the total number of counts indicate a statistical error of less than ±20 per cent at the 90 per cent confidence level.

The uranium determinations given in Table 1 were made by the fluorometric method (Adams and Maeck, 1954). The error in these determinations is estimated at less than ±15 per cent of the amount present. The ratio of α-activity, αcph, to fluorometric uranium concentration, U_f, is a linear function of the sought thorium-to-uranium ratio:

[From equation (1)] $$\frac{\alpha cph}{U_f} = \frac{\alpha_U}{U_f} + \frac{\alpha_{Th}}{U_f} \qquad (2)$$

$$\frac{\alpha cph}{U_f} = K_1 + \frac{\alpha_{Th}}{U_f} \qquad (3)$$

$$\frac{\alpha cph}{U_f} = K_1 + K_2\,(Th/U) \qquad (4)$$

Table 1

Sample number	Formation or source	Rock type	γ-Ray spectral analysis			Fluorometric uranium (p.p.m.)	Net α-counts/hr 20·3 cm²	Ratio Th_γ/U_γ	Ratio $\alpha cph/U_f$
			U_γ (p.p.m.)	Th_γ (p.p.m.)	K_γ (%)				
1	AEC standard	Pitchblende in dunite[c]	10[a]	0[b]	—	10[a]	110	0·0	11
2	AEC standard No. 5	Carnotite	780	0[d]	—	930[a]	9340	0·0	10
3	AEC standard No. 1	Phosphate Rock	240	4	1·1	250[a]	2200	0·02	8·8
4	Chattanooga	Black shale	80	5·2	2·7	67	575	0·07	8·3
			79	6·5	2·8	72		0·08	
						65			
						74			
5	Winchell	Limestone	4·1	0·6	0·0(4)	3·6	38	0·15	11
6	Heebner	Black shale	32	9·8	2·2	27	238	0·31	8·8
						26			
						29			
						24			
7	Morrow	Limestone	1·4	1·1	0·4	1·3 1·4	16	0·79	13
8	Marble Falls	Limestone	(3·3)[e]	(2·2)[e]	(0·5)[e]			(0·6)[e]	
			3·1[f]	2·7[f]	0·5[f]			0·87[f]	
						(2·3)[e]	(41)[e]		(18)[e]
						2·7[f]	48[f]		18[f]
9	Austin chalk	Limestone	1·7	1·6	0·3	1·8	27	0·94	15
						1·8			
						1·8			
10	Austin chalk	Limestone	(1·2)[e]	(2·0)[e]	(0·5)[e]			(1·7)[e]	
			1·3[f]	1·4[f]	0·5[f]			1·1[f]	
						(1·0)[e]	(17)[e]		(17)[e]
						1·1[f]	25[f]		22[f]
11	Austin chalk	Limestone	2·4	5·1	1·7	2·1	49	2·1	23
12	Lawrence	Underclay	4·2	13	2·4	2·4[g]	101	3·1	42
13	Lawrence	Shale	4·0	13	2·0	3·8	103	3·3	27
14	Smithwick	Shale	2·4	8·7	1·6	2·4	80	3·6	35
						2·3			
						2·4			
						2·0			
						2·4			
15	Loe	Sandy shale	3·7	14	2·5	1·9[g]	143	3·8	68
						2·2[g]			
						2·1[g]			
16	Del Rio	Shale	(1·2)[e]	(11)[e]	(2·0)[e]			(9·2)[e]	
			1·8[f]	12[f]	2·0[f]			6·7[f]	
						(1·0)[e]	(54)[e]		(54)[e]
						(2·6)[e]	(82)[e]		(59)[e]
						(3·0)[h]	(96)[h]		(32)[h]
17	Point Peak	Shale	1·9	13	8·5	1·9	93	6·8	49
						2·0			
						2·1			
18	Lawrence	Red shale	1·6	13	2·9	1·6	95	8·1	59
19	Oak Hall	Bentonite	4·0	34	3·8	4·3	303	8·5	71
20	Arkansas	Bauxite	6·4	96	0·3	6·4	745	15	116
21	Surinam	Bauxite	6·1	132	0·5	6·0	1088	21·6	181
22	AEC standard	Monazite in dunite[c]	0·4[a]	10[a]	—	0·4[a]	73	25[a]	182

[a] Certificate value for standard.
[b] No thorium detected in this pitchblende.
[c] Standards made at New Brunswick Laboratory, AEC, by diluting NBS Standards No. 2670 (pitchblende) and No. 2601 (monazite) with dunite.
[d] None detected.
[e] Value rejected because of poor homogeneity.
[f] Value accepted after thorough mixing.
[g] Sample may be weathered and deficient of an equilibrium amount of uranium.
[h] Value plotted in Fig. 1, but homogenization probably not adequate.

This relationship [equation (4)] should be useful experimentally, provided that radioactive equilibrium exists and that the α-emitter sites, absorption factors, and emanation accumulation do not seriously affect the measured α-activities. To test the useful range of this method, two standards from the National Bureau of Standards (samples 1 and 22 in Table 1) were measured. Rather than make

synthetic mixtures, rocks with intermediate thorium-to-uranium ratios were selected for study (Fig. 1 and Table 1). These rocks had the advantage of exhibiting some of the variation in concentration, emanation accumulation, absorption factors, and α-emitter sites that might be encountered in geochemical studies.

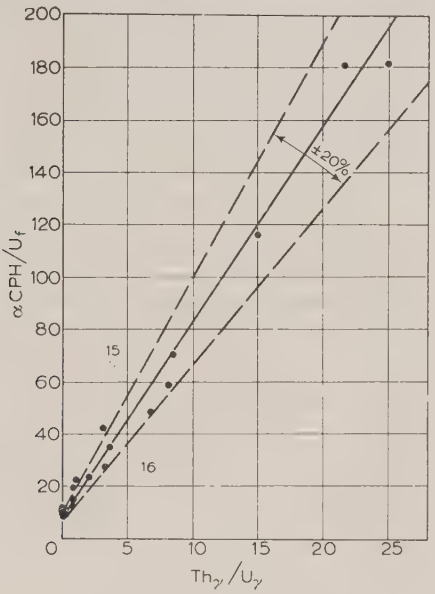

Fig. 1. $\alpha cph/U_f$ versus Th_γ /U_γ.

γ-Ray Spectral Method

For a natural rock, practically all of the γ-radiation comes from three sources: ^{40}K, the ^{238}U series, and the ^{232}Th series. The γ-rays from ^{238}U and ^{232}Th themselves are of so low an energy as to make direct measurements impractical. Where secular radioactive equilibrium prevails, the abundance of ^{238}U or ^{232}Th can be determined by measuring the activity of any daughter in the respective series. This follows from the constant ratios that exist between the concentrations of the various members of a series in an equilibrated sample. In like manner, a measurement of the ^{40}K isotope may be considered as characteristic of potassium, since the fractional abundance of this isotope has been found to be constant in nature (Rankama, 1954). Consequently, if secular equilibrium is assumed and if the γ-ray activity of a rock sample is measured at three different energies characteristic of potassium, uranium, and thorium respectively, three linear equations are available for calculating the three unknown concentrations. All necessary calibration constants can be determined from the spectra of standard samples.

Techniques of this type, capable of measuring the few parts per million of thorium and uranium present in common rocks, have been developed concurrently and independently by Hurley (1956) and by two of the present authors at the Shell Development Company. An adequate discussion of the γ-ray spectra of these elements and the most convenient means of calculating the concentrations from rock-sample measurements has been presented by Hurley.

Since the γ-rays concerned are from natural sources of low activity, it is necessary to maximize the total count-to-background ratio and to minimize instrumental drifts. This is done by using large, thallium-activated sodium iodide scintillation crystals with heavy shielding, and by stabilizing the instrumental characteristics as much as possible. Other than the shape and size of the crystal, the geometry used in the present instrument is very similar to that used by Hurley. The data presented in this paper were obtained with a $3\frac{1}{2}$ in. long by 3 in. dia., solid crystal as compared with the smaller, well-type crystal used by Hurley. The sample holders in the two instruments were essentially of the same shape, though differing in volume; about 600 g of powdered rock in the present holder compared to about 200 g in that of Hurley. For the present work, the sample filled an annular volume of about $\frac{1}{2}$ in. thickness around the lateral surface of the crystal and extended about 1 in. beyond the end of the crystal. All sample holders were sealed after being filled to prevent the loss of radon or thoron gas. The sample activity was then measured over a period of several days until no increase in activity was observed. This assured equilibrium between ^{226}Ra and ^{214}Bi, the isotope to be measured, although the equilibrium between ^{238}U and ^{226}Ra, both with very long half-lives, could only be assumed. Because of the shorter half-life of thoron, this procedure also insured equilibrium in the thorium series. The electronic equipment (photomultiplier tube, linear amplifier, single-channel pulse-height analyser, and scaler) were of conventional design.

The main difference between the two γ-ray techniques involves the choice of spectral energies. Hurley used three channels centred at the following energies: 0·180 and 0·238 MeV for uranium and thorium, and 1·46 MeV for potassium. With this choice of energies, the potassium interference at 0·180 and 0·238 MeV could be neglected only for samples containing more than 100 parts per million of equivalent uranium in equilibrium with its daughters. For the present work, higher energy γ-rays were chosen: 1·76 MeV from ^{214}Bi in the uranium series and 2·62 MeV from ^{208}Tl in the thorium series. With these energies, potassium can be ignored even when present in high concentrations, because its spectrum contributes no appreciable γ-ray pulse above 1·6 MeV. Thus, it is possible to determine the abundances of thorium and uranium from only two spectral measurements. For most rock samples the uranium contribution at 2·62 MeV can be ignored in determining thorium. Although this scheme has the advantage of less interference from higher energy γ-rays, it has the disadvantage of a lower counting rate.

Alternatively, use has been made of another choice involving three energies: 0·609 MeV from ^{214}Bi in the uranium series, 1·46 MeV from ^{40}K, and 2·62 MeV from ^{208}Tl in the thorium series. The agreement to within $\pm$15 per cent of the amount present of uranium and thorium calculated from the two choices has been a strong reason for confidence in the γ-ray method.

For calibration of the instrument, the following standards were used:

C.P. potassium chloride

NBS Sample No. 4987, 1 per cent thorium, 0·04 per cent uranium,

NBS Sample No. 4994, 0·1 per cent uranium.

The uranium contribution was subtracted from the thorium standard spectrum.

The thorium and uranium standards were available only in a quantity of 100 g. Therefore, the calibration had to be made with a geometry different from that of the rock samples. A small, flat sample holder was devised for the standards in which potassium chloride exhibited about the same specific activity as in the 600 g holder. The preservation of the spectral shapes of thorium, uranium, and potassium was confirmed with several rock samples in both geometries. These samples were chosen so as to cover a wide range of thorium-to-uranium ratios. From these measurements, a geometric correction factor of $0{\cdot}96 \pm 0{\cdot}03$ was obtained. All specific activities measured with large sample geometry were multiplied by this factor for correlation with the small sample geometry used for calibration. The effects of self-absorption in the standards and rock samples were measured and found to be the same to within the accuracy of the measurements (± 2 per cent).

Other than the errors inherent in this type of measurement and mentioned by Hurley, the results presented here are limited in accuracy by the degree of homogeneity of the standard sources and samples. Except for samples in which the thorium-to-uranium ratio is unusually high or low, the present method is believed to be accurate to within ± 15 per cent of the amount of thorium and uranium present and about ± 5 per cent of the amount of potassium present. Although greater accuracies are almost certainly attainable, the present procedure is more than sufficient for the geochemical studies now in progress.

Comparison and Discussion

In Fig. 1, the $\alpha cph/U_f$ values are plotted against the thorium-to-uranium ratios determined by γ-ray spectral analysis from the data listed in Table 1. A straight line was fitted to the solid points in Fig. 1 by the least-squares method. The equation for the straight line is:

$$\alpha cph/U_f = 7{\cdot}80 + 7{\cdot}57\ Th_\gamma/U_\gamma \qquad (5)$$

which is the experimental analogue of equation (4). The two constants are determined by the instrumentation used and are accurate to two significant figures. Nearly all of the 22 samples listed in Table 1 and plotted in Fig. 1 fall on or near the straight line, establishing for these samples: (1) the experimental usefulness of equations (4) and (5); (2) the accuracy of the two methods; and (3) as a consequence of (1) and (2), the presence of secular radioactive equilibrium for the samples near the straight line. The broken lines in Fig. 1 enclose the area within which must fall points deviating less than ± 20 per cent from the values on the straight line. Deviations of about ± 20 per cent would be the maximum expected if there were errors of about ± 10 per cent in each of the four measurements plotted in Fig. 1.* One rock sample that deviates widely from the straight

* Points that fall outside these limits are believed to represent samples that are out of secular radioactive equilibrium or poorly homogenized samples.

line is sample 15, the Loe Sandy shale. It is believed that this sample is deficient of a radioactive equilibrium amount of uranium because (1) it is an outcrop sample and some uranium may have been leached out; (2) if the γ-ray value for uranium is used instead of the fluorometric, the sample falls well within the limits of error; (3) there is no known mineralogical or chemical reason why the several fluorometric uranium determinations should be consistently low in only this sample (see Table 1). Sample 12 may also be weathered. Sample 16 is the other widely divergent point, and it is believed that this and most of the other divergencies from the straight line are caused by lack of homogeneity in the samples. A lack of homogeneity would also explain the poor reproducibility in all the measurements of sample 16 (see Table 1). It must be remembered that the γ-ray measurements require about 600 g of sample, whereas the fluorometric uranium determination uses less than 0·5 g, and the effective sample weight in the α-activity measurement is less than 0·2 g. Thus it was observed that, with the exception of the Loe Sandy shale, the samples that did not fall near the straight line were the samples with the poorest reproducibility in all the measurements, and they were the samples of heterogeneous grain size from rocks whose composition varied within a few centimetres or less (samples 8, 10, 16 in Table 1). Conversely, those samples that fell on or near the straight line were those with the most reproducible measurements and those with uniformly fine grains from homogeneous rocks (samples 4, 6, 9, 14, 19 in Table 1). In this connection it should be noted that samples 1 and 22 are particularly hard to homogenize for α-counting, because sample 1 consists of 0·0022 per cent dense pitchblende in 99·9978 per cent dunite with essentially all the activity in the pitchblende. Sample 22 has 0·012 per cent monazite as the α-active material. It is concluded that if the samples are well homogenized, naturally or artificially, the self-absorption and emanation variations are small relative to statistical counting and other errors. For zircon samples, Webber *et al.* (1956) have found a similar linear relationship between total α-activity and thorium plus uranium as determined by a γ-ray spectrometer. In general, the absolute uranium values determined by the two methods agree to well within the estimated errors (see Table 1). The U_f values are generally slightly lower than the U_γ values, which is to be expected from the losses due to the extraction efficiency and quenching in the fluorometric procedure (Adams and Maeck, 1954).

Values of K_1 and K_2, intercept and slope respectively of Equation (4), were estimated by means of the equations of Nogami and Hurley (1948). Assuming a minimum detectable residual range in argon of about 1 cm, the calculated value of K_1 agrees well with the measured value, shown in Equation (5), whereas the calculated value of K_2 is about one-third of the measured value. The comparison of theory with the measurements thus indicates that the α-counter has preferential sensitivity to the thorium series. This observation was reported by Breger (1955) and was attributed to insufficient flushing of the α-counter, although higher flow rates were not actually tried. In further work with the present instrument, higher flow rates, combined with a modified chamber for more efficient flushing, showed a significant reduction in sensitivity to the thorium series. Although high sensitivity to the thorium series has shown no effect on the reproducibility of

results or the linear relationship between the two methods presented here, it has emphasized the fact that an α-chamber must be carefully designed or else calibrated with standard samples as has been done in the present work. In order to calibrate the chamber by use of theoretically calculated sensitivities, the basic assumption of the NOGAMI–HURLEY theory must be fulfilled; namely, that all daughters remain localized in the position occupied by the original parent isotope. In view of the fact that radon and thoron do not remain localized, it is doubtful whether one would ever find complete agreement between the above theory and experiment. The agreement between theory and experiment is good in cases where the Th/U ratio is low (below about 1). At higher Th/U ratios the theoretical and experimental curves diverge more markedly, with the experimental curve being more sensitive to the thorium series. However, the results reported here demonstrate that the observed α-counts can be used in estimating the true Th/U ratio in the many varieties of sedimentary rocks studied.

The $\alpha cph/U_f$ method has the advantage of requiring only about 5 g of sample compared to the 600 g of common rock sample needed for the γ-ray method. With both methods, the higher the radioactivity the lower the sample requirement, but with the present γ-ray equipment, rarely can measurements be made on less than 50 g of sample. The $\alpha cph/U_f$ method is somewhat more sensitive; a measurement has been obtained on a limestone containing less than 0·1 part per million thorium and uranium. The γ-ray method permits a satisfactory measurement on samples containing more than about one part per million thorium and one part per million uranium. To date the $\alpha cph/U_f$ method has proved about 50 per cent faster, although more manipulative time is required for the fluorometric uranium determinations. The γ-ray method has the advantage that absorption, distribution of emitters, and emanation accumulation are less formidable problems. However, the good agreement between the two methods on such a variety of rock types demonstrates that the thick-source α-procedure is widely applicable, despite variations in the distribution of α-emitters, absorption factors, and the production of emanation from the interior of the thick source (BREGER, 1955; PICCIOTTO and SALVETTI, 1956).

Provided that the above concentration minima are exceeded and that there is secular radioactive equilibrium, either method should determine the thorium-to-uranium ratio to within less than ±20 per cent where the ratio exceeds 3. There is less accuracy with ratios below 1. Fortunately, the concentration minima are exceeded in nearly all rocks and the thorium-to-uranium ratio in the cosmos and in the earth averages about 3, with the terrestrial ratios varying widely (Fig. 1). Thus the working range is of use in many geochemical and geological problems and the accuracy of the measurements exceeds the sampling accuracy in many cases. The geologic discussion of these and other samples will be published elsewhere.

Acknowledgements—Mr. W. R. ORR, Shell Development Company, constructed or obtained all the electronic units of the γ-ray spectral analysis equipment. The laboratory assistance of Mrs. C. M. WADE, Shell Development Company, and Mr. R. PLILER and Mrs. H. JOHNSTON of the Rice Institute is acknowledged.

The work at The Rice Institute is part of a project on the geochemistry of thorium supported through the generosity of the Robert A. Welch Foundation.

Note added in proof: After the manuscript of this paper had been accepted for publication, several of the samples therein described were analysed independently for thorium (colorimetrically) and uranium (fluorometrically) by the Trace Elements Laboratory of the United States Geological Survey. These independent results are given below and it is gratifying that over 80 per cent of the values agree with those given above to within the cited limits of error. Space and the fact that this inter-laboratory calibration is only in a preliminary stage do not permit a more extended discussion at this time. The authors wish to thank E. S. Larsen, 3rd, F. S. Grimaldi and the staff of the Trace Elements Laboratory for the interesting results given below.

Sample	Thorium in p.p.m.	Uranium in p.p.m.
Chattanooga Black Shale	8·2, 8·1	74·0, 78·0
Heebner Black Shale	8·8, 8·9	34·5, 34·0
Lawrence Red Shale	11·7, 10·6	3·0, 2·7
Leo Sandy Shale	14·0, 13·4	5·2, 4·6
Arkansas Bauxite, RP–114	79·4, 79·8	7·0, 6·6
Surinam Bauxite, RP–113	130	

References

Adams J. A. S. (1954) Uranium and thorium contents of volcanic rocks. Chap. 2.2, *Nuclear Geology* (Edited by Henry Faul). Wiley, New York.

Adams J. A. S. (1955) The uranium geochemistry of Lassen Volcanic National Park, California. *Geochim. et Cosmochim. Acta* **8,** 74–85.

Adams J. A. S. and Maeck W. J. (1954) Fluorometric and colorimetric microdetermination of uranium in rocks and minerals. *Analyt. Chem.* **26,** 1635–1639.

Bates T. F. *et al.* (1954) Mineralogy and petrology of the Chattanooga Shale (abstract). *Bull. Geol. Soc. Amer.* **65,** 1230.

Beers R. F. and Goodman C. (1944) Distribution of radioactivity in ancient sediments. *Bull. Geol. Soc. Amer.* **55,** 1229–1253.

Birch F. (1954) Heat from radioactivity. Chap. 5, *Nuclear Geology* (Edited by Henry Faul). Wiley, New York.

Bowie S. H. U. (1954) Nuclear emulsion techniques. Chap. 1.15, *Nuclear Geology* (Edited by Henry Faul). Wiley, New York.

Breger I. A. (1955) Radioactive equilibrium in ancient marine sediments. *Geochim. et Cosmochim. Acta* **8,** 63–73.

Evans R. D. and Goodman C. (1941) Radioactivity of rocks. *Bull. Geol. Soc. Amer.* **52,** 459–490.

Facchini U., Forte M., Malvicini A. and Rossini T. (1956) Analysis of uranium and thorium minerals by α-spectrum. *Nucleonics* **14,** 126–131.

Faul H. (Editor) (1954) *Nuclear Geology.* Wiley, New York.

Guilbert J. M. and Adams J. A. S. (1955) α-particle autoradiography with liquid emulsions. *Nucleonics* **13,** 43.

Hurley P. M. (1956) Direct radiometric measurement by γ-Ray scintillation spectrometer. Part I and II, *Bull. Geol. Soc. Amer.* **67,** 395–412.

Koczy F. F. (1954) Chap. 2.4c, *Nuclear Geology* (Edited by Henry Faul). Wiley, New York.

Larsen E. S., Jr. and Phair G. (1954) The distribution of uranium and thorium in igneous rocks. Chap. 2.1, *Nuclear Geology* (Edited by Henry Faul). Wiley, New York.

Neuerburg G. J. (1956) Uranium in igneous rocks in the United States of America. P/16, *Peaceful Uses of Atomic Energy* **6,** 231–239. United Nations, New York.

Nogami H. H. and Hurley P. M. (1948) The absorption factor in counting α-rays from thick mineral sources. *Trans. Amer. Geophys. Un.* **29,** 335–340.

Picciotto E. and Salvetti F. (1956) Comptage d'α à bass temperature; une méthode pour éviter la diffusion du radon. *Il Nuovo Cimento, Serie X* **3,** 815–819.

Rankama K. (1954) *Isotope Geology.* McGraw-Hill, New York.

Webber G. R., Hurley, P. M. and Fairbairn H. W. (1956) Relative ages of Eastern Massachusetts granites by total lead ratios in zircons. *Amer. J. Sci.* **254,** 574–583.

Geochimica et Cosmochimica Acta, 1958, Vol. 13, pp. 280 to 292. Pergamon Press Ltd., London

Inert gases and the evolution of the atmosphere*

Paul E. Damon† and J. Laurence Kulp
Lamont Geological Observatory (Columbia University), Palisades, New York

(*Received* 12 *July* 1957)

Abstract.—The origin of the present isotopic composition of the inert gases in the atmosphere is reviewed. Using new data on the maximum rate of tritium, and hence ^{3}He, production in the atmosphere, the present rate of escape of ^{4}He and ^{40}A from the crust can be calculated. It is found that this rate is far too small to account for the quantity of ^{40}A in the atmosphere and that most of the ^{40}A presumably accompanied by some nitrogen and water was introduced into the atmosphere in the first billion years of earth history from the mantle and crust.

Introduction

Since the demonstration that the inert gases were preferentially lost during earth formation (Brown, 1949) and the recognition that most of the ^{40}A in the atmosphere must be due to ^{40}K decay followed by outgassing (von Weizsäcker, 1937; Brown, 1949), a number of authors have attempted to define the evolution of the atmosphere and hydrosphere (Tatel, 1950; Kulp, 1951; Birch, 1951; Rubey, 1951; Urey, 1951; Barth, 1952; Rankama, 1954; Poldervaart, 1955; Shilliber and Russell, 1955). These authors differed considerably on the relative contributions of the mantle and the crust, the total quantities involved, and the time pattern.

A number of factors make it possible to define atmospheric evolution with greater certainty. These include a more precise knowledge of the decay constants of ^{40}K (Wetherill *et al.*, 1956 geological limits; Damon and Kulp, 1957a review of data; Wetherill, 1957 new gamma measurement), the new work on the rate of formation of tritium and hence ^{3}He in the atmosphere (Begemann and Libby, 1956; Giletti *et al.*, 1957) and increased knowledge of the retention of helium and argon in minerals and rocks (Wetherill *et al.*, 1955; Wasserburg and Hayden, 1955; Reynolds, 1957; Carr and Kulp, 1957; Damon and Kulp, 1957b; Goldich *et al.*, 1957).

It is the purpose of this paper to evaluate the present rate of degassing of the inert gases, primarily helium and argon, and from this to draw conclusions concerning the evolution of the atmosphere. After reviewing the factors which have produced the present isotopic composition of the inert gases, the present rate of degassing is computed by using the production rate of tritium to obtain the ^{3}He production rate and hence the half-life for ^{3}He escape.‡ This rate permits calculation of the average effective temperature of the base of the exosphere and thus the ^{4}He escape rate from the atmosphere to space may be obtained. This, in turn,

---

* Lamont Geological Observatory No. 277.
† Present address: University of Arizona, Tucson, Arizona.
‡ This calculation was first suggested by Libby (1953).

determines the leak rate of helium and argon from the lithosphere into the atmosphere. Finally, the present leak rate of ^{40}A will be compared with the total amount of ^{40}A in the atmosphere and with the production rate in the crust and mantle during earth history.

Isotopic Composition of the Inert Gases in the Atmosphere

The present composition of the terrestrial inert gases (Hollander *et al.*, 1953) has been derived from several sources: the primeval gas captured and retained by the earth at the time of its formation, atoms formed subsequently by radioactive decay, loss to and gain from outer space, fission, cosmic radiation, and natural terrestrial nuclear reactions.

The modification as a result of radioactive decay is best shown by the unusually high abundance of ^{40}A in the atmosphere (Table 1). It was, in fact, this phenomenon which led von Weizsäcker (1937) to predict that ^{40}A was the product of

Table 1. Cosmic and atmosphere abundances of the inert gases and the atmospheric balance

Species	Cosmic abundance in atoms per 10,000 Si (Suess and Urey, 1956)	Number of atoms in atmosphere now (Rankama and Sahama, 1950)	Cosmos earth (Brown, 1947)	Probable ($T - 1/2$) for escape from atmosphere in years (this paper)	Probable rate of entry into atmosphere now in atoms/year (this paper)
Helium-3		$6{\cdot}4 \times 10^{32}$		$1{\cdot}4 \times 10^{6}$	$3{\cdot}1 \times 10^{26}$
Helium-4		$5{\cdot}29 \times 10^{38}$		5×10^{7}	7×10^{30}
Neon	86,000	$1{\cdot}96 \times 10^{39}$	10^{10}	very long	
Argon	1,500	$9{\cdot}85 \times 10^{41}$	10^{8}	very long	$1{\cdot}5 \times 10^{30}$
Krypton	0·51	$1{\cdot}02 \times 10^{38}$	10^{7}	very long	
Xenon	0·04	$8{\cdot}14 \times 10^{36}$	10^{6}	very long	

the K-capture decay of ^{40}K. It was not until six years later that Thompson and Rowlands (1943) demonstrated that the decay of ^{40}K involved ^{40}A, confirming the prediction. Atmospheric argon is 99·6 per cent pure ^{40}A, whereas the cosmic abundance of ^{36}A (from extrapolation of isotope abundance curves) is probably equal to or greater than that for ^{40}A (Suess, 1949). The major part of the ^{38}A in the atmosphere is probably of primordial origin, but Fleming and Thode (1953) have demonstrated the existence of naturally occurring nuclear reactions in pitchblende which produce this isotope, such as $^{35}\mathrm{Cl}(\alpha, p)^{38}\mathrm{A}$ and, $^{35}\mathrm{Cl}(\alpha, n)^{38}\mathrm{K} \xrightarrow{\beta+} {}^{38}\mathrm{A}$ and $^{41}\mathrm{K}(n, \alpha)^{38}\mathrm{Cl} \rightarrow {}^{38}\mathrm{A}$. Similar reactions can produce small amounts of ^{36}A. Recently Gerling and co-workers (Gerling *et al.*, 1956) have reported as much as 1 part of ^{38}A per 5×10^{4} parts of ^{40}A in potassium-containing minerals. Less than this amount of ^{38}A is present in the occluded argon occurring in beryl (Damon and Kulp, 1957c). Winchester is undertaking a search for the possible existence of long-lived ^{38}K, but preliminary work has thus far yielded negative results (J. W. Winchester, personal communication, 1957).

Although nuclear reactions have produced inert gases during earth history, it can be demonstrated that, with the exception of the helium isotopes and argon-40, most of the inert gases present in the atmosphere are of primordial origin. For example, the nuclear reactions suggested by the above workers could supply, at most, only 4 per cent of atmospheric ^{38}A. A convincing argument first advanced by WETHERILL (1954) also suggests that most of atmospheric neon is of primordial origin. WETHERILL measured $1{\cdot}22 \times 10^{-8}$ ^{21}Ne atoms per alpha particle in pitchblende from the Belgian Congo, which he ascribes to the reaction $^{18}O(\alpha, n)^{21}Ne$. A theoretical calculation by MORRISON and PINE (1955) predicts approximately 4×10^{-8} ^{21}Ne atoms per alpha particle for this reaction which, considering the small quantities involved, is in excellent agreement. If the age of the earth is taken to be $4{\cdot}55 \times 10^{9}$ years (PATTERSON, 1956), about $1{\cdot}5 \times 10^{42}$ alpha particles (helium atoms) have been produced in the earth's crust during this period of time. Multiplying this by the ^{21}Ne production ratio, we have 2×10^{-8} $^{21}Ne \times 1{\cdot}5 \times 10^{42} = 3 \times 10^{34}$ ^{21}Ne atoms. But there are 5×10^{36} atoms in the atmosphere (see Table 1) and thus, according to this argument, the alpha-particle induced ^{21}Ne constitutes less than 1 per cent of the ^{21}Ne in the atmosphere. This calculation is also conservative in that it assumes that all of the neon has been outgassed, which surely is not true. Similar arguments can be derived for the other inert gases. For instance, krypton and xenon are produced by neutron-induced fission (SIEGEL, 1946) and spontaneous fission (MACNAMARA and THODE, 1950), but calculations by KHLOPIN and GERLING (1948) and FESTA and SANTANGELO (1952) indicate that only a small fraction of the atmospheric krypton and xenon is of fissiogenic origin.

The terrestrial abundance of the inert gases is very low, compared to spectrographically observed cosmic sources and to their position on elemental and isotopic abundance curves. The neon-to-oxygen ratio in the planetary nebulae NGC7027 (ALLER, 1954) has been estimated to be 0·28. Argon has also been observed to be more abundant in certain cosmic sources (BROWN, 1949) than on earth, while helium, which is the second most abundant element in cosmic material, is a rare element on earth. Modern theories on the origin of the earth agree in ascribing the low terrestrial abundance of the inert gases to their inability to form compounds or liquid or solid phases except at very low temperatures. BROWN (1949, p. 265) has given a convincing demonstration that "during the process of earth formation the mechanism was such as to prohibit the retention of an appreciable fraction of any substance that existed at that time primarily in the gaseous state".

The heavier the gas the less probability it will have of exceeding the velocity necessary for it to escape from the present earth or the earth in a preplanetary form. Helium, which is much lighter than the other inert gases, is being produced by radioactivity and leaking into the atmosphere at a greater rate than argon, but it is less abundant in the atmosphere by a factor of over a thousand. The cause of this phenomenon is most certainly the tendency of the light helium atom to escape into space (SPITZER, 1947) at the present time as well as in the past. The heavier argon atom is now retained by the earth, but escaped during the preplanetary stage when the total mass of the earth was distended throughout a greater volume of space (KUIPER, 1949, p. 322).

Morrison and Pine (1955) have given a thorough review of the natural history of helium, and have been able to account for various natural sources of helium in a consistent and convincing manner. One key to an understanding of the origin of these helium sources is the abundance of ^{3}He, which is very rare on earth. ^{3}He is produced in the atmosphere by cosmic-ray spallation reactions in which ^{3}He and ^{4}He are "boiled" off from the excited target nucleus and by the neutron reactions on atmospheric nitrogen suggested by Libby (1946), i.e. $^{14}N(n, ^{12}C)^3H \rightarrow ^3He$ and $^{14}N(n, 3\alpha)^3H \rightarrow ^3He$. Reactions of the type $^6Li(n, \alpha)^3H \rightarrow ^3He$ first proposed by Hill (1941) are responsible for most of the lithospheric production of ^{3}He (Morrison and Pine, 1955). Aldrich and Nier (1948) have measured the ^{3}He content of various natural sources. They find the lowest terrestrial ^{3}He content for radioactive minerals and the highest content for the lithium-bearing mineral spodumene which provides a favourable environment for the neutron reaction on ^{6}Li. ^{4}He is also produced in this reaction (alpha particle), and the production of ^{4}He by radioactivity is so much more profuse that as a consequence the ratio of ^{3}He to ^{4}He is a very small number (i.e. 10^{-7}–10^{-6}). Thus, large lithospheric gas sources, such as the Panhandle helium field, have a lower ^{3}He/^{4}He ratio than has the atmosphere. When dealing with small sources, there is a possibility of local ^{3}He enrichment caused by derivation from a high lithium environment, such as observed for the mineral spodumene.

It has been suggested by Mayne (1956) that a significant amount of ^{3}He is introduced into the atmosphere by the capture of meteroritic dust containing ^{3}He. The estimate of the amount introduced in this way was based upon an erroneously high production rate of helium in the earth's crust (Damon, 1957) and the invalid assumption that the crust as a whole is being continuously and completely degassed (Mayne, 1956, p. 176; Mayne, 1957, p. 202). In addition, even if Mayne's revised figure of 2000 tons of meteoritic dust per day is used (which seems to be too high in view of the work of Smales and Wiseman (1955) on the Ni/Cu and Co/Cu ratios in deep-sea sediments), it appears impossible that such ^{3}He as was produced in the dust particles could have been quantitatively retained. The smaller the particle, the greater the probability that the ^{3}He will be ejected during spallation, and if it is initially retained that it will diffuse out subsequently. Finally, the addition of the quantity of ^{3}He necessitated by Mayne's assumption of complete degassing requires an improbably high average temperature at the base of the exosphere (2400°K).

In summary, the inert gases appear to be normally abundant cosmically, but rare terrestrially because of their peculiar properties which did not allow them to be captured and retained in cosmic proportions. That which was retained has been modified to a great extent by the radioactive decay products ^{4}He and ^{40}A and by the escape of ^{4}He into space. Nuclear reactions have produced small quantities of inert gas isotopes, which seem to be almost entirely of a secondary rather than a primordial origin, most notably ^{3}He. The atmospheric neon, krypton and xenon* isotopes and also ^{36}A and ^{38}A are essentially primordial in origin.

* ^{129}Xe is an exception. It has been, at least in part produced by beta decay of ^{129}I—$T_{1/2} = 1{\cdot}7 \times 10^7$ years (Suess and Brown, 1951).

The Atmospheric Balance

Early estimates of tritium production from cosmic-ray stars (e.g. spallation of ^{14}N and ^{16}O caused by collisions with cosmic-ray protons) and the $^{14}N(n, t)C^{12}$ reaction called for 0·4–0·9 tritons per cm² sec (Fireman, 1953).* More recent experimental estimates have lowered the production rate to between 0·1 and 0·3 T/cm² sec (Fireman and Rowland, 1955; Currie *et al.*, 1956). On the other hand, the tritium production estimated from hydrospheric balance considerations has considerably increased from the original estimate of between 0·1 and 0·2 T/cm² sec (von Buttlar and Libby, 1955). On the basis of new data on United States ground waters and rains, Begemann and Libby (1956) estimate 0·7/cm² sec; and using the same data, Craig (1957) obtains 1·2 T/cm² sec. With new tritium measurements of Atlantic Ocean water, Giletti *et al.* (1957) review the hydrospheric budget method of estimating tritium production, and obtain 1·1 T/cm² sec. They place the extreme limits as 0·5 and 2·5 T/cm² sec. On the basis of the present disparity between particle reaction experiments and the hydrospheric balance method, Craig (1957) has recently suggested a possible solar origin of natural tritium, while Giletti *et al.* (1957) suggest additional ^3H formation from reactions, including protons in the intermediate energy range.

The primary proton flux is approximately 0·5 protons/cm² sec (Kaufman, 1953; Winckler *et al.*, 1950) and the ratio of protons to helium nuclei in the primary cosmic-ray flux is about 4 (Alpher and Herman, 1950). This may be compared with a value of about 4·5 for the solar hydrogen-to-helium ratio. No experimental evidence has been found for the existence of ^3He in the sun, but from a theoretical point of view, the solar $^3He/^4He$ ratio has been estimated to be 0·02 (Greenstein, 1951). Thus, even if it is assumed that all of the primary cosmic-ray helium flux is from the sun, this yields only 0·002 ^3He atoms per cm² sec from the sun. The tritium flux required is over 100-fold greater than this.

It appears that the empirical evidence based on the material balance calculation is the most reliable means of estimating the ^3H production (Gilletti *et al.*, 1957) and hence the ^3He production rate in the atmosphere. If the average of the three latest such estimates, i.e. 1·0 T/cm² sec, is taken for the tritium production rate and the assumption made that except for the $^{14}N(n, t)$ reaction ($\sim$0·1 T/cm² sec), the tritium is produced by spallations which produce ^3He in approximately equal amounts; a value of 1·9 atoms per cm² sec is obtained for the atmospheric ^3He production. Multiplying by the total area of the earth's surface, $3{\cdot}1 \times 10^{26}$ ^3He atoms are produced within the atmosphere per year. According to Aldrich and Nier (1948), the atmospheric $^3He/^4He$ ratio is $\sim 1{\cdot}2 \times 10^{-6}$, and since the total ^4He content of the atmosphere is $5{\cdot}3 \times 10^{38}$ atoms, there must be about $6{\cdot}4 \times 10^{32}$ ^3He atoms present in the atmosphere (Table 1).

Therefore, assuming the helium content of the atmosphere is in a steady-state condition, the half-life for escape is:

$$(T_{1/2})_{^3He} = \frac{0{\cdot}693 \times \text{concentration in atmosphere}}{\text{production rate}} \qquad (1)$$

* The lithospheric production of tritium is sufficiently small to be neglected (Morrison and Pine, 1955).

Substituting the above numerical values:

$$(T_{1/2})_{^3\mathrm{He}} = \frac{0{\cdot}693 \times 6{\cdot}4 \times 10^{32}}{3{\cdot}1 \times 10^{26}} = 1{\cdot}4 \times 10^6 \text{ years}$$

On the basis of the above assumptions, this is an estimate of the most probable ^{3}He escape half-life and is probably correct to within ± 50 per cent. If the maximum tritium production rate computed by GILETTI is used (i.e. 2·5 T/cm^2 sec), the minimum half-life would by $5{\cdot}9 \times 10^5$ years.

The escape rate of ^{3}He allows the equivalent temperature of the exosphere* to be evaluated. SPITZER (1947) provides the following relationship for t_1, the time during which the atmospheric constituent would fall to $1/e$ of its initial value:

$$t_1 = \frac{6\pi C B e^Y}{3gY} \tag{2}$$

where C is the root-mean-square velocity, $Y = 3{v_\infty}^2/2C^2$, v_∞ being the velocity of escape from the earth's surface, g is the acceleration of gravity, and B, which very nearly equals 5×10^6 at all temperatures for light particles, is a factor which takes into consideration the difference in particle densities with altitude. This equation may readily be modified to a form more suitable for this work since:

$$C = (3RT/m)^{1/2}, \qquad Y = \frac{m{v_\infty}^2}{2RT}, \qquad \text{and} \qquad (T_{1/2})_{\mathrm{esc}} = 0{\cdot}693t_1$$

$$(T_{1/2})_{\mathrm{esc}} = \frac{2B}{3g{v_\infty}^2}(3RT_x/m)^{3/2} \exp \frac{m{v_\infty}^2}{2RT_x} \tag{3}$$

$R = 8{\cdot}3$ ergs $\times 10^7$ degree^{-1} mole^{-1}.
$B = 5 \times 10^6$ (above).
m = at. wt. in g/mole.
$v_\infty = 11{\cdot}3$ km/sec.
$g = 980$ cm/sec^2.
T_x = equivalent temp. for base of exosphere (critical level) in degrees Kelvin.

$$(T_{1/2})_{^3\mathrm{He}} = 6{\cdot}40 \times 10^{-5}\, T_x^{3/2} \exp \frac{2{\cdot}32 \times 10^4}{T_x} \quad \text{(years)} \tag{3a}$$

$$(T_{1/2})_{^4\mathrm{He}} = 4{\cdot}15 \times 10^{-5}\, T_x^{3/2} \exp \frac{3{\cdot}10 \times 10^4}{T_x} \quad \text{(years)} \tag{3b}$$

Solving equations (3a) and (3b) for different temperatures and plotting, the graph in Fig. 1 is obtained.

A temperature of 1880°K is required to produce the escape rate obtained from the tritium data ($1{\cdot}4 \times 10^6$ years). The maximum exospheric temperature corresponding to the extreme upper limit on tritium production would be 2040°K.

* The exosphere is that portion of the atmosphere in which collisions are a minimum, so that a significant fraction of light atoms originating in the denser regions below may soar up and being undeflected may escape the gravitational field of the earth (providing their velocity exceeds the escape velocity).

The evidence for a high-temperature zone above 300 km altitude in the earth's atmosphere has been reviewed by Bates (1954) and Spitzer (1947). The evidence consists of the study of the profiles of the emission lines in the night-sky spectrum, determinations of the half-thickness of the f_2 ionosphere layer by radio observers, etc. There seems little doubt that high temperatures must exist, but the average temperature has only been placed between 1500 and 2000°K. Direct observations by rockets have not yet been reported from this altitude, and the difficulties inherent in making temperature measurements from rockets are apparently not to

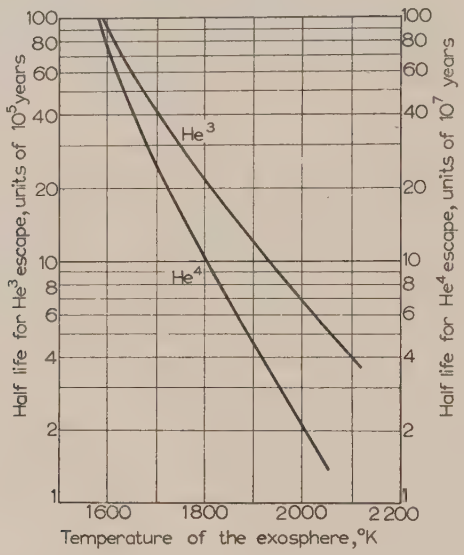

Fig. 1. Half-life for the escape of ^{3}He and ^{4}He from the exosphere vs. temperature of the exosphere.

be underestimated. There is also the possibility that the average temperature is less than 1500°K with short bursts during the sunspot cycle when the temperature might exceed 2000°K (Spitzer, 1947).

The most probable half-life of ^{3}He obtained from the tritium data may now be used to obtain the corresponding half-life for ^{4}He escape from Fig. 1.

$$(T_{1/2})_{^4\mathrm{He}} = 5 \times 10^7 \text{ years}$$

The ^{4}He leak rate into or out of the atmosphere, which corresponds to the above half-life, can now be obtained from a similar relationship to equation (1):

$$^4\text{He leak into atmosphere per year} = \frac{0{\cdot}693 \times \text{concentration in atmosphere}}{(T_{1/2})_{^4\mathrm{He}}}$$

Substituting numerical values:

$$^4\text{He leak into atmosphere} = \frac{0{\cdot}693 \times 5{\cdot}3 \times 10^{38}}{5 \times 10^7} = 7{\cdot}3 \times 10^{30} \text{ atoms/year.}$$

The ^{4}He and ^{40}A production rates in the crust are given in Table 2. These have been calculated from the abundances and decay constants listed in Table 3. The U and Th abundances are for an average crust composed of 10 per cent granitic, 35 per cent intermediate and 55 per cent basic igneous rock, which is about the same

Table 2. Production rate of helium and argon at present time

Species	Production rates (10^{30} atoms/year)		
	in crust	in mantle	crust + mantle
^{4}He(^{235}U)	4	21	25
^{4}He(^{238}U)	95	503	598
^{4}He(^{232}Th)	92	410	502
Total ^{4}He	191	934	1125
^{40}A	40	308	348

as average intermediate rock (Evans and Goodman, 1941). The abundance of K in the crust is taken as 1·9 per cent (Poldervaart, 1955). For the potassium content of the mantle, matter with the potassium content of stony meteorites (850 p.p.m. Edwards, 1955) has been assumed to have been differentiated to form both crust and mantle. Suess and Urey (1956) have reviewed the current data on

Table 3. Constants and abundances used in the calculations

Mass of crust	$= 23{\cdot}7 \times 10^{24}$ g	Poldervaart (1955)
Mass of mantle	$= 4{\cdot}060 \times 10^{24}$ g	Poldervaart (1955)
Area of earth	$= 5{\cdot}10 \times 10^{18}$ cm^2	Rankama and Sahama (1950)
Area of dry land	$= 1{\cdot}49 \times 10^{18}$ cm^2	Rankama and Sahama (1950)
Abundance of K in crust	$= 1{\cdot}9\%$ K_2O	Poldervaart (1955)
Abundance of uranium in crust	$= 1{\cdot}3$ p.p.m.	Evans and Goodman (1941)
Abundance of thorium in crust	$= 5{\cdot}0$ p.p.m.	Evans and Goodman (1941)
Potassium content of stony meteorites	$= 850$ p.p.m.	Edwards (1955)
Potassium content of mantle (assumed)	$= 710$ p.p.m.	This paper
Uranium content of mantle (assumed)	$= 0{\cdot}01$–$0{\cdot}1$ p.p.m.	Suess and Urey (1956)
Thorium content of stony meteorites	$= 0{\cdot}035$–$0{\cdot}35$ p.p.m.	Suess and Urey (1956)
Uranium content of mantle	$= 0{\cdot}04$ p.p.m.	This paper
Thorium content of mantle	$= 0{\cdot}13$ p.p.m.	This paper

^{40}K decay constants: $\lambda_\beta = 0{\cdot}492 \times 10^{-9}$ year^{-1}, $\lambda_e = 0{\cdot}581 \times 10^{-10}$ year^{-1}
^{238}U, ^{235}U and ^{232}Th decay constants $= 0{\cdot}1541 \times 10^{-9}$ year^{-1}
$0{\cdot}9722 \times 10^{-9}$ year^{-1}, $0{\cdot}4987 \times 10^{-10}$ year^{-1} respectively

uranium and thorium in meteorites. The values for the uranium and thorium content of the mantle have been estimated from their data.

Since the production rate of helium is about 191×10^{30} atoms/year for the crust and 934×10^{30} atoms/year for the mantle compared with the 7×10^{30} atoms/year that are currently leaking into the atmosphere, it appears that the earth is not being outgassed extensively and in fact only a few per cent of the helium now forming is being liberated.

Even if the upper limit for the atmospheric ^{3}He production (8×10^{26} atom ^{3}He/year) is used (based upon GILETTI's estimate of the maximum tritium production), and MAYNE's improbable meteoritic dust contribution included, the total ^{3}He increment into the atmosphere is only $13{\cdot}9 \times 10^{26}$ atoms ^{3}He/year. This corresponds to an equivalent exospheric temperature of 2180°K (^{3}He half-life $= 3{\cdot}1 \times 10^5$ years; ^{4}He half-life $= 7{\cdot}2 \times 10^6$ years), which requires a leak rate of 51×10^{30} atoms ^{4}He/year. In this extreme case only 27 per cent of the ^{4}He being produced in the crust is being liberated.

Complete degassing* of the crust requires an average exospheric temperature equal to 2420°K. The ^{3}He half-life would then be $1{\cdot}1 \times 10^5$ years. The ^{4}He half-life would equal $1{\cdot}9 \times 10^6$ years and the ^{3}He increment into the atmosphere would need to be greater by a factor of 13 than the estimate of the probable value based upon GILETTI's calculation of the tritium production (40×10^{26} atoms ^{3}He/year). If meteoritic dust contained the 3×10^{-5} cm^3/g hypothecated by MAYNE, 14,000 tons/day of meteoritic dust would be required to maintain the atmospheric balance of ^{3}He. Since dust particles would not retain all the ^{3}He produced within them, this is probably a lower limit on the required amount of cosmic dust, assuming a complete crustal degassing. There is no evidence for such large increments of meteoritic dust (SMALES and WISEMAN, 1955) or for such high average exospheric temperatures (SPITZER, 1947; BATES, 1954) as would be required by the assumption of complete outgassing of the crust.

Past changes in the cosmic-ray flux could alter the calculation of the escape half-life. If the present cosmic-ray flux is higher than in the past, the average rate of degassing is even less than the value calculated assuming constant flux. If, however, the present cosmic-ray flux is less than in the past, the rate of degassing may be greater than calculated. It has been suggested to the authors that while a strong case may be made for constancy up to 5×10^4 years ago, the flux may have been considerably greater prior to this time. A simple calculation shows that, if the hypothecated increase took place suddenly 5×10^4 years ago, complete degassing would require the flux to have been 16·5-fold greater. If the hypothecated change took place gradually or at an earlier time, complete degassing would require the increase to be even greater than the factor of 16·5. Here again only large factors indeed can seriously affect the validity of the argument.

As a consequence of the above analysis it may be concluded with considerable confidence that the earth's crust is not being completely outgassed at the present time. Since argon has a higher retentivity in minerals than has helium, it cannot

* Complete degassing is defined here as the condition existing when the rate of degassing is equal to the production rate. This, of course, allows for some storage time.

leak at a greater rate than helium. Thus at the present time, assuming no leakage from the mantle, the crust is outgassing argon at the maximum rate of about $1{\cdot}5 \times 10^{30}$ atoms/year corresponding to the calculated helium leak rate of 7×10^{30} atoms/year.

The Evolution of the Atmosphere and Hydrosphere

Table 4 gives the total number of ^{40}A atoms produced in the crust and mantle during the period from the present to the designated time, using the data in Table 3.

Table 4. Total number of ^{40}A atoms produced from present to designated time in billions of years

Time	Atoms produced in units of 10^{40} atoms	
	Crust	Mantle
0·5	3	21
1·0	5	40
1·5	9	70
2·0	14	111
2·5	21	162
3·0	30	230
3·5	42	321
4·0	57	439
4·5	77	596

If the present rate of leakage of argon from the lithosphere into the atmosphere were constant back to the beginning of the earth ($4{\cdot}5 \times 10^9$ years; Patterson, 1956), the total argon input to the atmosphere would only be 1 per cent of the $98{\cdot}5 \times 10^{40}$ atoms which are now present in the earth's atmosphere. Even this result is perhaps not too surprising when the large areas of exposed rocks older than 2 billion years which have retained most of their argon are considered. Furthermore, this is consistent with the demonstration (Damon and Kulp, 1957c) that beryl and cordierite, which incorporate inert gases during formation under magmatic conditions, contain exponentially more helium and argon the older the rock.

These results provide definite evidence that the outgassing of the earth was not linear and that all of the argon now in the atmosphere could not have come from the crust.* The argument is strengthened by the fact that the crust appears to have grown significantly with time, so that the values for the crustal production in Table 4 are certainly too large. Since the argon was not present in the initial atmosphere, for reasons given earlier, it is clear that considerable outgassing must have occurred in the first fraction of earth history.

During the early history of the earth as a planet, it appears that the temperature of the crust and upper mantle were considerably higher than now† (Jacobs,

* It should be pointed out that this result is not critically dependent upon the precise temperature at the base of the exosphere. The ^3He half-life is determined from the abundance of ^3He in the atmosphere and the rate of introduction of ^3He into the atmosphere. This in turn defines an equivalent average temperature. All that is required of the model is that, given the ^3He escape rate, the equations must provide an approximate corresponding ^4He escape rate.

† A cooler protoplanet stage could very well have preceded the high-temperature phase, as suggested by Urey (1951).

1956, p. 399). Some independent evidence for this is the absence of rocks preserved from this period and the high partial pressure of helium and argon in the most ancient magmatic gases (Damon and Kulp, 1957c). If during this early period (1 billion years) the crust and mantle lost about 30 per cent of the argon that was formed, all of the argon in the atmosphere could be accounted for.

It remains now to answer the arguments for a linear growth of the atmosphere and those that would ascribe all atmospheric argon to the crust. Rubey (1951, 1955) reviewed the chemical and geological evidence for the origin of the atmosphere and hydrosphere and concluded that they accumulated gradually throughout geologic time. According to Rubey, a dense primitive atmosphere would result in the deposition of large quantities of limestone which are absent from the geologic record (1951, p. 1120). However, little or no evidence remains of the geologic record prior to 3 billion years ago, and the chance of survival of a subsequent Keewatin deposit, in particular a shallow water deposit, is not great. There is also the possibility of Keewatin carbonate deposition in deep-sea sediments which are not now accessible. Thus the evidence does not permit a categorical denial of limestone formation. Further, as Turner and Verhoogen (1951, p. 489) have said: "in Precambrian and other once deep-seated terrains which have been affected by regional metamorphism and simultaneous large-scale intrusion of granitic magma, it may also be difficult to distinguish between amphibolites formed from limestones by metasomatic introduction of Al, Fe, Mg and Si from magmatic solutions, and amphibolites derived from basic igneous rocks." Of course, at the time of Rubey's analysis the large gap between the oldest rocks and the beginning of earth history had not been established. Rubey found that the total output of volcanic gases including hot springs and fumeroles was of the right order of magnitude to account for the "excess volatiles" added to the earth's surface, but the actual juvenile content of these waters has yet to be established. Finally, the method of geochemical balance used by Rubey leads to a low "erosion rate" and does not take into account the recycling of sediments to igneous rocks by the granitization process. The recycling of sediments provides the continuous addition of carbon dioxide which Rubey requires to prevent brucite from becoming the common marine sediment.

Rankama (1953) assumes all ^{40}A comes from the weathering of igneous rock and then computes the quantity of rock weathered. He then argues that the result indicates that the ^{40}A comes from the crust alone, in disagreement with Kulp (1951) who proposed that a deeper source was required. This argument is open to criticism on three counts: (1) this is a circular argument; (2) the total mass of eroded rock thus obtained is considerably greater than the entire mass of the crust above the Mohorovícíc discontinuity (Poldervaart, 1955); (3) Rankama assumes all ^{40}A produced in the crust has been lost, which, of course, is not the case.

Shillibeer and Russell (1955) concluded that most atmospheric argon could have been derived by release of radiogenic argon from crustal rocks as they are built into continental masses. The age of the earth derived in this way is significantly greater than the age of the earth as determined by Patterson (1956), and to bring these results into agreement it would be necessary to assume some contribution of ^{40}A from the mantle, as suggested by these authors (Shillibeer and

Russell, 1955, pp. 19–20). It is concluded that the early outgassing is required by the data.

As pointed out several years ago (Kulp, 1951), water should probably have accompanied argon from the mantle in roughly proportional quantities at the temperature involved. Assuming the mantle initially had the water content of stony meteorites, a quantity of water on the order of magnitude of the ocean must have left the mantle early in earth history. The oceans cannot be growing more or less linearly, as has been proposed, but were most rapidly evolved in the first billion years of earth history followed by the continuous addition of much smaller quantities throughout geologic time. The important atmospheric constituents such as nitrogen, carbon dioxide and hydrogen sulphide would also have been involved in this early outgassing phenomenon.

Conclusions

(1) At the present time helium and argon are accumulating in the earth's crust as a whole.

(2) The rate of leakage of both gases from the lithosphere is so small that the bulk of the argon content of the atmosphere appears to have been evolved at an earlier time.

(3) It does not seem that the argon content of the atmosphere can be derived entirely from the crust, even given 4·5 billion years of earth history.

(4) Most of the ^{40}A and much of the water now on the surface of the earth were probably introduced from the mantle during the first billion years of earth history. Subsequent lesser additions occurred through the weathering of surface rocks and the growth of continents.

Acknowledgements—This work was made possible by the generous support of the Research Division, Atomic Energy Commission, under Contract AT(30–1)–1669. Prof. Arie Poldervaart and Dr. Bruno J. Giletti contributed helpful discussion and criticism.

References

Aldrich L. T. and Nier A. O. (1948) *Phys. Rev.* **74,** 1590–1594.
Aller L. H. (1954) *Astrophys. J.* **120,** 401–412.
Alpher R. A. and Hermann R. C. (1950) *Rev. Mod. Phys.* **22,** 153.
Barth T. F. W. (1952) *Schweiz Min. Petr. Mitt.* **32,** 354–360.
Bates D. R. (1954) *The Earth as a Planet* (Edited by G. P. Kuiper) pp. 576–636. Univ. of Chicago Press.
Begemann F. and Libby W. F. (1956) *ASTIA Document No.* AD110381, p. 26.
Birch F. (1951) *J. Geophys. Res.* **56,** 107.
Brown H. (1947) *Rev. Mod. Phys.* **21,** 625–634.
Brown H. (1949) *Atmospheres of the Earth and Planets* (Edited by G. P. Kuiper). pp. 260–268. Univ. of Chicago Press.
von Buttlar H. and Libby W. F. (1955) *J. Inorg. Nucl. Chem.* **1,** 75–91.
Carr D. R. and Kulp J. L. (1957) *Bull. Geol. Soc. Amer.* **68,** 763–784.
Craig H. (1957) *Phys. Rev.* **105,** 1125–1126.
Currie L. A., Libby W. F. and Wolfgang R. L. (1956) *Phys. Rev.* **101,** 1557–63.
Damon P. E. (1957) *Geochim. et Cosmochim. Acta* **11,** 200–201.
Damon P. E. and Kulp J. L. (1957a) *Amer. J. Sci.* **255,** 697–704.
Damon P. E. and Kulp J. L. (1957b) *Trans. Amer. Geophys. Un.* **38,** 945–953.
Damon P. E. and Kulp J. L. (1957c) *Amer. Min.* In press.

Edwards G. (1955) *Geochim. et Cosmochim. Acta* **8,** 285–294.
Evans R. D. and Goodman C. (1941) *Bull. Geol. Soc. Amer.* **52,** 459–490.
Festa C. and Santangelo M. (1952) *Ann. Geofis.* **3,** 489.
Fireman E. L. (1953) *Phys. Rev.* **91,** 922–926.
Fireman E. L. and Rowland F. S. (1955) *Phys. Rev.* **97,** 780–782.
Fleming W. H. and Thode H. G. (1953) *Phys. Rev.* **90,** 857.
Gerling E. K., Levski L. K. and Afanas'eva L. T. (1956) *Dokl. Akad. Nauk SSSR* **109,** 813.
Giletti B. J., Kulp J. L. and Bazan F. (1957) *Trans. Amer. Geophys. Un.* In press.
Goldich S. S., Baadsgaard H. and Nier A. O. (1957) *Trans. Amer. Geophys. Un.* **38,** 597.
Greenstein J. L. (1951) *Astrophys. J.* **113,** 531.
Hill R. D. (1941) *Phys. Rev.* **59,** 103.
Hollander J. M., Perlman I. and Seaborg G. T. (1953) *Rev. Mod. Phys.* **25,** 459–651.
Jacobs J. A. (1956) *Handbuch der Physik* Band XLVII, pp. 325–333. Geophysik I, Springer-Verlag, Berlin.
Kaufmann S. (1953) *The Natural Distribution of Tritium.* Ph. D. Dissertation, Univ. Chicago.
Khlopin V. G. and Gerling E. K. (1948) *Dokl. Akad. Nauk SSSR* **58,** 1415; *Chem. Abstr.* **44,** 7735a.
Kuiper G. P. (1949) *Atmospheres of the Earth and Planets* (Edited by G. P. Kuiper) pp. 306–405. Univ. of Chicago Press.
Kulp J. L. (1951) *Bull. Geol. Soc. Amer.* **62,** 1555.
Libby W. F. (1946) *Phys. Rev.* **69,** 671.
Libby W. F. (1953) *Proc. Natl. Acad. Sci.* **39,** 245–247.
MacNamara J. and Thode H. G. (1950) *Phys. Rev.* **80,** 471–472.
Mayne K. I. (1956) *Geochim. et Cosmochim. Acta* **9,** 174–183.
Mayne K. I. (1957) *Geochim. et Cosmochim. Acta* **11,** 202–203.
Morrison P. and Pine J. (1955) *Ann. N.Y. Acad. Sci.* **62,** 69–92.
Patterson C. (1956) *Geochim. et Cosmochim. Acta* **10,** 230–237.
Poldervaart A. (1955) *Crust of the Earth* (Edited by A. Poldervaart) Geol. Soc. Amer. Special Paper 62, 119–145.
Rankama K. (1954) *Geochim. et Cosmochim. Acta* **5,** 81–84.
Rankama K. and Sahama Th. G. (1950) *Geochemistry.* Univ. of Chicago Press.
Reynolds J. H. (1957) *Geochim. et Cosmochim. Acta* **12,** 177–184.
Rubey W. W. (1951) *Geol. Soc. Amer. Bull.* **62,** 1111–1147.
Rubey W. W. (1955) *Crust of the Earth* (Edited by A. Poldervaart) Geol. Soc. Amer. Special Paper 62, 631–650.
Shillibeer H. A. and Russell R. D. (1955) *Geochim. et Cosmochim. Acta* **8,** 16—21.
Siegel J. M. (1946) *J. Amer. Chem. Soc.* **68,** 2411–2442.
Smales A. A. and Wiseman J. D. H. (1955) *Nature, Lond.* **175,** 464.
Spitzer L., Jr. (1947) *Atmospheres of the Earth and Planets* (Edited by G. P. Kuiper) pp. 213–250. Univ. of Chicago Press.
Suess H. E. (1949) *J. Geol.* **57,** 600.
Suess H. E. and Brown H. (1951) *Phys. Rev.* **81,** 1071.
Suess H. E. and Urey H. C. (1956) *Rev. Mod. Phys.* **28,** 68–69.
Tatel H. E. (1950) *J. Geophys. Res.* **55,** 329.
Thompson F. C. and Rowlands S. (1943) *Nature, Lond.* **152,** 103.
Turner F. J. and Verhoogen J. (1951) *Igneous and Metamorphic Petrology.* McGraw-Hill, New York.
Urey H. C. (1951) *Geochim. et Cosmochim. Acta* **1,** 209.
Wasserburg G. J. and Hayden R. J. (1955) *Geochim. et Cosmochim. Acta* **7,** 51.
von Weizsäcker C. F. (1937) *Phys Z.* **38,** 623.
Wetherill G. W. (1954) *Phys. Rev.* **96,** 679.
Wetherill G. W. (1957) *Science* **126,** no. 3273, 545–549.
Wetherill G. W., Aldrich L. T. and Davis G. L. (1955) *Geochim. et Cosmochim. Acta* **8,** 171–172.
Wetherill G. W., Wasserburg G. J., Aldrich L. T., Tilton G. R. and Hayden R. J. (1956) *Phys. Rev.* **103,** 987.
Winckler J. R., Stix T., Dwight K. and Sabin R. (1950) *Phys. Rev.* **79,** 656–669.

Geochimica et Cosmochimica Acta, 1958, Vol. 13, pp. 293 to 302. Pergamon Press Ltd., London

Alkali elements in potash feldspar from the pre-Cambrian of Southern Norway

S. R. Taylor and K. S. Heier
Department of Geology and Mineralogy, Oxford

(*Received* 6 *May* 1957)

Abstract—Li, Na, K, Rb, and Cs have been determined in 50 alkali feldspars from the pre-Cambrian of South Norway. The rock types range from gneisses, augengneisses, gneiss granites, granites to aplites and pegmatites. Rubidium enrichment occurs in some diapire (post-orogenic) granites and in some of the large pegmatites from the Telemark formation. Normal K/Rb ratios are found for the large pegmatites from Kragerø and Arendal as well as the gneisses, etc. Enrichment in rubidium was found in all feldspars examined from east of the Oslo fiord.

Introduction

The development of greater precision in spectrochemical analysis (see, for example, Ahrens, 1954) coupled with the attainment of greater accuracy through the use of reliable standards such as G-1 and W-1 (Fairbairn *et al.*, 1951) makes it possible to apply certain trace-element data to the solution of geological problems not previously amenable. One of the more outstanding geochemical problems is the behaviour of chemical elements during metamorphic and ultrametamorphic to magmatic processes resulting in the formation of the "granitic" shield complexes. Opinion has long been divided on the importance of transfer and migration of elements under such conditions. Since precise spectrographic methods are available for the determination of Li, Rb and Cs, and since their geochemical behaviour is moderately well known, it was decided to investigate the distribution of these elements in potash feldspars from the pre-Cambrian basement rocks of Southern Norway.

The rocks chosen for investigation have chemical and mineralogical granitic affinities when this is understood in its widest sense. Petrographically they can be divided into types ranging from gneisses, augengneisses, gneiss granites, granites, aplites to pegmatites.

The origin of the rocks is controversial and will be explained differently according to the view one has on these rocks in general.

The map (Fig. 1) gives a simplified picture of the geology of the region concerned. Two pre-Cambrian areas are separated by the Skagerak and the Permian igneous rocks within the Oslo graben. The relations between the two are not known. Age determinations carried out on uranium-bearing minerals from pegmatities indicate 850×10^6 years for the eastern (Østfold) area and 1050×10^6 years for the area to the west.* The latter age was obtained for minerals from pegmatites from both sides of the large breccia separating the western area into the Bamble formation in the east and the Telemark formation in the west. The importance

* These are uranium–lead ages carried out about 20 years ago. New age determinations are being undertaken, but no results are yet published.

of this breccia is not known. Bugge, (1928, 1941) maintains that it separates two pre-Cambrian rock complexes of entirely different age, the Bamble formation being the oldest, while the Telemark formation is contemporaneous with the Østfold area in the east and belongs to the Gotidic orogeny. Barth (1935), points to the increase in the regional metamorphism from west to east in the Bamble formation and considers that this formation represents the deeper zones of the Telemark orogeny. Holtedahl (1953) suggests that the difference in age measured

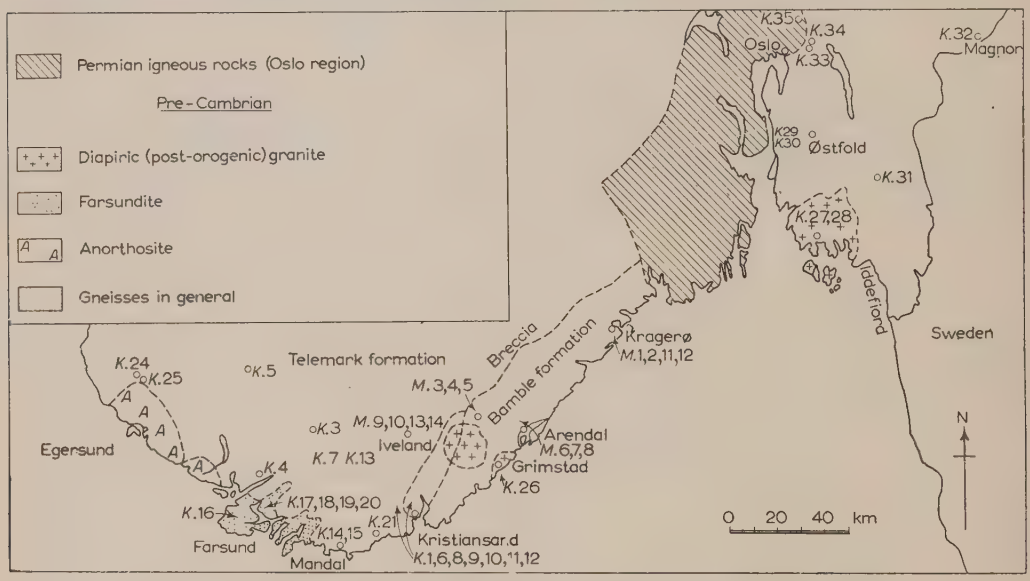

Fig. 1. Geological sketch map of Southern Norway, showing sample localities.

from pegmatite minerals on the two sides of the Oslo fiord may be explained by a difference in origin of the pegmatites concerned, the pegmatites in the western area being formed by ultrametamorphism during the orogenesis, while he connects the pegmatites in the east with the post-orogenic Iddefjord granite (diapire granite). Still another area has been separated out as a formation of its own, different from these already discussed. This is the Egersund–Sogndal formation of anorthositic, noritic, and charnockitic rocks in the far south-west of the map. The relations between this area and the granodioritic gneisses towards NE are unknown, but a general increase in regional metamorphism, as evidenced by the gneisses and migmatites, takes place in a SW direction from the central part of the Telemark complex and thus a common orogenetic relationship with increasing depths of erosion levels exposed towards SW may be assumed (Heier, 1956, 1957).

The Østfold area

Granitized mica schists and leptites of undoubtedly supracrustal origin occur immediately south of Oslo and close to the Oslo fiord. In a central part more homogeneous gneiss-granites (Hobøl granite, K.30) develops within the gneisses and in the far south a homogeneous post-orogenic granite, the Iddefjord granite

(K.27–K.28), is intruded with migmatitic contacts against the gneisses. The Østfold area is covered by the samples K.27–K.35. K.33–K.35 are found within, or close to the Permian igneous rocks and were exposed to Permian thermal metamorphism.

The Bamble formation

Banded gneisses occupy most of this area. Two post-orogenic (diapire) granites in many respects similar to the Iddefjord granite also occur. Sample K.26 is taken from the smallest of these (Grimstad granite). In addition we have only samples from pegmatites close to Kragerø, (M.1, M.2, M.11, M.12) and Arendal (M.6, M.7, M.8).

The Telemark formation

We are concerned only with the rocks south of the thick series of orogenically folded supracrustral rocks. Younger than these is the Telemark granite (gneiss granite), which grades into the huge southern gneiss complex. The Iveland pegmatites (M.9, M.10, M.13, M.14) are most certainly formed in connexion with this granite. The Lauvrak (M.3, M.4) and Hinnebu pegmatites (M.5) occur between these and the Arendal pegmatites. They are found within the Bamble formation, but may be connected with the post-orogenic Birkeland granite. The Iveland pegmatites are found within a large complex of amphibolite gabbro. The contacts against the surrounding gneiss are gradational.

The majority of our samples are from the southern part of this gneiss complex and cover a number of rock-types grading into each other. Field evidence strongly supports ultrametamorphic processes being responsible for their formation.

A more homogeneous granite (Farsundite) (K.16, K.17), is found to the far south. This rock differs, however, from the post-orogenic granites previously mentioned in that amphibole may be a dominant femic mineral.

The pegmatite body at Rømteland (K.18–20) must be genetically connected with the farsundite in which it occurs.

Sample Preparation and Analytical Method

The feldspar fractions were obtained by separation of the rocks, using magnetic separation and heavy liquids (acetylene tetrabromide and acetone). When the feldspars formed large porphyroblasts, as in some of the augengneisses, pure potash feldspar fractions were obtained by handpicking. Thus rather pure potash feldspar fractions were obtained, 95 per cent and better, the impurities being mostly quartz and plagioclase.

The samples were ground in agate mortars to pass 120-mesh bolting cloth. Sodium and potassium were determined by flame photometer. The spectrographic procedure utilized the variable internal standard method described by Ahrens (1954, Sect. 5–4, pp. 55–59), sodium being used as the internal standard. The samples were arced at a low current until the alkali metals had completed distillation. This time was rather uniform at 120 sec for the electrodes used.

Details are as follows: Spectrograph: Hilger large quartz and glass. Glass optics. Wavelength range: 4600–9600 Å. Kodak IRER plate. Lower electrode (anode) 1·6 mm i.d. × 5 mm depth, Johnson Matthey 4B graphite. Upper electrode (cathode) "Ship" carbon 5 mm diameter. Current: 4·4 A d.c. Slit 15 μ. Exposure time: 120 sec. Plates developed in Kodak D-19b for 5 min.

G-1 (granite) and W-1 (diabase) were used as the primary standards. The following values were used

Li—G-1; 22·5 p.p.m.;	W-1: 9 p.p.m.
Rb—G-1: 220 p.p.m.;	W-1: 25 p.p.m.
Cs—G-1: 2·5 p.p.m.	

Since extrapolation beyond these values was necessary particularly in the case of rubidium, synthetic standards using an alkali feldspar base were prepared in the usual way from "Specpure" chemicals to cover higher concentrations. Since these standards fitted along the G-1, W-1 curve, it is believed that little systematic error exists.

The following lines were used: Li-6707, Rb-7947 and Cs-8521. Na-5682 was the internal standard line. Duplicate results were within 5 per cent of the arithmetical mean. Working curves are shown in Fig. 2. The location of the samples is shown on the map (Fig. 1) and the analytical data are listed in Table 1.

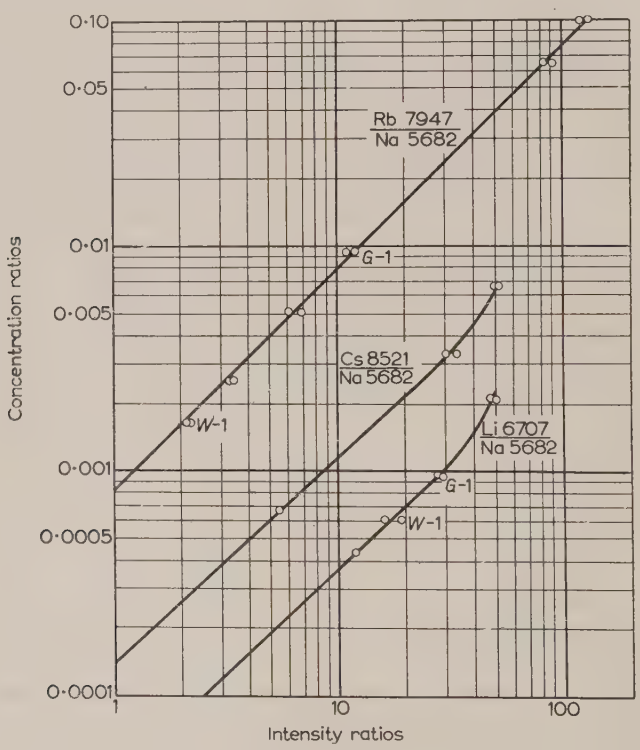

Fig. 2. Working curves for determination of Li, Rb and Cs in feldspars.

Sodium and potassium

The K/Na ratio of the potash feldspars varies as would be expected. The ratio indicates the minimum temperature of the feldspar formation and when related to the sodium content of the coexisting plagioclase a more exact definition of the temperature of formation may be possible (Barth, 1951, 1956). The temperatures thus determined are listed together with the analytical data in Table 1. The ordinary gneisses seem to have reached a temperature of 400°C, which represents a background level. For the granite gneisses, Barth assigns a temperature of

Table 1. Alkali element content of potash feldspars

A: South Norwegian gneisses and granites located between the Telemark granite and the Egersund region

No.	Rock type	Rock No.	Locality	T°C	% Na_2O	% K_2O	p.p.m. Li	% Na	% K	p.p.m. Rb	p.p.m. Cs
K.13	Coarse gneiss		Röyrås	420	1·20	14·76	2·2	0·89	12·25	690	3·1
K.23	Gneiss		Spangereid		2·28	9·56	5·1	1·69	7·94	500	2·7
K.3	Augengneiss	5	Hille	680	3·56	10·66	6·2	2·64	8·85	450	—
K.4	Augengneiss	4	Feda	640	2·88	11·71	12	2·14	9·72	320	—
K.5	Augengneiss	7	Haughom-Tonstad	640	3·17	11·94	21	2·35	9·91	500	—
K.7	Gneiss granite	3	Sögne chapel, Holskogen	430	1·26	14·34	5·8	0·94	11·90	750	16
K.1	border facies granite (anatexe)	14	Glattetrevn.	400	1·52	13·96	2·8	1·13	11·59	770	38
K.8	Oddersja granite (anatexe granite)	13	Varden, Skråstadhgd.	450	1·32	14·64	3·7	0·98	12·15	860	15
K.10	Oddersjå granite (anatexe granite)	12	Södal	430	1·22	14·22	2·6	0·91	11·80	740	—
K.11	Anatexe granite	15	Path from Urdalen	450	1·32	14·56	16	0·98	12·09	360	—
K.12	Fine grained granite (anatexe)	17	Granite between faults, Oddersjå	400	1·10	14·92	0·9	0·82	12·38	910	9·2
K.14	Holum granite (anatexe)		Erland	520	1·90	13·50	1·6	1·41	11·21	570	2·3
K.15	Holum granite (anatexe)		Ljosvann	550	2·10	13·00	2·2	1·56	10·80	530	1·9
K.26	Diapire granite		Fevig (Grimstad)	550	2·48	13·08	1·3	1·84	10·86	910	22
K.16	Farsundite (Diapire granite)	20	Udal-Lista	550	2·34	13·18	5·1	1·74	10·94	1100	3·4
K.17	Farsundite (Diapire granite)		2–2 Km from Rømteland, Osestad.	590	3·07	11·64	5·0	2·28	9·66	470	20
K.18	Pegmatite (large)		Rømteland 1.	450	1·83	13·92	4·2	1·36	11·55	3400	100
K.19	Pegmatite (large)		Rømteland 2.	600	3·13	12·77	2·0	2·32	10·60	2300	44
K.20	Pegmatite (large)		Rømteland 3.	590	2·91	12·77	4·6	2·16	10·60	1400	10
K.24	Pegmatite (small)		Lakssvelefjeld		3·06	11·54	3·7	2·27	9·58	500	—
K.25	Pegmatite (small)		Ålgård		2·51	12·44	20	1·86	10·33	1150	—
K.9	Small pegm. vein in Oddersjå granite	9	Varden, top 260	550	2·56	13·12	4·5	1·90	10·89	640	1·9
K.6	Aplite	16	Varden, Skråstadhgd.	430	1·28	14·88	3·0	0·95	12·35	940	22

B: East Norwegian gneisses and granites

K.31	Gneiss		Heller gård, Askim		1·32	14·45	7·2	0·98	12·00	1050	6·5
K.32	Gneiss		Magnor		1·67	14·32	160	1·24	11·89	1260	9·5
K.33	Gneiss		Gamle Strömsvn,		1·90	13·54	43	1·41	11·24	1250	38
K.34	Gneiss		Skarervn. Lörenskog		2·00	13·55	70	1·48	11·25	930	22
K.35	Gneiss		Gjelleråskrysset, Oslo, inclusion in Permian Nordmarkite		3·03	10·87	7·9	2·25	9·02	420	4·6
K.30	Hoböl granite, (gneiss granite)		Greåker, Hvidsten, Hoböl		1·42	13·25	3·2	1·05	11·00	1250	8·0
K.29	Pegmatite in Hoböl granite		Hytteåsen, Hoböl		2·59	12·66	2·0	1·92	10·51	1200	18
K.27	Iddefjord granite (diapire)		3 km. NW. of Fredrikstad		1·46	12·43	8·9	1·08	1032	1300	3·8
K.28	Iddefjord granite (diapire)				1·32	14·52	7·3	0·98	12·05	3300	13

C: Large pegmatite bodies

No.	Locality	% Na_2O	% K_2O	p.p.m. Li	% Na	% K	p.p.m. Rb	p.p.m. Cs
M.1(a)	Kalstad, Kragerø	2·88	11·98	0·5	2·14	9·94	510	2·7
M.1(b)	Kalstad, Kragerø	3·30	11·51	0·8	2·45	9·55	840	3·8
M.2(a)	Lindvikskollen, Kragerø	2·85	12·67	0·2	2·11	10·52	610	1·1
M.2(b)	Lindvikskollen, Kragerø	3·24	12·12	0·3	2·40	10·06	550	1·9
M.11	Tangen, Kragerø	3·32	12·15	0·1	2·46	10·09	880	14
M.12	Tangen, Kragerø	3·68	10·85	0·4	2·73	9·01	740	8
M.6	Gloserhei, Froland, Arendal	2·77	12·41	0·1	2·06	10·30	640	0·8
M.7	Gloserhei, Froland, Arendal	2·58	12·75	0·1	1·91	10·58	620	1·5
M.8	Gloserhei, Froland, Arendal	2·84	12·83	0·1	2·11	10·65	790	1·5
M.3	Lauvrak, øst-Agder	1·88	13·78	1·5	1·39	11·44	1600	23
M.4	Lauvrak, øst-Agder	1·74	14·03	0·3	1·29	11·65	2000	25
M.5(a)	Hinnebu, øst-Agder	2·03	13·30	2·0	1·51	11·04	1400	13
M.5(b)	Hinnebu, øst-Agder	2·27	13·48	3·1	1·68	11·19	1400	15
M.9	Tuftan, Iveland	2·99	12·55	3·7	2·22	10·42	1230	11
M.10	Tuftan, Iveland	2·79	12·84	3·1	2·07	10·66	1150	11
M.13	Eretveit, Iveland	2·32	13·12	0·1	1·72	10·89	790	6·1
M.14	Eretveit, Iveland	2·56	12·98	0·1	1·90	10·78	630	5·7

The rock numbers are those used by Barth (1956)
T°C: temperature of formation determined by the feldspar geologic thermometer, Barth (1956).
—: not detected.

430°, and for the anatexe granites, 450°. The diapire granites are formed in the range 550–590°, while the highest temperatures (580–680°) are obtained for the augengneisses (Barth, 1956, Fig. 7).

Lithium

The absence of 6-fold (octahedral) co-ordination positions in the feldspar lattice excludes Li^+ (0·68 Å) from structural positions. Nevertheless, it is present in all the samples examined, and although usually not more than a few parts per million, is occasionally much more. Ahrens and Liebenberg (1945) note that amounts greater than 5 p.p.m. Li are rare in feldspar. It is in general more abundant than caesium in the feldspars. However, the crustal abundance of Li (32 p.p.m.) is about 6·5 times that of caesium (5 p.p.m.) (Rankama, 1954). An examination of the Li/Cs ratios indicates that with the exception of two samples (K. 32, 34) the ratios are markedly less than this and average 0·42. The feldspars containing high Li are mainly from the gneisses and augengneisses (without detectable Cs) and this may indicate sample contamination. On the other hand, the large pegmatites, in particular, are very low in Li (and in the Li/Cs ratio). While Li and Cs both have difficulty in entering the feldspar lattice, the ratios suggest that Cs enters more freely than Li. The area east of Oslo fiord is in general higher in Li.

Rubidium

The close relationship between K and Rb in minerals, rocks and meteorites has been shown by AHRENS *et al.* (1952) and forms an outstanding example of close geochemical coherence. Figs. 3, 4 and 5 show plots of percentage K versus

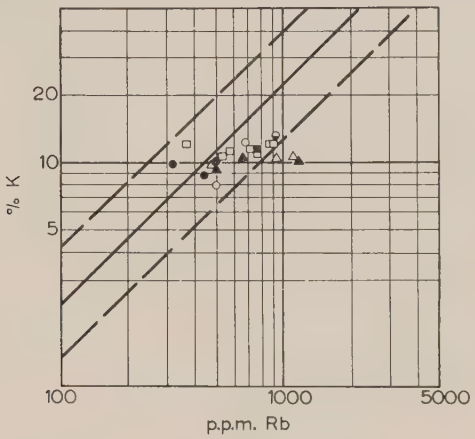

Fig. 3. K/Rb relationship for feldspars from west of Oslo fiord (excluding large pegmatites) superimposed on AHRENS *et al.* (1952) K/Rb curve. Broken lines indicate limits of normal scattering.

● augengneiss
○ gneiss
■ gneiss granite
□ anatectic granite
△ diapire granite
◒ aplite
▲ small pegmatites
— — limits of scatter

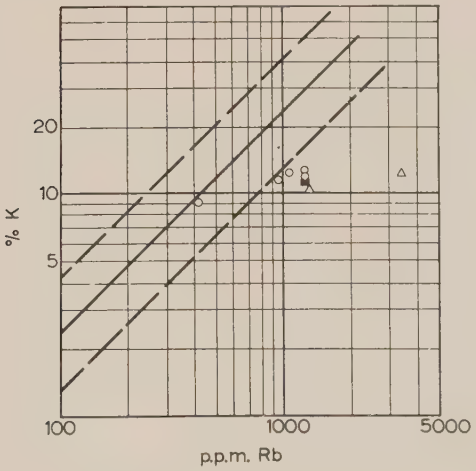

Fig. 4. K/Rb relationship for feldspars from east of Oslo fiord.

■ gneiss granite
△ diapire granite
○ gneiss
— — — limits of scatter

p.p.m. Rb for the feldspars superimposed on the K/Rb curve of Ahrens *et al.* (1952, Fig. 2). This curve has been adjusted to conform to more recent rubidium determinations on G-1 and W-1, which were used as standards by Ahrens (see Taylor *et al.*, 1956).

Distinctive enrichment in rubidium may be assumed if points fall well to the right of the curve, providing that results are calibrated against G-1 and W-1

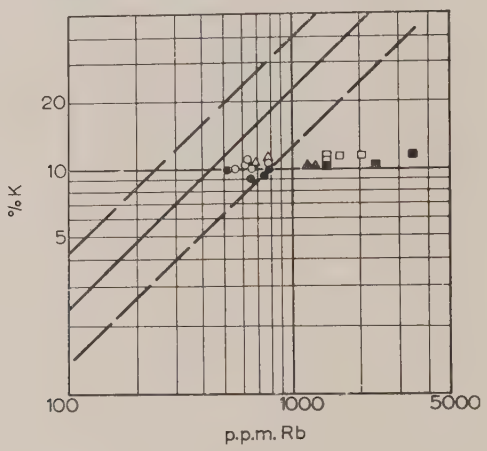

Fig. 5. K/Rb relationship for large pegmatites.
● Krager ø
○ Arendal
□ øst-Agder
▲ Iveland (Tuftan)
△ Iveland (Eretveit)
■ Rømteland
— — — limits of scatter

and also that the spread is outside the limits of error. On Fig. 3 are plotted K and Rb figures for feldspars (excluding those from large pegmatites) from South Norway. The K/Rb ratios are within the limits of normal scatter except for two diapire granites, K.16 (Farsundite) and K.26 (Grimstad) and one of the small pegmatites (K.25). These three specimens show mild enrichment in rubidium.

Fig. 4 indicates that, with the exception of one gneiss, [K.35, inclusion in Permian Nordmarkite] all the rocks from east of the Oslo fiord are enriched in rubidium. These rocks are also high in Li and Cs. The K/Rb plots for the large pegmatites (Fig. 5) indicate that about half are enriched in Rb, while the remainder are not. The pegmatites from Kragerø and Arendal are not enriched. Oftedal (1954) notes that feldspars from these pegmatites are poor in lead, and qualitative analysis of our samples confirms this, none having more than about 10 p.p.m. The large pegmatites from Tuftan, Hinnebu and Lauvrak are enriched in Rb (M.13, M.14). These feldspars (including Eretveit) are also rich in Pb (Oftedal, 1954) and our samples contain about 50–100 p.p.m. Pb. Oftedal (1954) in discussing the lead data considers that the Bamble pegmatites (low in Pb and Rb) are formed by "incipient granitization processes or vestiges of granitization processes which have been going on at greater depth".

The rubidium and lead-rich pegmatites of the Telemark formation "may have formed through granitization of rock complexes locally enriched in Pb but in many cases it is more probable that they are connected with larger palingenic granitic bodies in the classical way" (Oftedal, 1954).

The data from the large Rømteland pegmatite show that different degrees of Rb enrichment are found within the same pegmatite. The feldspars from Rømteland 2 and 3 are both from the main pegmatite, while no. 1 (very high in Rb) is from a younger vein cutting the pegmatite (T. Sverdrup, personal communication). This suggests extreme Rb enrichment in the very late hydrothermal stage. (Note also the much lower temperature of formation of this feldspar relative to the other two.) Rb enrichment in the late hydrothermal stage may also be the explanation of the varying Rb content within the same diapiric granites (Farsundite and Iddefjord granites).

Taylor *et al.* (1956) report distinct Rb enrichment in magmatic granites which apparently represent a very late stage of crystallization where the composition of the magma is more comparable to a pegmatitic stage.

In the rocks examined by us biotite is the only other important potassium mineral in which Rb can be contained. According to Rankama amd Sahama (1950), Rb is enriched in biotites relative to feldspars.

In summary, enrichment of Rb relative to K occurs in some diapire granites and large pegmatites. It seems likely that extreme conditions (e.g. hydrothermal stage of differentiation) are necessary to affect seriously the K/Rb coherence. If large-scale transfer of material takes place during granitization processes, K and Rb seem to participate nearly to the same degree.

It is difficult to say, with such a small number of samples, if the uniform enrichment of Rb in the area east of the Oslo fiord represents a regional effect. This is perhaps unlikely in view of the established close coherence of K and Rb.

Caesium

Because of its much greater ionic radius (Cs^+ 1·67 Å), Cs shows little geochemical coherence with K and tends to accumulate in the last residual liquids. The concentration of Cs in the late hydrothermal stage is in our case illustrated by the high Cs content of the feldspars (K.18, K.19) from the Rømteland pegmatite. Apart from this it is evident that some significant Cs enrichment is traceable in the rocks which would be thought of as most differentiated (diapire granites and large pegmatites).

Of interest is the very low Cs content of the augengneisses and small pegmatites. These feldspars have also comparatively low Rb contents (except the Ålgård pegmatite). This may support the view that these rocks are formed by metamorphic recrystallization *in situ* and not by large-scale material transport.

Rankama (1954) lists the average Cs content in igneous rocks at 5 p.p.m. Our results suggest that Cs must be relatively enriched in the micas.

Summary

A very general trend of Rb enrichment occurs in the potash feldspar from the series augengneisses–gneisses–diapiric granites to large pegmatites. The potash

feldspars from the large pegmatites of Kragerø and Arendal and the small pegmatites have values quite similar to the gneisses in which they occur and this may be taken as evidence of formation *in situ* following the ideas of Ramberg (1956). It was thought that significant differences would be observed among the feldspars from the gneisses, gneiss granites and anatectic granites. The processes by which these are formed do not seem to be capable of producing any marked variation. Thus, migration of elements during granitization may be quite local, so that no large-scale differences are produced. This seems to be particularly so with the high-temperature augengneisses. On the other hand, the Rb enrichment exhibited by some of the diapire granites, and large pegmatites indicates that conditions have been extreme enough to cause enrichment in Rb. These conditions may have been those of the late hydrothermal or "pegmatitic" stage of crystallization.

Further work on the distribution of gallium, lead, thallium, barium and strontium in the feldspars is in progress, and work on the coexisting micas is planned.

Acknowledgements—Thanks are due to Prof. T. F. W. Barth, Dr. H. Neumann and Dr. T. Sverdrup for many of the samples. Mr. S. Moorbath kindly made available the large pegmatite samples (M.1 to M.14). The authors are grateful to Miss Penelope Bailey for performing the spectrographic analyses.

References

Ahrens L. H. (1954) *Quantitative Spectrochemical Analysis of Silicates*. Pergamon Press, London.

Ahrens L. H. and Liebenberg W. R. (1945) Lithium in mica and feldspar. *Trans. Geol. Soc. S. Afr.* **48,** 75.

Ahrens L. H., Pinson W. H. and Kearns M. M. (1952) Association of rubidium and potassium and their abundance in common igneous rocks and meteorites. *Geochim. et Cosmochim. Acta* **2,** No. 4, 229–242.

Barth T. F. W. (1935) The large pre-Cambrian intrusive bodies in the southern part of Norway. Report XVI Int. Geol. Congress, Washington, 1933.

Barth T. F. W. (1945) Geological map of the western Sørland. *Norsk Geol. Tidsskr.* **25,** 1.

Barth T. F. W. (1951) The feldspar geologic thermometers. *Neues Jb. Miner.* **82,** 143–154.

Barth T. F. W. (1956) Studies in gneiss and granite. *Skr. Norske Vidensk. Akad. I. Mat.-Naturv. Klasse* **1956,** No. 1.

Bugge A. (1928) En forkastning i det syd-norske grundfjeld. *Norg. Geol. Unders.* 130.

Bugge A. (1941) En oversikt over arbeidet i det sydnorske grundfjeld. *Norsk. Geol. Tidssk.* **21,** No. 2–3, 230–238.

Fairbairn H. W. *et al.* (1951) A co-operative investigation of precision, and accuracy in chemical, spectrochemical and modal analyses of silicate rocks. *Bull. U.S. Geol. Surv.* 980.

Heier K. S. (1956) The geology of the Ørsdalen district, Rogaland, S. Norway. *Norsk Geol. Tidssk.* **36,** No. 3, 167–211.

Heier K. S. (1957) Phase relations of potash feldspars in metamorphism. *J. Geol.* **65,** 468–479.

Holtedahl O. (1953) Norges Geologi. *Norg. Geol. Unders* **164,** 1.

Oftedal I. (1954) Some observations on the regional distribution of lead in South Norwegian granitic rocks. *Norsk Geol. Tidssk.* **33,** 135–161.

Ramberg H. (1956) Pegmatites in West Greenland. *Bull Geol. Soc. Amer.* **67,** 185–214.

Rankama K. (1954) *Isotope Geology*. Pergamon Press, London.

Rankama K. and Sahama Th. G. (1950) *Geochemistry*. Chicago University Press.

Taylor S. R., Emeleus C. H. and Exley C. S. (1956) Some anomalous K/Rb ratios in igneous rocks and their petrological significance. *Geochim. et Cosmochim. Acta* **10,** No. 4, 224–229.

Geochimica et Cosmochimica Acta, 1958, Vol. 13, pp. 303 to 321. Pergamon Press Ltd., London

The constitution of the mantle—I

Thermodynamics of the olivine–spinel transition

A. E. Ringwood
Dept. of Geology, University of Melbourne

(*Received* 3 *December* 1956)

Abstract—A method of calculating the pressure required to cause Mg_2SiO_4 to invert from the olivine to the spinel structure is described. It is based upon the fact that Mg_2SiO_4 displays limited solid solubility in nickel orthogermanate (Ni_2GeO_4) at high temperature. Ni_2GeO_4 has a spinel structure. By means of a thermodynamic treatment of Ni_2GeO_4—Mg_2SiO_4 spinel solid solutions and their phase equilibria with olivine solid solutions, it is possible to calculate the free energy of the olivine–spinel transition for Mg_2SiO_4. This is found to be 70,000 ± 10,000 J/mole at 1500°C.

The lattice constant of Mg_2SiO_4 spinel is found by extrapolating the lattice constants of the spinel solid solutions. This, together with the lattice constants of Ni_2SiO_4 and Mg_2GeO_4 spinels obtained in an analogous manner, indicate that the increase in density when olivine transforms to spinel is 11 ± 3 per cent.

The free-energy difference between the two forms when they are subjected to high pressures is $P\Delta V$, where ΔV is the difference in molar volume at a pressure P_1. When this function becomes equal to the free energy of transition at zero pressure (obtained above), olivine will invert to spinel. Calculations on this basis indicate that a pressure equivalent to that at a depth of approximately 500 ± 140 km within the earth will cause inversion. This result is in good agreement with the depth of the 20° discontinuity found by seismology.

Introduction

Seismological data, combined with investigations of density and electrical conductivity strongly suggest the presence of inhomogeneity in the upper levels of the mantle. Indications are that the inhomogeneity is most marked at a depth of about 400 km. Jeffreys (1952) has inferred the presence of a discontinuity at this depth—the "20° discontinuity". Birch (1952) has produced evidence suggesting that the inhomogeneity occurs over a substantial depth range—perhaps from 300 to 800 km. Above and below these limits the mantle appears to be homogeneous.

Jeffreys and Bernal (see Jeffreys, 1952) have suggested that the inhomogeneity and discontinuity are caused by a polymorphic inversion in olivine. Bernal (1936) pointed out that Mg_2GeO_4, which is closely related to Mg_2SiO_4, is dimorphous, displaying both olivine and spinel structures. Bernal therefore suggested that at high pressures, olivine-type Mg_2SiO_4 might undergo inversion to a spinel form, possessing higher density. Subsequent laboratory compression experiments upon olivine have failed to produce the spinel polymorph, however.

Before the Jeffreys–Bernal hypothesis can be adequately assessed, some means of estimating the pressure required to produce this inversion must be found. In the following pages, such a method is described. It is based upon an investigaton of sub-solidus phase equilibria in the system Ni_2GeO_4—Mg_2SiO_4. Nickel orthogermanate (Ni_2GeO_4) possesses a spinel structure. The ions Ni^2 and Mg^2 are similar in crystal chemical properties, and able to replace each other in many crystals and minerals. A similar resemblance occurs between Si^4 and Ge^4. Therefore it seemed possible that some Mg^2 and Si^4 might be able to replace Ni^2 and Ge^4

in Ni_2GeO_4. This proved to be the case, and Ni_2GeO_4 spinel was found to take up to 9 per cent of Mg_2SiO_4 into solid solution at 1500°C. By a study of the properties of these solid solutions, and a thermodynamic investigation of their phase equilibrium relationships to co-existing olivine solid solutions, sufficient data may be secured to predict the stability range of Mg_2SiO_4 spinel.

2. Determination of Free Energy of Transition

(a) *Experimental—The system* Ni_2GeO_4–Mg_2SiO_4

Sub-solidus phase equilibria in this system were investigated in the 1200–1500°C range. The raw materials—GeO_2, MgO—were of reagent grade. NiO was formed by igniting nickel nitrate and calcining the product at 1200°C. SiO_2 was prepared from pure quartz crystal which was crushed and leached with HCl.

After preliminary drying treatment, GeO_2, SiO_2, MgO and NiO were weighed out in amounts corresponding to various desired proportions of Ni_2GeO_4 to Mg_2SiO_4. The mixture (amounting to 1 g for any preparation) was thoroughly ground together under benzene in order to secure intimate mixing, dried, and then formed into tablets in a small press. Tablets were held in air in a platinum-wound electric furnace which could be controlled at any desired temperature. Temperature was measured using a calibrated Pt–Pt 10 per cent Rh thermocouple. The length of the run varied according to the time necessary to achieve equilibrium, and the amount of GeO_2 which was being lost by volatilization. (This becomes appreciable above 1400°C and must be corrected for.) The times necessary were determined by experience, and varied from 40 hr at 1200°C to 30 min at 1500°C. The tablet was then removed from the furnace, cooled in air, recrushed and reformed, and the procedure was repeated. In most cases this was sufficient to ensure equilibrium; sometimes, however, a third crushing was required.

The above procedure served to establish the approximate positions of phase boundaries; however, for more precise determination of the boundary on the spinel side, additional precautions were necessary. The main difficulty in sub-solidus studies is the attainment of a high degree of homogeneity in the sample so that complete equilibrium is ensured. To attain this, NiO—MgO and GeO_2—SiO_2 were weighed out, mixed and formed into tablets separately. The NiO—MgO tablets were held at 1400°C for several hours, crushed, and the procedure repeated twice. Similarly the GeO_2—SiO_2 tablets were melted at 1300°C for 2 hr, recrushed, and so on. These components which were by then individually homogeneous were weighed in the correct proportions to form a tablet of desired composition, which was then treated as above.

Samples so prepared were examined by optical and X-ray methods. The spinel solid solutions appear as green isotropic crystals under the petrographic microscope, whereas the olivine solid solutions are anisotropic and possess a high birefringence. Accordingly, it is possible to locate the two-phase boundary by observing the composition at which birefringent crystals make their appearance among the isotropic spinels. The location of the two-phase boundary on the olivine side of the system may be found in an analogous manner. Refractive indices of the spinels were determined using sulphur-selenium melts, whilst ordinary high RI liquids

sufficed for the olivines. By determining the refractive indices of the olivine solid solutions, the two-phase boundary may be located more accurately.

X-ray powder patterns of samples also locate the two-phase boundaries, and the results were found to agree with the optical examination. Trials with mixtures of NG_{100} and $NG_{40}MS_{60}$ ($NG = Ni_2GeO_4$, $MS = Mg_2SiO_4$) demonstrated that the

Table 1. Phase equilibrium data and refractive indices for spinel solid solutions

Composition (mole %)	Temperature (±10°C)	Phases present	Refractive index ±0·005
NG_{100}	1360	Homogeneous spinel	2·082
$NG_{97}MS_3$	1360	Homogeneous	2·068
$NG_{94}MS_6$[a,b]	1272	Two-phase	
$NG_{94}MS_6$	1360	Homogeneous	2·061
$NG_{94}MS_6$[a]	1411	Homogeneous	
$NG_{94}MS_6$	1439	Homogeneous	
$NG_{94}MS_6$[a]	1509	Homogeneous	
$NG_{93}MS_7$	1439	Homogeneous	
$NG_{92}MS_8$[a]	1272	Two-phase	
$NG_{92}MS_8$[a]	1411	Homogeneous	
$NG_{92}MS_8$[a]	1509	Homogeneous	
$NG_{91}MS_9$	1470	Two-phase	2·046
$NG_{91}MS_9$	1439	Two-phase	
$NG_{90}MS_{10}$[a]	1272	Two-phase	
$NG_{90}MS_{10}$[a]	1411	Two-phase	
$NG_{90}MS_{10}$	1439	Two-phase	
$NG_{90}MS_{10}$[a]	1509	Two-phase	
$NG_{88}MS_{12}$	1470	Two-phase	2·042
$NG_{88}MS_{12}$	1528	Two-phase	
$NG_{85}MS_{15}$	1470	Two-phase	2·037

[a] These samples were prepared using the special precautions to ensure homogeneity outlined previously.
[b] The inhomogeneity found in this sample was originally assumed to represent equilibrium, and consequently in the phase diagram first published (Ringwood, 1956) the spinel solvus was given a steep positive slope. However, subsequent work showed that it was impossible to obtain equilibrium at 1200°C, and hence it seemed possible that the inhomogeneity found in this run (1272°C) might be due to non-attainment of equilibrium. To check this, a sample of $NG_{90}MS_{10}$ was held at 800°C in a "squeezer" type apparatus under a pressure of 12,000 bars. The product was fairly well crystallized, but gave a rather diffuse X-ray powder pattern. Optical and X-ray examination did not reveal the presence of olivine. Most of the Mg_2SiO_4 must therefore be in solid solution. Accordingly the result referred to is probably not representative of equilibrium and the slope of the spinal solvus (Fig. 1) has been modified.

222 line of $NG_{40}MS_{60}$ (olivine) could usually be identified when $3\frac{1}{2}$ per cent of the olivine was present among the spinel. This corresponded to a tolerance of 2 per cent of pure Mg_2SiO_4. X-ray investigation also provided information on the lattice parameters of the spinel solid solutions and their structure.

(b) *Results*

Results of these investigations are set out in Tables 1 and 2. The principal conclusions may be summarized:

(i) Between 1300 and 1500°C, Ni_2GeO_4 spinels dissolve about 9 per cent of Mg_2SiO_4 (Fig. 1).

(ii) Between 1200°C and 1500°C, Mg_2SiO_4 olivines dissolve from 27 to 49 per cent of Ni_2GeO_4 (Fig. 1).

(iii) The system is binary in the single-phase fields but ternary in the two-phase field.

Alpha and gamma refractive indices of homogeneous olivine solid solutions have been plotted in Fig. 2 on a mole per cent basis. The variation is linear in the

Table 2. Phase equilibrium data and refractive indices for olivine solid solutions

Composition (mole %)	Temperature ±10°C	Phases present	Refractive index of olivine ±0·01	
			Alpha	Gamma
MS_{100}	1600	Homogeneous olivine	1·635	1·670
$NG_{20}MS_{80}$	1387	Homogeneous	1·687	1·745
$NG_{30}MS_{70}$	1396	Homogeneous	1·711	1·780
$NG_{30}MS_{70}$	1187	Two-phase (just)	1·700	1·750
$NG_{40}MS_{60}$	1187	Two-phase	1·710	1·770
$NG_{40}MS_{60}$	1387	Homogeneous	1·741	1·810
$NG_{45}MS_{55}$	1285	Two-phase	1·725	1·785
$NG_{50}MS_{50}$	1396	Two-phase	1·751	1·810
$NG_{50}MS_{50}$	1500	Two-phase	1·755	1·825
$NG_{50}MS_{50}$	1527	Homogeneous	1·763	1·840
$NG_{50}MS_{50}$	1411	Two-phase	1·740	1·815
$NG_{60}MS_{40}$	1396	Two-phase	1·760	1·820
$NG_{60}MS_{40}$	1411	Two-phase	1·750	1·820
$NG_{60}MS_{40}$	1500	Two-phase	1·765	1·840
$NG_{60}MS_{40}$	1527	Two-phase	1·770	1·855
$NG_{70}MS_{30}$	1411	Two-phase	1·760	1·830
$NG_{70}MS_{30}$	1500	Two-phase	1·770	1·845
$NG_{80}MS_{20}$	1411	Two-phase	1·775	—
$NG_{80}MS_{20}$	1500	Two-phase	1·780	1·855
$NG_{85}MS_{15}$	1470	Two-phase	1·790	1·860

single-phase field. Refractive indices are probably uncertain by ±0·01 because of slight inhomogeneity in the samples and differential volatilization of GeO_2 during formation. This error would tend to make $(\gamma - \alpha)$ values somewhat too high.

Refractive indices of spinel solid solutions are plotted in Fig. 3. The values are the mean of many determinations and are probably internally consistent to ±0·005. Here too, the variation is linear in the single-phase field, within the limits of error of refractive index determination.

Although the system is binary in the single-phase field, it becomes ternary when the two-phase field is entered. This behaviour is due to the ability of Ni^2 and Mg^2 to replace one another in crystals independently of Ge^4 and Si^4. In the single-phase region, Mg^2 and Si^4 can only enter Ni_2GeO_4 in the fixed ratio $(2Mg^2 + Si^4)$. Similarly, in the olivine single-phase field, Ni^2 and Ge^4 can only enter Mg_2SiO_4 in the fixed ratio $(2Ni^2 + Ge^4)$. However, these fixed ratios are not necessary in the two-phase field. Consequently, Fig. 1 can only be used to show the phases

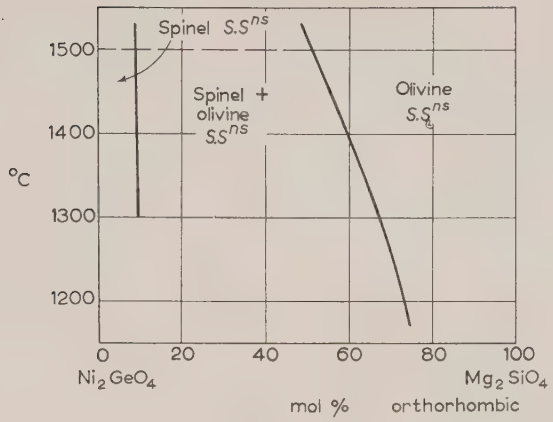

Fig. 1. Sub-solidus phase equilibria in pseudobinary system Ni_2GeO_4—Mg_2SiO_4.

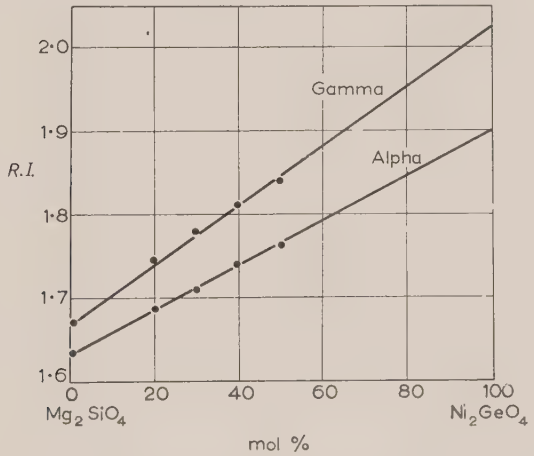

Fig. 2. Alpha and gamma indices of Mg_2SiO_4—Ni_2GeO_4 olivine-type solid solutions.

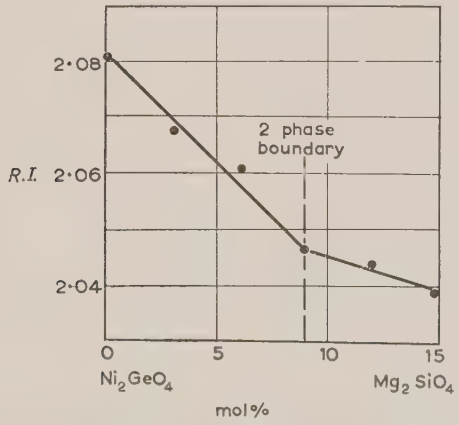

Fig. 3. Indices of refraction of Ni_2GeO_4—Mg_2SiO_4 spinel-type solid solutions.

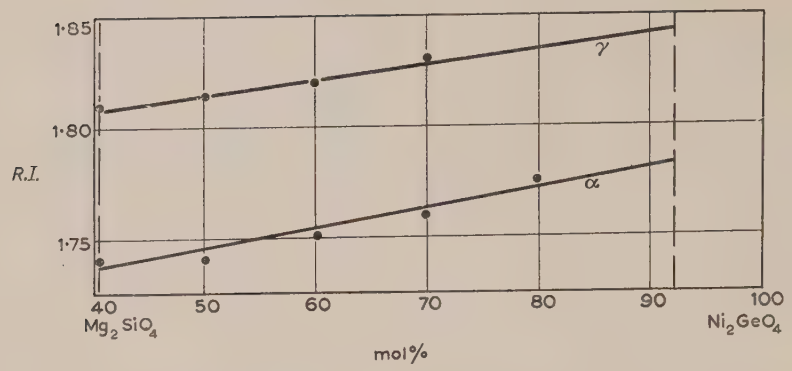

Fig. 4. Alpha and gamma indices of refraction of Ni_2GeO_4—Mg_2SiO_4 solid solutions across two-phase field at 1400°C. Broken lines indicate two-phase boundary.

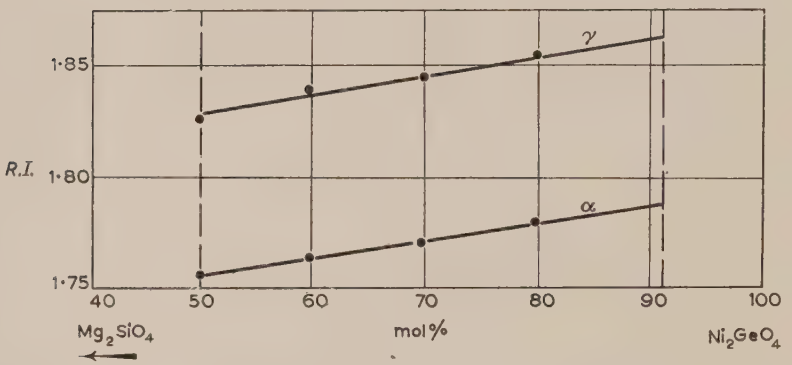

Fig. 5. Alpha and gamma indices of refraction of Ni_2GeO_4—Mg_2SiO_4 solid solutions across two-phase field at 1500°C. Broken lines indicate two-phase boundary.

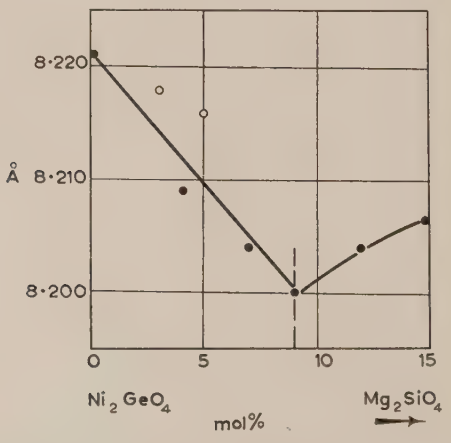

Fig. 6. Lattice constants of Ni_2GeO_4—Mg_2SiO_4 spinel-type solid solutions. Broken line indicates two-phase boundary. O—Anomalous values—see text.

present and their composition in the single-phase region. It does not give compositions of phases in equilibrium in the ternary region.

The effects of this deviation from binary equilibrium are shown in Figs. 3, 4, 5 and 6. In Figs. 4 and 5 refractive indices of olivines are plotted on a mole per cent basis across the two-phase field. Across this field they rise on the average by 0·035. Similarly, the refractive indices of spinels (Fig. 3) continue to decrease when they cross the two-phase boundary, but at a very much reduced rate. The same effect is seen in the lattice parameters of spinel solid solutions, which decrease with increasing content of Mg_2SiO_4 until the two-phase boundary is reached, and then begin to increase very slightly (Fig. 6, Table 3).

Table 3. Lattice parameters of spinel solid solutions

Composition	Å
NG_{100}	8·221
$NG_{97}MS_3$	8·218*
$NG_{96}MS_4$	8·209
$NG_{95}MS_5$	8·216*
$NG_{93}MS_7$	8·204
$NG_{91}MS_9$	8·200
·····Two-phase boundary·····	
$NG_{88}MS_{12}$	8·204
$NG_{85}MS_{15}$	8·206

* These values appear to be anomalous—Fig. 6. The particular samples were prepared by annealing the tablets for 100 hours at 1250°C, followed by crushing and heating for 3 hours at 1450°C. It is possible that equilibrium was not attained during the final heat treatment.

For the purpose of thermodynamic treatment it is necessary to find the composition of the olivine which is in equilibrium with spinel at the two-phase boundary on the spinel side of the diagram. This non-binary behaviour must therefore be analysed in greater detail.

The system NiO—MgO—GeO_2—SiO_2 is a quaternary system which may be expressed in terms of the usual tetrahedral model. A plane through the orthosilicate–orthogermanate composition in the tetrahedron is depicted in Fig. 7. In order to construct the olivine solvus, the compositions of olivines in the two-phase fields of the binary systems NG—MG, and NG—NS at 1500°C are required. These have been obtained (unpublished data) and were found to be $NG_{26}MG_{74}$ in the former system and $NG_{42}MG_{58}$ in the latter. The olivine solvus for the system NG—MS at 1500°C is $NG_{48}MS_{52}$ (Fig. 1). These data enable the olivine solvus for the orthosilicate–orthogermanate plane in the quaternary system to be constructed (Fig. 7). The corresponding spinel solvus has been approximately indicated, the only point known with precision being E, on the join NG—MS.

If the system NG—MS was behaving as a binary, then the spinel at E would be in equilibrium with olivine F on the binary join NG—MS. It was found (Fig. 4), however, that the refractive indices of the olivine in equilibrium with spinel E

($\alpha = 1{\cdot}79$, $\gamma = 1{\cdot}86$) were higher than those of olivine F ($\alpha = 1{\cdot}76$, $\gamma = 1{\cdot}835$). The composition of the unknown olivine must lie along the olivine solvus. The refractive indices of Mg_2GeO_4 (Ringwood, 1956b), Ni_2SiO_4 (Ringwood, 1956a), Mg_2SiO_4, are known, whilst the indices of the fictive olivine type Ni_2GeO_4 can be found by extrapolation (Fig. 2). Accordingly, the refractive index variation of olivines along the olivine solvus can be found and the position of the unknown olivine G thus located.

By this method it is found that spinel of composition $NG_{91}MS_9$ is in equilibrium at 1500°C with olivine of composition $(N_{60}M_{40})_2(G_{45}S_{55})O_4$ along the tie line EG.

The accuracy of this result is determined principally by the probable accuracy

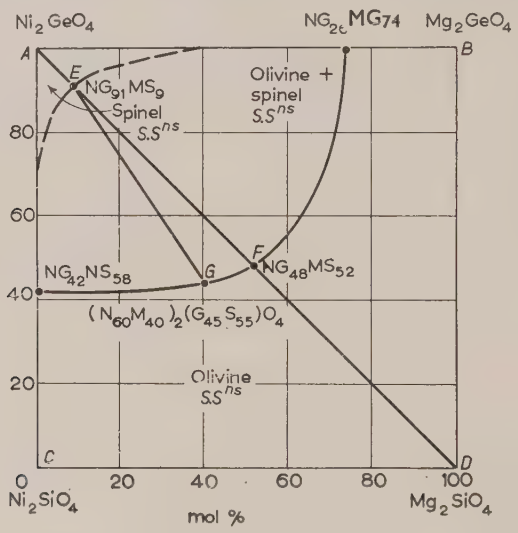

Fig. 7. Sub-solidus phase equilibria at 1500°C in system NG—MG—NS—MS

in measurement of refractive index ($\pm 0{\cdot}01$). This gives rise to a ± 4 per cent uncertainty in the Mg and Si fractions.

The assumption underlying the above derivation is that refractive indices of the solid solutions vary linearly with molar composition. Accumulated data on the optical behaviour of analogous solid solutions, e.g. Winchell (1933), Bowen and Schairer (1935), Ringwood (1956a), Ringwood (1956b), provide ample justification for this assumption. (See also appendix on "ideality".)

In fact, the correction for non-binary behaviour discussed in detail in the previous pages has only a minor effect upon the precision of later calculations compared to other sources of error, since the concentration factor involved is logarithmic. However, it was necessary to determine its order of magnitude.

The composition of the spinel solid solution at the two-phase boundary is $NG_{91}MS_9$ at 1500°C. The uncertainty is estimated at ± 1 per cent Mg_2SiO_4. This value is used as a basis for the calculations in the next section. Compositions at lower temperatures have not been utilized, since it seems doubtful whether true equilibrium was always reached at temperatures below 1350°C.

In most cases, powder patterns of spinel phases gave evidence of slight lattice

distortion. The introduction of Mg_2SiO_4 into the lattice causes a splitting of the high-angle reflection lines. The distortion is very slight—the width of splitting corresponds to a distance smaller than 0·02 Å and the crystals remain isotropic under the microscope. The distortion must involve a reduction in symmetry. This distortion was not found in all samples, and it may be a displacive transition brought on during cooling. The transition is apparently capricious. Quenching specimens from 1350°C failed to stabilize the undistorted form, but sometimes when specimens were annealed for long periods at 1200°C and then heated at 1450°C until equilibrium was reached, undistorted patterns were obtained, which were suitable for lattice constant determination (Table 3).

(c) *Theory*

When Mg_2SiO_4 becomes dissolved in Ni_2GeO_4 the process may be pictured in two stages. First, energy must be supplied to the stable form (olivine) of Mg_2SiO_4 in order to invert it to a hypothetical spinel form. Secondly, both spinels, Ni_2GeO_4 and Mg_2SiO_4, undergo mixing and solid solution. There is a balance between the amount of (free) energy required to perform the inversion and the (free) energy involved in the mixing of Ni_2GeO_4 and Mg_2SiO_4. If the energy of inversion is high, then only a small amount of Mg_2SiO_4 will be able to enter into solid solution. If the inversion energy is low, then a considerable range of solid solutions may be formed. It is clear from this qualitative argument that there is a relationship between the free energy of transition between olivine and spinel Mg_2SiO_4 and the amount of solid solution possible between Mg_2SiO_4 and Ni_2GeO_4. This relationship will now be analysed more rigidly.

In the preceeding section the compositions of coexisting olivine and spinel solid solutions in equilibrium at 1500°C were determined. Mg_2SiO_4 was a component of both solid solutions.

Let μ_1 represent the chemical potential of Mg_2SiO_4 in the olivine phase, and μ_2 represent the chemical potential of Mg_2SiO_4 in the spinel.

$$\therefore \qquad \mu_1 = \mu_1^0 + RT \ln a_1$$

$$\mu_2 = \mu_2^0 + RT \ln a_2$$

where μ_1^0 = chemical potential of the pure olivine form of Mg_2SiO_4 at 1500°C, and μ_2^0 = chemical potential of the pure spinel form of Mg_2SiO_4, whilst a_1 = activity of Mg_2SiO_4 in the olivine phase and a_2 = activity of Mg_2SiO_4 in the spinel phase.

At equilibrium, $\mu_1 = \mu_2$

$$\therefore \qquad \mu_2^0 - \mu_1^0 = RT \ln \frac{a_1}{a_2} = \Delta F^0$$

where ΔF^0 is the difference in chemical potential of the two pure modifications of Mg_2SiO_4, i.e. ΔF^0 is the molar free energy of transition of Mg_2SiO_4 from olivine to spinel at 1500°C.

In order to find the difference in molar free energy between olivine and spinel-type Mg_2SiO_4 it is therefore necessary to determine the activities of Mg_2SiO_4 in

both solid solutions in equilibrium. To obtain these, the assumption is made that the solid solutions are *ideal*. The validity of this assumption is examined in detail in the appendix. In effect, ideality requires that Ni^2 and Mg^2 ions mix randomly at their lattice positions with zero heat of mixing, and likewise for Ge^4 and Si^4.

If the solid solutions behave ideally, then the activity a of an ion becomes equal to its ionic fraction n. The ionic fraction is the ratio of the number of specified ions to the total number of lattice sites available to them.

$$\text{i.e. } a_{Mg} = \frac{n_{Mg}}{n_{Mg} + n_{Ni}} = [Mg]$$

Similar relations hold for a_{Ni}

whilst $$a_{Si} = \frac{n_{Si}}{n_{Si} + n_{Ge}} = [Si] \qquad \text{(similarly for } a_{Ge})$$

The activity of a complex component such as Mg_2SiO_4 is given not by $[Mg_2SiO_4]$, but by $[Mg]^2[Si]$—Tempkin (1945)*.

Accordingly, $$\Delta F^0 = RT \ln \left\{ \frac{[Mg_1]^2[Si_1]}{[Mg_2]^2[Si_2]} \right\} \qquad (1)$$

At 1500°C the composition of olivine and spinel in equilibrium have been determined (see previous section).

$$Mg_2 = 0{\cdot}09, \qquad Si_2 = 0{\cdot}09, \qquad Mg_1 = 0{\cdot}40, \qquad Si_1 = 0{\cdot}55$$

$$R = 8{\cdot}314 \text{ J/mole deg.}$$

Substituting these values in (1), the molar free energy of transition between olivine and spinel type Mg_2SiO_4 may be found.

$$\Delta F^0 = 70{,}000 \text{ J/mole at } 1500°C.$$

When the probable experimental error in composition determination is considered (Section 2b), a value of

$$\Delta F^0 = 70{,}000 \pm 10{,}000 \text{ J/mole at } 1500°C \text{ is found.}$$

The value for ΔF^0 when the composition correction for deviation of olivine from binary composition is not applied is 71,000 J/mole. It appears therefore that the correction calculated in Section 2b was not really significant. It was, however, necessary to determine its magnitude.

3. Effect of Pressure upon Transition

According to Le Chatelier's theorem, increasing pressure should tend to favour the stability of the polymorph with the higher density, in this case the spinel modification.

At the transition point where the two polymorphs are in equilibrium, their free energies (F) are equal.

* This follows, since Mg_2SiO_4 cannot be considered as an individual molecule mixing ideally with Ni_2GeO_4 molecules, in which case Raoult's law would apply, and the activity of Mg_2SiO_4 would be equal to its mole fraction. In this case Mg^2 and Ni^2 ions mix ideally at octahedral lattice sites, whilst Si^4 and Ge^4 are entirely separate, mixing ideally at tetrahedral sites. The entropy of mixing is therefore calculated on an entirely different basis and gives rise to the expression above.

The Gibbs free energy is given by

$$F = E + PV - TS$$

where S = entropy, V = molar volume and E = internal energy.

At equilibrium, $F_1 = F_2$, $P_1 = P_2$, $T_1 = T_2$

$$E_1 + PV_1 - TS_1 = E_2 + PV_2 - TS_2$$

$$(E_1 - TS_1) - (E_2 - TS_2) = P(V_2 - V_1) = P\,\Delta\,V$$

The quantity on the left is the difference in free energy between the two phases at zero pressure, which has already been determined as 70,000 J/mole at 1500°C.

$\therefore$ at equilibrium, $P\Delta V = 70{,}000$

where ΔV is the difference in molar volume between the two polymorphs.

The next step is to find ΔV. The density (and hence the molar volume) of olivine are known. It becomes necessary to find the density of Mg_2SiO_4 spinel. This can be calculated from the lattice constant of the spinel. This quantity may be obtained by several methods.

(a) The lattice constant of $MgSiO_4$ spinel may be derived from data on Ni_2GeO_4—Mg_2SiO_4 solid solutions (Fig. 6, Table 3). The value of the lattice constant of Mg_2SiO_4 spinel found by extrapolation is 7·99 Å. This leads to a spinel density 14 per cent higher than that of the olivine.

This result has been obtained assuming the applicability of Vegard's law—i.e. that the lattice constants of the solid solutions vary linearly with molar composition. This assumption depends upon whether the solid solutions are essentially ideal—a subject which is discussed in the appendix. Anticipating the discussion, it may be said that there is sufficient justification for the application of Vegard's law.

(b) Roy and Roy (1954) have prepared the spinel and olivine modifications of Mg_2GeO_4, a compound closely analogous to Mg_2SiO_4. They found a density difference between the two forms of 8 per cent. Although this does not necessarily imply that the corresponding density difference in Mg_2SiO_4 is also 8 per cent, it furnishes a useful approximation.

Bernal (1936) calculated a density difference of 9 per cent for the olivine - spinel transition based upon X-ray data of Goldschmidt (1931). This data is now known to be inaccurate, and hence the agreement between Bernal's result and that of Roy and Roy is somewhat fortuitous.

(c) Spinel solid solutions of Ni_2SiO_4 in Ni_2GeO_4 have been prepared and their lattice parameters determined (Table 4, Fig. 8). A lattice constant of 8·026 Å for Ni_2SiO_4 spinel is found by extrapolation. Calculations on this basis give rise to a 9 per cent density difference between the olivine and spinel forms of Ni_2SiO_4. The lattice parameters of Ni_2SiO_4 olivine were determined by Taylor (1930).

(d) The olivine–spinel transition in Mg_2SiO_4 involves a rearrangement of oxygen ions into a close-packed cubic structure with the Mg^2 and Si^4 occupying octahedral and tetrahedral holes respectively. In silicates, the nearest approach to the close-packed spinel structure is given by pyrope $Mg_3Al_2(SiO_4)_3$. The

unit cell of pyrope contains 96 oxygen ions and has a lattice parameter of 11·51 Å. If the oxygen ions in Mg_2SiO_4 spinel are as close-packed as in pyrope, the corresponding lattice constant for the spinel (32 oxygen ions per unit cell) would be 7·98 Å, in good agreement with the 7·99 Å deducted by direct extrapolation (Method (a)). This value involves a density difference between olivine and spinel of 14·5 per cent.

Table 4. Lattice parameters of Ni_2GeO_4(NG)—Ni_2SiO_4(NS) solid solutions

Composition	Lattice constant Å
NG_{100}	8·221
$NG_{96}NS_4$	8·216
$NG_{92}NS_8$	8·205
$NG_{90}NS_{10}$	8·201
$NG_{88}NS_{12}$	8·199
NS_{100} (extrap.)	8·026

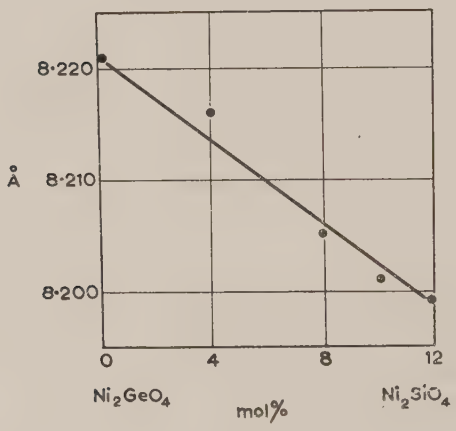

Fig. 8. Lattice constants of Ni_2GeO_4—Ni_2SiO_4 solid solutions.

(e) An approximate lattice constant for Mg_2SiO_4 spinel can be calculated directly, based upon the geometry of the spinel lattice which is constructed from MgO_6 octahedra and SiO_4 tetrahedra. The Mg—O distance in magnesium oxide is 2·10 Å and the O—O distance is 2·60 Å. Using these values, a figure of 8·14 Å is obtained for the lattice constant of Mg_2SiO_4 spinel. This involves a density difference of 8·5 per cent with the olivine. In fact, this derivation assumes an arrangement of perfect tetrahedra and octahedra in the spinel lattice. It is likely that there is some distortion and reduction of bond lengths because of sharing effects leading to a higher density than that calculated. Accordingly, the 8·5 per cent density difference calculated on this basis is likely to prove a minimum estimate.

From the preceding independent methods, the increase in density associated with the olivine–spinel transition may be placed at 11 $\pm$ 3 per cent. This gives rise to a difference in molar volume (ΔV) between the two polymorphs of 4·4 $\pm$ 1 cm^3 at 1 atmosphere pressure. In general, since ΔV is to some extent a function of pressure and temperature, it becomes necessary to investigate the behaviour of ΔV under high P,T conditions. It is a fortunate occurrence that olivines and spinels have characteristically small compressibilities and coefficients of thermal expansion. Because of this, ΔV is relatively unaffected over the wide range of high temperature and pressure conditions which might be expected in the mantle.

Preliminary calculations indicate that Mg_2SiO_4 olivine might be expected to invert to spinel at pressures corresponding to depths of 300–600 km in the mantle. Birch (1952) has calculated the strain of the constituents of the mantle as a function of depth, and finds that the strain at 400 km is about 3 per cent equivalent to a 9 per cent volume decrement.

Accordingly, the difference in molar volume of the two polymorphs in the transition region may be placed at 4·0 $\pm$ 1 cm^3. (This approximation ignores the effect of differing compressibilities for olivine and spinel polymorphs, but trial calculations show that this correction is not significant.)

Accordingly, the difference in free-energy ΔF, due to differential compression of the two polymorphs as a function of pressure, is $P\Delta V = 4{\cdot}0\ P$ cm^3 bar $= 0{\cdot}4\ P$J (P in bars). When ΔF equals the free energy of transition of the two forms at zero pressure, found previously to be 70,000 J at 1500°C, the two polymorphs will be in equilibrium.

$$\therefore \qquad 0{\cdot}40P = 70{,}000$$

$$P = 1{\cdot}75 \times 10^5 \text{ bars}$$

The probable range of error is found calculating the accumulated errors in the various steps which have led to this result. Accordingly, the maximum pressure which is required to produce equilibrium between the two forms is $2{\cdot}33 \times 10^5$ bars, whilst the minimum is $1{\cdot}20 \times 10^5$ bars. Thus the equilibrium pressure for the olivine–spinel transition at 1500°C may be placed at $(1{\cdot}75 \pm 0{\cdot}55) \times 10^5$ bars.

4. Inversion of Olivine in the Mantle

Before these results are applied to the mantle, the effect of other variables must be examined.

The temperature at which the transition pressure was deduced was 1500°C. Most estimates of temperature in the mantle in the region where the transition was predicted range from 1500 to 2500°C (Gutenberg, 1951). Therefore the effect of increasing temperature upon the equilibrium pressure must be examined.

It will be shown in Part II that the effect of increasing temperature above 1500°C will be to increase the free energy of transition. This is due to the fact that olivine has a higher entropy than spinel. Accordingly, the pressure required to cause inversion will be greater than that calculated for temperatures above 1500°C. This aspect will be treated in detail in Part II.

A second factor of some relevance is that the olivine of the mantle probably contains about 5–10 per cent of Fe_2SiO_4 in solid solution. A second component

in a solid solution may raise or lower the transition free energy for the polymorphic inversion of the pure form. The direction in which this particular transition would be affected is not known, but from analogy with solid–liquid phase equilibria, and other polymorphic inversions in ideal solid solutions, the effect is not likely to modify the results previously obtained to any large extent.

There is some evidence that Fe_2SiO_4 may have a greater tendency to take on the spinel structure than Mg_2SiO_4, in which case it would lower the transition free energy. This is suggested by the work of Romeijn (1953), who observed that Ni_2GeO_4 and Co_2GeO_4 both possessed the spinel structure, whilst the stable form of Mg_2GeO_4 possessed the olivine structure. Romeijn suggested that the spinel structure of transition metal ortho germanates may be favoured by a magnetic interaction of the transition ions.

If this is the case with Fe_2SiO_4, the spinel solid solution with Mg_2SiO_4 would have a somewhat greater content of Fe_2SiO_4 than the olivine with which it was in equilibrium. An investigation of this point is at present in progress.

In Part II, it is pointed out that spinels can take into solid solution compounds with ABO_3-type formulae at high temperatures, and that if a spinel–olivine transition occurred in the mantle, the spinel would probably dissolve $MgSiO_3$, and excess Al, Ca, Cr, and Ti which form separate phases in the upper mantle. If this occurs, the preferential solubility of these components in the spinel would have the effect of stabilizing the spinel at the expense of olivine at *smaller* pressures than those previously calculated.

The previous calculations have been made using the assumption of ideality for NG—MS solid solutions. In the appendix, evidence supporting this assumption is cited. However, if some deviation from ideality does occur, it is probable that the deviation would be positive in nature. This would also make the equilibrium transition pressure *smaller* than that calculated.

Conclusions

The preceding calculations indicate that a spinel modification of Mg_2SiO_4 should become thermodynamically stable at 1500°C in the pressure range $(1{\cdot}75 \pm 0{\cdot}55) \times 10^5$ bars. In the mantle these pressures are reached at depths of 500 ± 140 km. The following extraneous factors present could modify the actual depth of transition.

(i) Increase of temperature above 1500°C in the mantle would increase the transition pressure.

(ii) The effect of Fe_2SiO_4 in solid solution is not known. Some evidence suggests it would decrease the transition pressure.*

(iii) The presence of $MgSiO_3$, Al_2O_3, Cr_2O_3, CaO, TiO_2, which are likely to be preferentially soluble in the spinel phase, will decrease the transition pressure.

(iv) Departures from ideality in NG—MS solid solutions will probably decrease the transition pressure.

It therefore seems that these factors if present may have the net effect of decreasing the transition pressure. Accordingly, it is concluded the olivine in the

* Since confirmed (Author's note).

mantle probably begins to invert to spinel at depths less than 500 km. The bearing of this result of the constitution of the mantle is discussed in Part II.

Appendix

Ideal behaviour of solid solutions

An ideal solution is defined as one which obeys Raoult's law—i.e. the activity of a component is equal to its mole fraction. The most important properties of an ideal solid solution are that the mutually replacing ions (or atoms) are distributed at random in their appropriate lattice positions and that the heat of mixing is zero ($\Delta H = 0$). These conditions are likely to be approached most closely when the replacing ions are similar in size and charge.

The following indirect methods enable the ideality of a solid solution to be investigated.

(i) The heat of mixing of the components of an ideal solid solution is zero. Therefore the heats of solution of members of an ideal solid-solution series in a suitable solvent will vary linearly with composition. This may be investigated directly by means of solution calorimetry.

(ii) The volume change of mixing for an ideal solution is zero. Accordingly, the densities of members of an ideal solid-solution series will vary linearly with composition. This may be studied directly, or by X-ray methods. Vegard's law, which states that the lattice parameters of members of an ideal solid-solution series vary linearly with composition, is a consequence of this property.

The volume change of mixing for any solid solution (ΔV) is also a reflection of ΔH. A negative value of ΔV reflects a negative value of ΔH, since it implies that the ions are closer together in the solution due to an increase in bonding energy. The opposite applies for positive values of ΔV.

(iii) If a close resemblance exists between crystal chemical properties and thermochemical properties of components, then a close approach to ideality at high temperature may be expected.

In the case of the olivine and spinel solid solutions under consideration, the discussion may be conveniently broken into three parts, although it should be realized that this division is somewhat artificial.

(a) Data relating to the ideality of the Ni^2—Mg^2 replacement.

(b) Data relating to the ideality of the Ge^4—Si^4 replacement.

(c) Structural effects arising from double replacement in the solid solution—particularly lattice distortion.

(a) *The* Ni^2—Mg^2 *diadochy*. Ni^2 and Mg^2 ions possess the same charges and similar ionic radii ($Ni^2 = 0{\cdot}69$ Å, $Mg^2 = 0{\cdot}66$ Å). Ni^2 has a substantially higher ionization potential resulting in a more pronounced tendency to form bonds with some covalent and directed character. However, in oxide compounds the bonds are octahedrally directed, and since the ionic co-ordination of Ni^2 with oxygen is also octahedral, no complexities are to be expected from this factor. The principal effect is a slight shortening of the effective radius of Ni^2, giving NiO and MgO similar lattice constants.

Calorimetic data are not available for solid solutions of Ni—Mg compounds.

However, heats of solution in hydrofluoric acid have been determined for solid solutions of Fe_2SiO_4—Mg_2SiO_4 and $MgSiO_3$—$FeSiO_3$. Since there is generally a closer resemblance between corresponding Ni^2 and Mg^2 compounds than between Fe^2 and Mg^2 compounds, data upon these Fe^2—Mg^2 solid solutions are illuminating.

Sahama and Torgeson (1949) found that the heats of solution of members of these solid solutions varied linearly between end members. This means that the Mg^2—Fe^2 diadochy must be ideal in these cases. Bowen and Schairer (1935) calculated latent heats of melting from phase equilibria in the system Fe_2SiO_4—Mg_2SiO_4, and from their results concluded that the system behaves ideally. In view of these results, the conclusion seems justified that analogous Ni^2—Mg^2 mix-crystals are probably ideal.

Table 5. Lattice constants of NG—MG and CG—MG solid solutions

NG = Ni_2GeO_4
MG = Mg_2GeO_4
CG = Co_2GeO_4

Composition	Lattice constant (Å)
NG_{100}	8·221
$NG_{90}MG_{10}$	8·224
$NG_{85}MG_{15}$	8·225
MG_{100}(extrap.)	8·25
CG_{100}	8·321
$CG_{90}MG_{10}$	8·314
MG_{100} (extrap.)	8·25

This conclusion is supported by an examination of lattice constants of solid solutions of Mg_2GeO_4 in Ni_2GeO_4 and Co_2GeO_4 (Table 5). The lattice constant of Mg_2GeO_4 spinel has been obtained by extrapolating the values given in Table 5. In both solid-solution series the extrapolated lattice constant is 8·25 $\pm$ 0·02 Å. This agrees with the value of 8·255 Å found directly by Roy and Roy (1954).

In view of the large extrapolation involved, the lattice parameters of the solid solutions must to a high degree vary linearly with composition. A slight deviation from linearity (i.e. from Vegard's law) would have thrown these values far out. Accordingly, the Mg^2—Ni^2 and Mg^2—Co^2 diadochies in germanate spinels probably display a close approach to ideality.

(b) *The* Ge^4—Si^4 *diadochy.* Ge^4 and Si^4 have similar charges, and both tend to form tetrahedrally directed bonds with appreciable covalent character. There are pronounced differences in ionic radii—Si^4 0·42 Å, Ge^4 0·53 Å, but this is not significant, since their bonds with oxygen are only about 50 per cent ionic. When Ge^4 substitutes for Si^4 in a crystal, it has only a small effect on the lattice constants, indicating that Ge^4 and Si^4 have about the same size in crystals (Goldschmidt, 1931).

In Table 6, the melting temperatures of isostructural silicates and germanates are compared. In each case, the m.p. of the germanate is very similar to that of the silicate, and slightly below. The melting temperature of a crystal is a property which is very sensitive to changes in the internal energy balance and distribution within a crystal. The fact that substitution of Ge^4 for Si^4 has such a slight effect on melting point is strong evidence pointing towards the equivalence of Ge^4 and Si^4 in crystals—i.e. of ideality.

Table 6. Melting temperatures of isostructural silicates and germanates (°C)

Mg_2SiO_4	(1)	1890
Mg_2GeO_4		1830
Zn_2SiO_4	(2)	1512
Zn_2GeO_4		1490
$NaAlSi_3O_8$	(3)	1118
$NaAlGe_3O_8$		1067
$KAlSi_3O_8$	(3)	1170
$KAlGe_3O_8$		1122

(1) Ringwood (1956)
(2) Ingerson, Morey and Tuttle (1948)
(3) Goldsmith (1950)

In the former two examples in Table 6, complete solid solutions with very small melting intervals and a continuous melting curve of the Roozeboom I type are found. With regard to these, Goransen (1942) has stated: "However, it is found from a study of silicate equilibria relations that systems which are miscible in the solid as well as the liquid state approach this condition of ideality, and when miscible in all proportions both in the liquid and solid state may be treated as ideal".

Further evidence of ideality may be derived from Ni_2GeO_4—Ni_2SiO_4 spinel solid solutions (Table 4, Fig. 8). In Section 3 it was shown that the calculated density difference between Ni_2SiO_4 spinel and olivine based upon the above results was 8·5 per cent. This figure is consistent with the corresponding values obtained by several independent methods and suggests that the Ge—Si diadochy in the spinel must be obeying Vegard's law.

(c) *Structural effects arising from double replacement in the solid solution.* In the previous sections, evidence has been put forward indicating that when Ni^2—Mg^2 or Ge^4—Si^4 replacement occurs separately in crystals, the replacement is essentially ideal. On general grounds, therefore, it would be expected that when double replacement occurs—i.e. when Ni^2Ge^4 replace Mg^2Si^4, the replacement would also approach ideality. This is indicated by the lattice constant data for the NG—MS spinel solid solutions. The lattice constant for Mg_2SiO_4 spinel found by extrapolation leads to results for the density difference between spinel and olivine Mg_2SiO_4 which are in reasonable agreement with the corresponding density

differences found by other methods (Section 3). This implies that Vegard's law is being accurately obeyed and that the double replacement is essentially ideal at high temperatures.

However, at low temperatures the NG—MS spinels are found to be slightly distorted (Section 2b). This is indicated by splitting of high-angle diffraction lines, corresponding to differences in interplanar spacing of 0·02 Å. This distortion therefore involves a reduction of symmetry. The amount of distortion is, however, very small and unlikely to affect free-energy relationships to any significant degree. At high temperatures the distortion evidently disappears, giving rise to a normal series of spinels (Table 3).

This distortion may cause a positive deviation from ideal behaviour. Although separate replacement of Ni^2 by Mg^2 and Ge^4 by Si^4 might be ideal, it can happen that when two foreign ions such as Mg^2 and Si^4 are introduced simultaneously into a lattice, some strain is set up. This is because lattice stabilities are dependent upon ionic radius ratios, and although Mg^2 and Si^4 might be able to fit satisfactorily into a spinel lattice structure separately, the radius ratio Mg^2/Si^4 is such that some strain is introduced when both enter together. This has apparently happened here. Solution of Mg^2 and Si^4 separately is found not to cause splitting.

Although the conclusion is drawn that high-temperature solid solutions of Ni_2GeO_4 and Mg_2SiO_4 are probably essentially ideal, the above point is important, since it indicates that *if deviation from ideality did occur, the deviation is most likely to be positive in nature*, i.e. tending towards segregration of phases.

The calculations in Section 2c show that the effect of this non-ideal behaviour will be to produce inversion from olivine to spinel at a *shallower* depth in the mantle than is found assuming ideal behaviour.

Acknowledgements—The author is greatly indebted to Mr. A. J. Gaskin of C.S.I.R.O., Mr. G. M. Willis of the Metallurgy Department, Prof. J. S. Anderssen, F.R.S., of the Chemistry Department, Melbourne University, and to Prof. J. B. Thomson of the Geological Department, Harvard University, for the benefit of constructive criticism and helpful discussion. He also acknowledges gratefully the encouragement given to the project by Prof. E. S. Hills, F.R.S., of the Geology Department, Melbourne University.

References

Bernal J. D. (1936) *Observatory* **59,** 268.
Birch F. (1952) *J. Geophys. Res.* **57,** 227.
Bowen N. L. and Schairer J. F. (1935) *Amer. J. Sci.* **29,** 151–217.
Goldschmidt V. M. (1931) *Nachr. Ges. Wiss. Göttingen.* **1,** 184.
Goldsmith J. R. (1950) *J. Geol.* **58,** 518.
Goransen R. (1942) *Handbook of Physical Constants.* Bull. Geol. Soc. Amer. Spec. Paper No. 36, p.226.
Gutenberg B. (1951) *Internal Constitution of the Earth* Chap. 7. Dover. Pub. Inc.
Ingerson E, Morey G. W. and Tuttle O. F. (1948) *Amer. J. Sci.* **246,** 31.
Jeffreys H. (1952): *The Earth* (3rd ed.). Cambridge Univ. Press.
Ringwood A. E. (1956a) *Geochim. et Cosmochim. Acta* **10,** 297.
Ringwood A. E. (1956b) *Amer. J. Sci.* **254,** 707.
Ringwood A. E. (1956c) *Nature. Lond.* **178,** 1303.
Romeijn F. C. (1953) *Phillips Res. Rep.* **8,** 304.

Roy D. M. and Roy R. (1954) *Amer. Min.* **39,** 957.
Sahama Th. G. and Torgeson D. R. (1949) *J. Geol.* **57,** 255.
Taylor N. W. (1930) Die kristallstrukturen des verbindungen Zn_2TiO_4, Zn_2SnO_4, Ni_2SiO_4, $NiTiO_3$. *Z. Phys. Chem.* B. **9,** 241.
Tempkin M. (1945) *Acta Physicochem. U.R.S.S.* **20,** 411.
Winchell A. N. (1933) *Elements of Optical Mineralogy* Part II. John Wiley, New York.

Geochimica et Cosmochimica Acta, 1958, Vol. 13, pp. 322 to 334. Pergamon Press Ltd., London

The concentration and isotopic abundances of atmospheric carbon dioxide in rural areas

Charles D. Keeling*
Division of Geological Sciences, California Institute of Technology, Pasadena, California

(*Received* 6 *June* 1957)

Abstract—Fifty samples of rural air collected near the Pacific coast of North America have been analysed for carbon dioxide reporting, in addition to concentration in air, the isotopic abundances of C^{13} and O^{18}. A correlation observed for all samples between C^{13} isotope abundance and concentration in air can be explained by assuming an initial composition for atmospheric carbon dioxide of 0·031 volume per cent in air, C^{13}/C^{12} ratio −7·0 per mil., to which is added carbon dioxide of plant origin with a ratio of approximately −23 per mil. Minimum concentrations and associated carbon isotope ratios at different stations show very little variation (0·0307–0·0316 per cent, −6·7 to −7·4 per mil) and are believed to be representative of Pacific maritime air. Oxygen isotope abundances are approximately the same as for carbon dioxide in chemical equilibrium with average ocean water, but individual samples show variations which generally do not correlate with changes in concentration in air and are as yet unexplained.

Introduction

Carbon dioxide in the atmosphere has been studied for more than a hundred years. Nineteenth century measurements showed its concentration to vary, especially over continental areas. Causes for variation were not always understood, but the activity of plants explained the diurnal periodicity often observed for rural air, and the burning of fuel accounted for the high values of urban air reported (Lundegårdh, 1924, Chapter 1). New data in this century have confirmed these general features of continental air (Hutchinson, 1953), and more extensive measurements over the open ocean have established smaller but still significant variations for ocean air (Buch, 1939, 1948). No accurate measurements have been reported for air far enough above the earth's surface to be completely removed from local influences. For this reason the often quoted figure of 0·03 per cent for the mean concentration of atmospheric carbon dioxide is only a rough approximation.

Several investigators have measured the abundance of the C^{13} isotope of atmospheric carbon dioxide and have shown that the carbon is appreciably lighter (lower C^{13}/C^{12} ratio) than that of the bicarbonate of natural waters or that of the carbonate of marine sediments. The first isotope measurements (Murphy and Nier, 1941) are probably somewhat in error because of an isotopic effect attending the absorption of the carbon dioxide in hydroxide solution, but the recent measurements of Craig (1953) employing carbon dioxide condensed from air at liquid nitrogen temperature are believed to be correct. The present study was undertaken to determine what relationships might exist between variations in concentration and variations in the isotopic ratios of carbon dioxide in the atmosphere. To investigate the problem systematically, Craig's extraction method was modified to shorten the time required to process individual samples, oxygen isotope measurements were instituted, and a manometer was constructed to measure accurately the quantity of carbon dioxide for each sample.

* Present address: Scripps Institution of Oceanography, University of California, La Jolla, California.

Experimental

Air samples were collected in evacuated five litre flasks under circumstances where local human influences were not likely to affect the air being sampled. Simultaneously with collection, the temperature and, where possible, humidity, wind, and barometric pressure, were recorded. The flasks were returned to the laboratory where the carbon dioxide was extracted and prepared for mass spectrometer analysis. Sample flasks were attached to a vacuum line, the sample pressure and temperature measured under laboratory conditions, and the sample pumped through a large spherical liquid nitrogen trap at reduced pressure. The condensate was freed from water-vapour by fractional distillation at dry ice temperature and the resulting gas, which could be verified by mass spectrometric analysis to be pure carbon dioxide, was condensed in a constant volume manometer constructed after a design of Germann (1914), where the quantity was measured. The purified gas was analysed in a modified double collector mass spectrometer as described by McKinney *et al.* (1950)

Isotope measurements are expressed per mil by the function:

$$\delta = \left(\frac{R_{\text{sample}}}{R_{\text{standard}}} - 1 \right) 10^3$$

where R is the absolute ratio of the abundance of two isotopes being compared. Differences in carbon-13 abundance between sample and standard are reported in terms of the relative carbon isotope ratio, δC^{13}, for which $R = C^{13}O^{16}O^{16}/C^{12}O^{16}O^{16}$, differences in oxygen-18 abundance in terms of δO^{18} for which $R = C^{12}O^{16}O^{18}/C^{12}O^{16}O^{16}$. The δ values were calculated from the experimental mass ratios 46/44 and 45/44 of sample and standard carbon dioxide gas by a method explained in detail by Craig (1957). The standard carbon dioxide gas to which analyses are referred is prepared from a particular sample of calcium carbonate obtained from a belemnite of the Pee Dee formation (Chicago standard "*PDB*-1") which has been previously employed as a primary standard by Craig (1953, 1957), Epstein and Mayeda (1953), and Jeffery (1955).

Carbon dioxide concentrations are reported as parts per million (p.p.m.) of original air by volume (M_{CO_2}), water-vapour concentrations as volume per cent of original air (M_{H_2O}). Carbon dioxide concentrations in parts per million of dry air are also reported for samples for which humidity data are available.

Isotope ratios are considered to be accurate to $\pm 0{\cdot}20‰$ although analyses frequently agree within $\pm 0{\cdot}05‰$. Carbon dioxide concentrations are considered to be accurate to $\pm 1{\cdot}0$ p.p.m.

Analysis of Data

The results of sampling at rural stations in Washington and California are presented in Table 1. Diurnal graphs of concentration and isotopic abundance for each station have been prepared to illustrate the data (Figs. 1–6). These data exhibit two salient features: minimum concentrations are nearly the same at all stations (Fig. 7); variations in the carbon isotope ratio are proportional to the reciprocal of molar concentration, i.e.

$$\delta C^{13} = I(C^{13}) + M(1/\mu_{CO_2}). \qquad (1)$$

The smooth curves in Figs. 8 and 9 represent this relationship with coefficients $I(C^{13})$ and M calculated from the experimental data by the method of least-squares (Worthing, 1943) separating the California and Washington data.

Values of $I(C^{13})$ and the average experimental deviation of δC^{13} from the least square relationship, separating the data of each station, are presented in Table 2, together with observed minimum concentrations and associated isotope ratios at each station. The average deviation of δC^{13} is nearly within experimental error

Table 1. Carbon dioxide composition and meteorological data for rural air*

California stations	Local time (hr min)	Air temp. (°C)	Wet bulb temp. (°C)	Rel. hum. (%)	μ_{H_2O} (vol. %)	Bar. press. (mm/Hg)	Wind (speed and direction) (knots)	Cloud (fraction and type)	μ_{CO_2} (moist) (p.p.m)	μ_{CO_2} (dry) (p.p.m)	δC^{13} (‰)	δO^{18} (‰)
Big Sur State Park	12·15	24·7	15·3	34	1·05	754·0	2–4	clear	316·0	319·3	−7·41	+1·15
Elevation 70 m (coastal	18·15	18·3	14·4	66	1·38		calm	clear	321·0	325·5	−7·47	+1·16
redwood grove, 1 m above Big	20·15	13·9	12·2	82	1·30		calm	clear	339·4	343·9	−8·36	+1·57
Sur River on footbridge,	22·00	12·8	11·7	88	1·30		calm	clear	366·0	370·8	−9·43	+1·60
18–19 May 1955)	2·30	10·0	10·0	100	1·22		calm	clear	368·9	373·4	−9·80	+0·78
	5·30	8·3	8·3	100	1·09		calm	clear	388·6	392·9	−10·38	+1·14
	6·30	8·3	8·3	100	1·09		calm	clear	383·2	387·5	−10·18	+1·09
	8·30	15·6	13·3	78	1·38		calm	clear	344·7	349·5	−8·40	+1·47
	11·30	25·6	17·8	46	1·50		calm	clear	329·8	334·8	−7·80	+1·23
Yosemite National Park	10·00	11·1	5·0	41	0·68	606·0	—	clear	321·4	323·6	−7·43	+0·04
Tamarack Flats, elevation	12·30	12·8	8·3	58	1·06		—	clear	312·9	316·2	−7·06	+1·31
1950 m (west slope of Sierra	18·00	10·6	7·8	71	1·12		—	clear	333·8	337·6	−8·07	+1·37
Nevada mountain range in	22·00	3·9	3·9	100	1·00		—	clear	356·1	359·7	−8·86	+2·86
mixed conifer forest, 1 m	2·30	0·6	0·6	100	0·79		—	clear	356·0	358·8	−9·04	+1·95
above Tamarack Creek on	5·45	0·6	0·6	100	0·79		—	clear	363·3	366·2	−9·36	+1·68
footbridge, 2–3 June 1955)	8·00	3·9	3·3	92	0·92		—	clear	360·8	364·2	−9·03	+1·34
Yosemite National Park	10·00	10·6	3·9	33	0·63	567·0	—	clear	313·9	315·9	−7·04	+0·55
Lake Tenaya, elevation												
2500 m (50 m west of lake on												
open granite field, 3 June												
1955)												
Yosemite National Park	11·45	11·7	—	—	—	529·0	—	clear	318·3	319·8	−7·20	+0·35
Tioga Pass, elevation 3000 m												
(100 m north of pass on snow												
field, 3 June 1955)												
Inyo Mountains	2·00	−2	—	—	—	482·8	SW 8	clear	311·5	—	−6·88	+0·07
Mt. Barcroft Station, elevation	8·30	1	—	—	—	482·9	W 10	clear	313·3	—	−6·98	+0·07
3800 m (100 m west of building	13·45	9	—	—	—	483·3	W 11	clear	313·5	—	−6·90	+0·32
on snow field, 8 July 1955)												
Inyo Mountains	18·30	9	—	—	—	483·8	W 23	clear	313·7	—	−6·94	+0·63
Mountain Divide, elevation	22·00	3	—	—	—	482·9	SW 10	clear	315·2	—	−7·09	+0·43
4000 m (1 km north of Mt.	2·00	1	—	—	—	482·1	SW 14	0·5 Ci	317·6	—	−7·15	+0·39
Barcroft station on top of	6·00	2	—	—	—	—	SW 16	0·5 Ci	319·2	—	−7·01	+0·44
rock pile, 8–9 July 1955)	11·30	6	—	—	—	480·9	S 6	0·5 Ci	316·4	—	−7·19	+0·27
	15·15	7	—	—	—	481·2	SW 7	0·5 Ci	314·5	—	−7·13	+0·23

elevation 4300 m (on top of rock pile, 9 July 1955)	14·00	0	—	—	—	—	—	0·5 Ci	313·5	—	−7·04	+0·32
Washington stations												
Hart's Pass	13·00	20·0	—	—	—	—	W 5–10	clear	313·7	—	−7·41	−0·45
Elevation 1900 m (crest of	18·30	12·2	—	—	—	—	0–1	clear	311·7	—	−6·98	−0·21
Cascade Mountains, in middle	23·00	6·7	—	—	—	—	calm	clear	321·4	—	−7·38	−0·30
of gravel road, 31 August–	5·45	5·6	—	—	—	—	calm	clear	319·7	—	−7·51	−0·27
1 September 1955)	14·00	18·9	—	—	—	—	W 2–5	clear	307·4	—	−6·84	+0·08
Olympic National Park	9·45	12·2	—	100	—	—	S 5–10	clear	309·6	314·1	−6·88	+0·29
Beach Trail no. 6, elevation	Next day											
sea level, (Pacific coast, on	15·15	14·4	—	100	—	—	SW 10–15	1·0 St	308·7	313·8	−6·85	−0·21
sand beach, 6–7 September 1955)												
Olympic National Park	13·00	18·9	—	68	1·77	765·0	calm	1·0 Sc rain at 14·00	346·2	352·5	−8·45	+0·20
Hoh River Ranger Station, elevation 170 m (500 m												
northwest of ranger office, in	17·30	17·2	—	75	1·70	748·0	calm	0·4 Sc	343·0	348·9	−8·07	+0·49
dense rain forest, 1 m above	21·30	12·8	—	94	1·50	760·5	calm	clear	332·3	337·4	−7·97	−0·16
Taft Creek on footbridge,	1·45	13·1	—	100	1·50	759·7	calm	1·0 Sc	404·1	410·2	−10·79	−1·93
6–7 September 1955)	6·15	12·5	—	100	1·46	759·2	calm	1·0 Sc	392·3	398·2	−10·54	−1·79
	9·15	13·1	—	100	1·50	759·5	calm	0·7 Sc	382·0	387·9	−9·77	−1·69
	13·00	15·8	—	69	1·33	759·2	S 1–2	1·0 Sc	308·5	312·6	−6·66	+0·43
Rock Lake	14·45	29·4	—	—	—	—	SW 5–10	clear	312·3	—	−6·99	+0·17
Elevation 600 m (2 km from	18·00	29·2	—	—	—	—	calm	clear	311·9	—	−7·01	+0·13
north end of 1 x 30 km lake	22·30	14·7	—	—	—	—	E 0–1	clear	328·4	—	−7·93	−0·49
on west sloping hill above	2·30	11·1	—	—	—	—	E 0–1	clear	336·3	—	−8·23	−0·63
lake, in very dry grassland	6·00	11·1	—	—	—	—	E 2–4	clear	319·4	—	−7·49	−0·03
with scattered pine trees in	9·30	15·6	—	—	—	—	SW 5–15	clear	311·0	—	−6·85	+0·19
lake basin area. Air collected 0·3 m above roof of low shack, 10–11 September 1955)	12·30	21·9	—	—	—	—	SW 5–15	clear	309·4	—	−6·83	+0·36

**Big Sur and Yosemite stations:* air temperature and wet bulb by sling psychrometer to ±0·5°F (±0·3°C); mean barometric pressure for station estimated from altitude by an approximate barometric formula, value used in determining relative humidity. *Inyo Mountain stations:* air temperature by mercury thermometer to ±0·5°C; barometric pressure by mercury barometer to ±0·1 mm/Hg; wind vector by recording cup anemometer and wind vane. *Hart's Pass, Olympic and Rock Lake stations:* air temperature by mercury thermometer to ±0·3°C. *Olympic stations:* humidity based on dry and wet bulb readings measured at Hoh River Ranger Station, humidity assumed at Beach Trail no. 6, barometric pressure by aneroid barometer to approximately ±0·01 in/Hg (±0·3 mm/Hg). At all stations except Inyo Mountains, wind vector estimated visually. Cloud estimated visually at all stations: Ci = cirrus, Ac = altocumulus, Sc = stratocumulus, St = stratus, m = meter, km = kilometre.

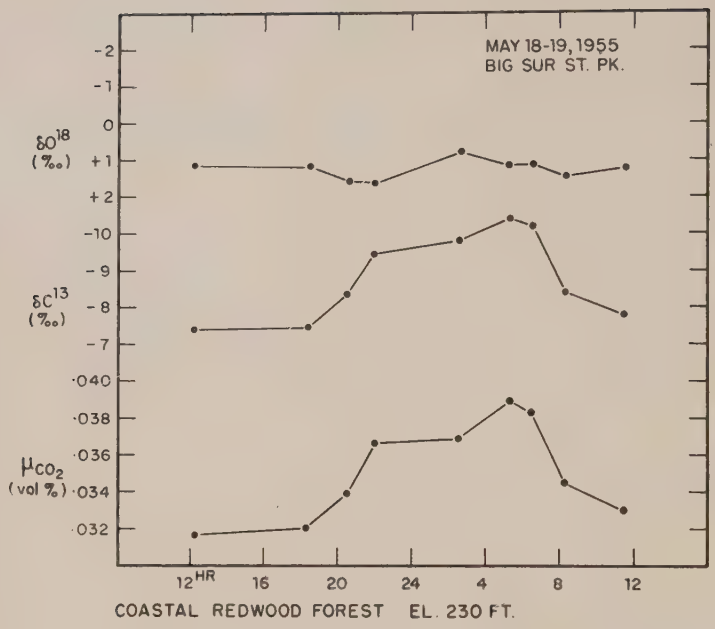

Fig. 1. Diurnal variation in the concentration and isotope ratios of atmospheric carbon dioxide in a coastal redwood forest of California.

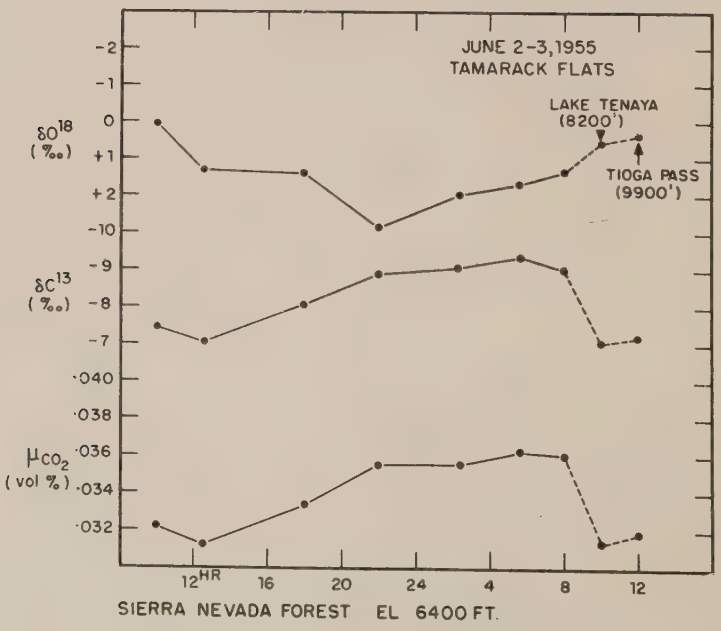

Fig. 2. Diurnal variation in the concentration and isotope ratios of atmospheric carbon dioxide in a forest of the Sierra Nevada.

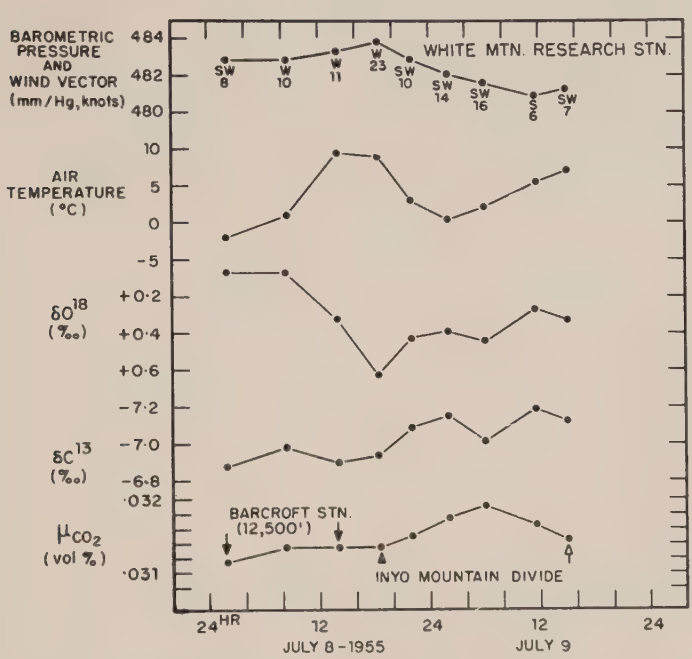

Fig. 3. Diurnal variation in the concentration and isotope ratios of atmospheric carbon dioxide and variations in barometric pressure, wind vector, and air temperature over barren ground near White Mountain Research Station in the Inyo Mountains of California.

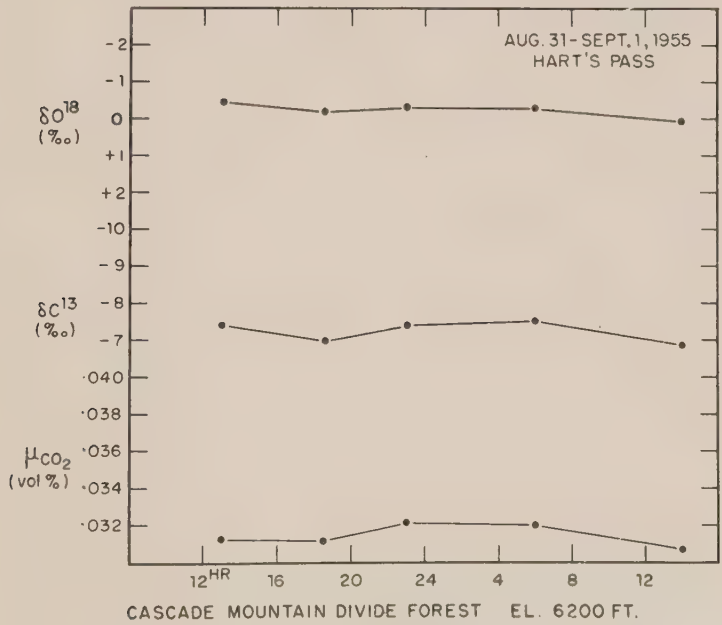

Fig. 4. Diurnal variation in the concentration and isotope ratios of atmospheric carbon dioxide in a forest at the crest of the Cascade Mountain range of Washington.

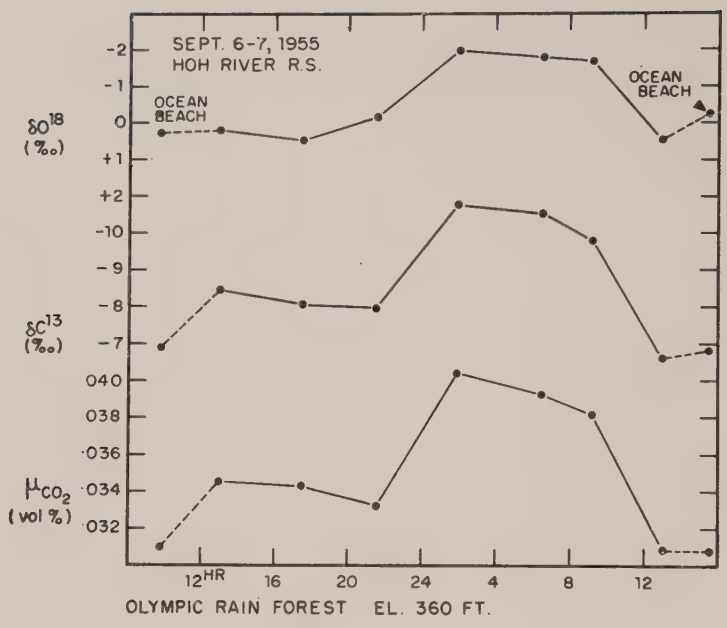

Fig. 5. Diurnal variation in the concentration and isotope ratios of atmospheric carbon dioxide in a rain forest of the Olympic Peninsula of Washington.

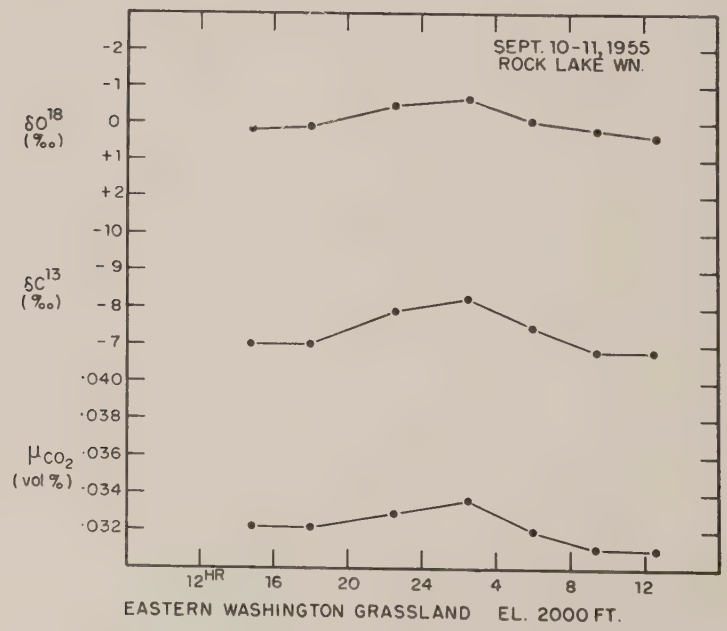

Fig. 6. Diurnal variation in the concentration and isotope ratios of atmospheric carbon dioxide in grassland of eastern Washington.

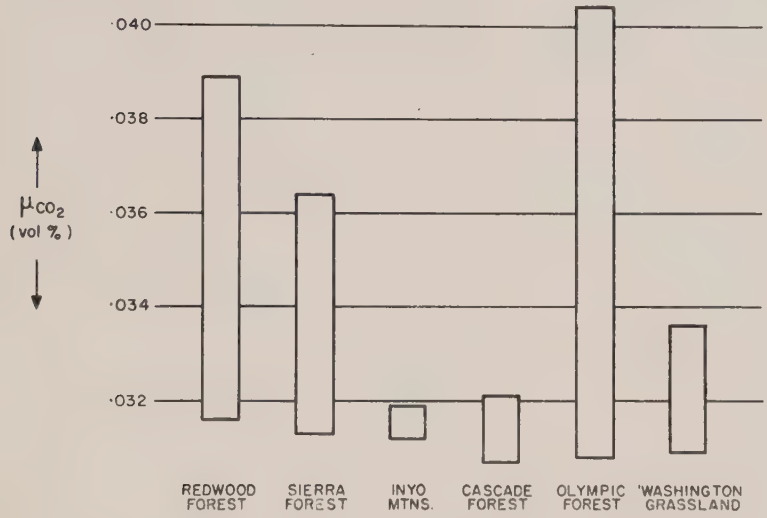

Fig. 7. Range in concentration of atmospheric carbon dioxide at various stations in Washington and California.

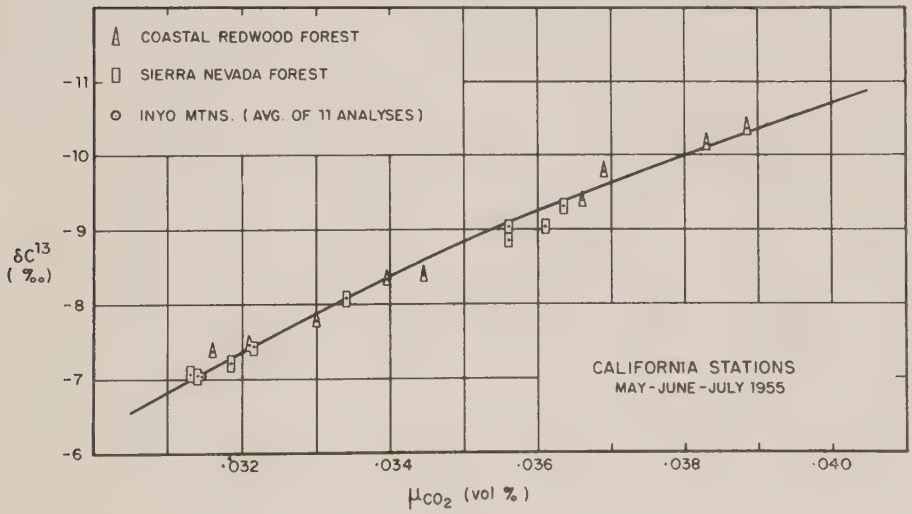

Fig. 8. Relation between carbon isotope ratio and concentration of atmospheric carbon dioxide for California stations.

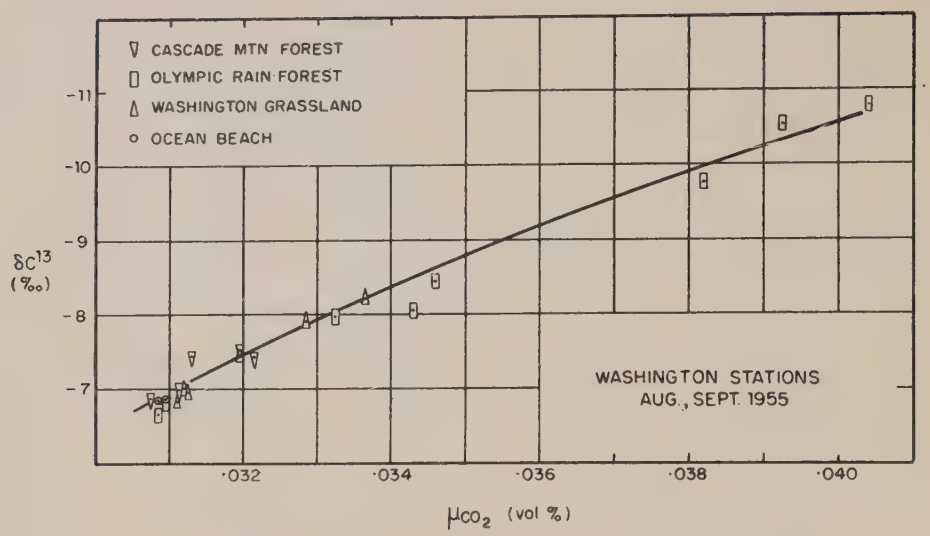

Fig. 9. Relation between carbon isotope ratio and concentration of atmospheric carbon dioxide for Washington stations.

at all stations. Minimum concentrations and carbon isotope ratios fall in a narrow range (307 to 316 p.p.m., −6·7 to −7·4‰), oxygen isotope ratios in a somewhat wider range (+1·2 to −0·2‰). Average minimum concentrations and associated carbon isotope ratios for forest and grassland stations (311 p.p.m., −6·96‰) agree closely with values for stations over barren ground (312 p.p.m., −6·92‰), oxygen isotope ratios agree less closely (+0·67 and +0·14‰, resp.).

At Washington stations, variations in the oxygen isotope ratio appear to be nearly proportional to concentration (Fig. 10) although values scatter more than

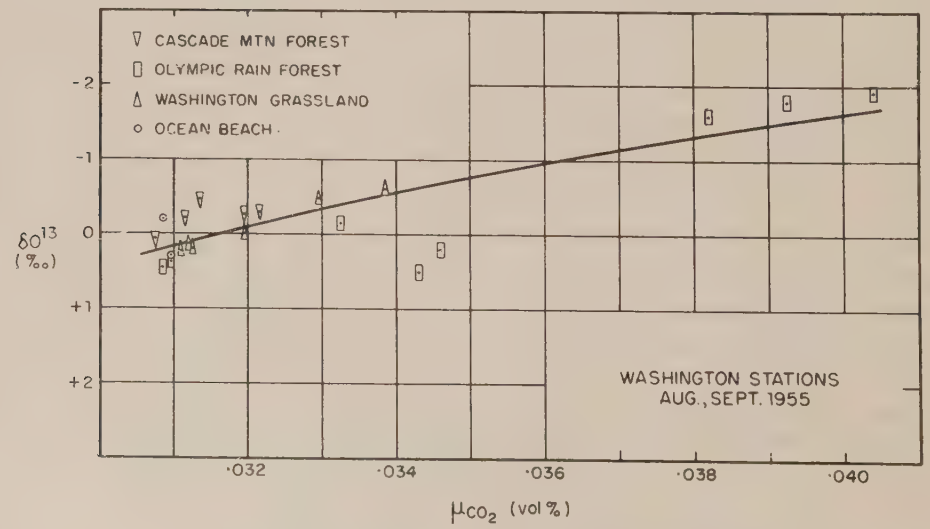

Fig. 10. Relation between oxygen isotope ratio and concentration of atmospheric carbon dioxide for Washington stations.

Table 2. Characteristic composition of atmospheric carbon dioxide

Station	Month of 1955	Minimum μ_{CO_2} (p.p.m.)	δC^{13} at minimum μ_{CO_2} (‰)	δO^{18} at minimum μ_{CO_2} (‰)	$I(C^{13})$ (‰)	$I(O^{18})$ (‰)	Av. dev. in δC^{13} (‰)	Av. dev. in δO^{18} (‰)	No. of analyses
Forest or Grassland									
Big Sur State Park	May	316	−7·41	+1·15	−24·1	—	0·098	—	9
Yosemite National Park	June	313	−7·06	+1·31	−23·1	—	0·076	—	7
Hart's Pass	August	307	−6·84	+0·08	−21·0	−6·4	0·120	0·116	5
Olympic National Park	September	309	−6·66	+0·43	−24·2	−10.9	0·134	0·39	7
Rock Lake	September	309	−6·83	+0·36	−25·0	−11·7	0·046	0·047	7
Barren Ground									
Yosemite National Park	June	314	−7·04	+0·55	—[a]	—	—[b]	—	2
Inyo mountains	July	312	−6·88	+0·07	—[a]	—	0·063	—	11
Olympic National Park	September	309	−6·85	−0·21	—[a]	—	—[b]	—	2

[a] Concentration variation too small to establish value.

[b] Insufficient data to establish value.

for carbon. Values of $I(O^{18})$ based on a relationship for oxygen analogous to equation (1) have been calculated for these stations by the method of least squares and appear in Table 2. The average experimental deviation of δO^{18} is nearly the same as for δC^{13} at two stations but is considerably greater at the other (Olympic rain forest). For California stations no proportionality with concentration is apparent at all, but for the Inyo mountain station a correlation may exist between the oxygen isotope ratio and barometric pressure (Fig. 3).

Discussion

Rural air samples were all collected from the layer of air close to the ground, and, except for Inyo Mountain and ocean beach samples, were collected under circumstances where the metabolic activity of plants might be expected to influence the carbon dioxide composition of the air. This is so because plants exchange carbon dioxide with the atmosphere by means of respiration and assimilation and also because carbon dioxide is evolved from the ground through decay of organic material in the soil and respiration of plant roots. Air was sampled at least three metres from any living plants to be out of range of extremely local carbon dioxide gradients. In three cases (coastal redwoods, Sierra Nevada forest, Olympic rain forest) a bridge over a small stream afforded a good location, conveniently removed from low lying plants but at the same elevation as ground level air in the vicinity of the stream. In another instance (Washington grassland) the roof of a low shed beside a railroad track was used; at Hart's Pass (Cascade mountain crest) the middle of a dry gravel road. At all these five stations the data suggested minimum carbon dioxide concentrations in the afternoon and maximum concentrations in the late evening or early morning hours. Similar alternations have almost always been noted in the carbon dioxide content of air over land. Numerous observations going back to the early nineteenth century indicate the generality of this effect (Lundegårdh, 1924), and with little doubt, it may be attributed to the metabolic activity of terrestrial plants and the respiration of the soil.

The pronounced regularity with which the carbon isotope ratio follows changes in carbon dioxide concentration suggests a simple cause for mutual variation in these quantities. When to air is added carbon dioxide differing in carbon isotopic abundance by a constant amount from the carbon dioxide initially present in the air, changes in the carbon isotope ratio of the total atmospheric carbon dioxide will be proportional to the reciprocal of molar concentration. If equation (1) is used to describe this relationship, the carbon isotope ratio of the carbon dioxide which brings about the change in concentration will be equal to the term, $I(C^{13})$. Computed values of this term vary, for different stations, from -21 to $-25‰$, a range in isotope ratio which agrees well with the range found generally for the carbon of terrestrial plants (Wickman, 1952; Craig, 1953). Thus the relationship between carbon isotope ratio and molar concentration observed for the carbon dioxide of rural air is explained if carbon dioxide is added to or subtracted from the atmosphere by plants or their decay products.

On the other hand, the uniform concentration and carbon isotope ratio of afternoon air samples cannot be primarily a result of biological activity. In a

restricted air supply but under average conditions of light, temperature and mineral fertilization, plants are able to reduce the concentration of carbon dioxide to significantly lower values than have ever been observed under natural conditions (Egle and Schenk, 1952), and until the minimum concentration is reached where plant assimilation and respiration of carbon dioxide just balance, there is no known biological regulatory process which will predict the same concentration of carbon dioxide for such widely varied plant environments as are represented in the present data. The observed uniformity must therefore be a result of some rather general meteorological circumstance which operated at the times when these samples were collected. Such a recurring characteristic composition strongly implies that all local influences of vegetation have been wiped out at these times by mixing of ground level air with air from above or beyond the zone of vegetation influence, and that this mixed air over these rather widely separated stations during several months of the year, at least, was conspicuously constant in carbon dioxide composition. At several locations samples were deliberately taken under circumstances where vegetation would have no influence on the air even near the ground. The data for the Olympic beach station represents air blowing briskly off the Pacific Ocean. In the Inyo Mountains and Sierra Nevada (Lake Tenaya and Tioga Pass) air was collected above almost completely barren ground and always in a good wind. The concentrations and carbon isotope ratios at these stations agree very closely with those of forest and grassland stations at times of minimum concentration (Table 2). The concentrations are consistent with those of maritime polar air collected north of Iceland with a range 309–317 p.p.m. (Buch, 1948) and, quite probably, the data represent a carbon dioxide composition characteristic of the maritime polar air which is nearly always present over the Pacific coast of North America (Pettersen, 1940, p. 165).

Oxygen isotope ratios agree approximately with carbon dioxide in equilibrium with mean ocean water at 25°C, for which $\delta O^{18} = -0{\cdot}1‰$) (Epstein and Mayeda, 1953, as corrected by Craig, 1957). Samples associated with minimum concentrations range from $+1{\cdot}3$ to $-0{\cdot}2‰$, forest and grassland samples from $+2{\cdot}9$ to $-1{\cdot}9‰$.

Most of the individual values do not appear to correlate with any measured meteorological or chemical quantity, but an interesting relationship is suggested by the data for the Inyo Mountains. During the period before the passage of a pressure wave, indicated by maximum barometric pressure near 18·00 on 8 July, the oxygen isotope ratio changed noticeably, reflecting the change in barometric pressure, while the carbon isotope ratio and carbon dioxide concentration were constant within the precision of measurement. The slight rise in concentration after the maximum pressure was reached was reflected in the carbon isotope ratio but appeared to have only a small influence on the oxygen isotope ratio which continued to follow the barometric pressure. The effect, if real, must be explained by a process which affects only the oxygen isotope ratio. The isotopic equilibrium of the oxygen of carbon dioxide with the oxygen of ocean water is such a process. Since the equilibrium fractionation between phases is temperature dependent with a coefficient of approximately $-0{\cdot}2$ per thousand per degree centigrade (Urey, 1947), a correlation with barometric pressure could be the result of partial

mixing of air from different air masses which were equilibrated with water of differing oxygen isotopic composition or at different temperatures.

Acknowledgements—The author thanks those who co-operated or assisted in the collection of air samples, especially John C. Preston and his staff at Yosemite National Park, and Messrs. Paul Manis, William Roche, and Peter Miljanich of the University of California's White Mountain Research Station staff.

The author is particularly indebted to Dr. Samuel Epstein and Dr. Harrison Brown of the California Institute of Technology, whose interest in the geochemistry of carbon and oxygen was an important factor in directing him to a study of atmospheric carbon dioxide. In addition, he thanks Mr. Charles McKinney, Dr. Epstein, and Dr. Robert Clayton for advice and assistance in the laboratory, Mr. William Otto for generous help with mounting the constant volume manometer, and Mrs. Franca Bressler, Mrs. Barbara Jones, Mrs. Lillian Baum, and Dr. Hector Rubalcava, who performed the mass-spectrometer analyses. This work was supported by the Atomic Energy Commission, Contract *AT*(11–1)–208.

References

Buch K. (1939) Beobachtunge nüber das Kohlensäuregleichgewicht und über den Kohlensauereaustausch zwischen Atmosphäre und Meer im Nordatlantischen Ozean, Abo, Finland, Akademi. *Acta Math. Phys.* **11,** 1–32.

Buch K. (1948) Der Kohlendioxydgehalt der Luft als Indikator der meteorlogischen Luftqualität, Helsinki, Finland. *Eripainos Geophys.* **3,** 63–79 (*Chem. Abstr.* **47,** 9682*i*, 1953).

Craig H. (1953) The geochemistry of the stable carbon isotopes. *Geochim. et Cosmochim. Acta* **3,** 53–92.

Craig H. (1954) Carbon-13 in plants and the relationship between carbon-13 and carbon-14 variations in nature. *J. Geol.* **62,** 115–149.

Craig H. (1957) Isotopic standards for carbon and oxygen and correction factors for mass-spectrometric analysis of carbon dioxide. *Geochim. et Cosmochim. Acta* **12,** 133–149.

Egle K. and Schenk W. (1952) Untersuchungen über die Reassimilation der Atmungskohlensäure bei der Photosynthese der Pflanzen. *Beitr. Biol. Pfl.* **29,** 75–105.

Epstein S. and Mayeda T. (1953) Variations of O^{18} content of waters from natural sources. *Geochim. et Cosmochim. Acta* **4,** 213–224.

Germann A. F. O. (1914) A modified precision manometer. *J. Amer. Chem. Soc.* **36,** 2456–2462.

Hutchinson G. E. (1953) The biochemistry of the terrestrial atmosphere. *The Earth as a Planet* (Edited by G. P. Kuiper) Chap. 8. University of Chicago Press, Chicago, Illinois.

Lundegårdh H. G. (1924) *Der Kreislauf der Kohlenäsure in der Natur* p. 308. Gustav Fischer, Jena.

McKinney C. R., McCrea J. M., Epstein S., Allen H. A. and Urey H. C. (1950) Improvements in mass spectrometers for the measurement of small differences in isotope abundance ratios. *Rev. Sci. Instrum.* **21,** 724–730.

Murphy B. F. and Nier A. O. (1941) Variations in the relative abundance of the carbon isotopes. *Phys. Rev.* **59,** 771.

Petterssen S. (1940) *Weather Analysis and Forecasting* pp. 562–581. McGraw-Hill, New York.

Urey H. C. (1947) The thermodynamic properties of isotopic substances. *J. Chem. Soc.*

Wickman F. E. (1952) Variations in the relative abundance of the carbon isotopes in plants, *Geochim. et Cosmochim. Acta* **2,** 243–254.

Worthing A. G. (1943) *Treatment of Experimental Data.* Wiley, New York.

Geochimica et Cosmochimica Acta, 1958, Vol. 13, pp. 335 to 338. Pergamon Press Ltd., London

Comments on two papers by John F. Lovering concerning a typical parent meteorite body

Harold C. Urey
Enrico Fermi Institute for Nuclear Studies
University of Chicago

In a recent paper, Lovering (1957b) has presented data and arguments in regard to the subject of this note. He summarizes his conclusions in Table 6 (p. 260). I believe that the conclusions presented in this table are most doubtful or that they have been presented previously. I shall take up the items in this table in the order in which he lists them.

(1) *Silicate/metal nickel fractionation in stony meteorites*

Some years ago Brown and Patterson (1948) attempted to estimate the pressures within a primitive planet assumed to be the parent of the meteorites, from the distribution of nickel between the silicate and metal phases of stone meteorites. Lovering notes that the chondrites are secondary objects and that the previous estimate is unreliable. He then presents new data on nickel in the olivine and metal phases of pallasites. He finds 150 p.p.m. of nickel in Admire and Allim and 350 p.p.m. in Brenham and Springwater. He averages these to secure 250 p.p.m. and points out that this is three times the amount expected on the basis of Zur Strassen's observations. It seems possible and perhaps likely that some metallic impurity was included in the olivine samples. This was the criticism of Urey and Craig (1953) in regard to the Brown and Patterson work. At least a variation by a factor of 2·3 between the amount of nickel in Brenham and Springwater and that of Admire and Albin needs to be explained in some way, which Lovering does not attempt to do. Moreover, the temperature chosen by Lovering is arbitrary in the extreme. He assumes 2000°K for this at some time in the past, but also assumes that cooling to 700°K occurred during some 10^9 years or so. Surely diffusion of nickel over some millimetres or a centimetre would occur during this time and no well-defined equilibrium temperature could exist. Moreover, he uses volume data for pure phases at ordinary temperatures instead of partial molal volumes at high temperatures. Any deduction of pressures on such a basis is so doubtful as to be meaningless.

(2) *Metal/sulphide nickel fractionation in stony-iron meteorites, and*

(3) *Metal/sulphide nickel fractionation in iron meteorites*

Lovering reports analyses for nickel in the troilite and metal phases of the Rio Loa, Henbury and Toluca irons and the Brenham and Springwater pallasites, and calculates a mean distribution coefficient for each group, namely 0·06 and 0·03 respectively. (I cannot repeat his calculation of these averages from his data.) The differences of these two averages is puzzling, but the differences between the individual distribution coefficients calculated from the five sets of data are even larger, i.e. by about a factor of 10. Thus, if equilibrium was established and if the data are reliable, these iron and stony-irons must have been formed under very different conditions and averaging equilibrium constants can give only doubtful results. Moreover, I cannot repeat the calculation he uses for Zur Strassen's equilibrium constant. Jander and Rothschild (1928) give values for $([FeSiO_3][NiS])/([NiSiO_3][FeS])$ at various concentrations of nickel in an equilibrium mixture. The values

vary, but an extrapolation to zero nickel content gives ~1 for the equilibrium constant of the reaction

$$NiSiO_3 + FeS = FeSiO_3 + NiS, \qquad K = 1$$

ZUR STRASSEN (1930) gives many data for the reaction

$$Ni + FeSiO_3 = Fe + NiSO_3, \qquad K = 6{\cdot}53 \times 10^{-3}$$

and finds no trend with concentration. The first reaction was studied at 1700°C* and the second at 1480°C. Calculating the constant for the latter temperature to its value at 1700°C, assuming that the entropy change for the reaction is zero, gives $2{\cdot}5 \times 10^{-2}$. Now, adding the equations gives

$$Ni + FeS = Fe + NiS, \qquad K = 2{\cdot}5 \times 10^{-2}$$
$$T = 1973°K.$$

Thus the calculated equilibrium constant and LOVERING's very rough observed values agree without pressure correction of any kind at ~2000°K. LOVERING gives $K = 1$ at 1200°K in his Table 1, but uses 2000°K in Table 6.† At lower temperatures the higher value of K may be correct, but the imperfections of solid solutions are so great that equilibrium constants extrapolated from the liquid state or calculated from thermodynamic data for pure phases are so uncertain that any conclusions in regard to the effect of pressure on the distribution would be quite inconclusive.

(4) *Depression of the γ–α transformation temperatures in the iron meteorites and time to form Widmansättten pattern*

LOVERING accepts the high pressures suggested by UHLIG (1954) and reviews further data on the temperature pressure coefficient. So far as the writer is aware, the argument for high pressures is given by UHLIG (*loc. cit.* pp. 289, 293), and this argument can hardly be regarded as certain. In fact, UHLIG says, "The factor of pressure, therefore, may conceivably prevent transformation of >13 per cent alloys (which at 10^5 atm transform below 460°C) even though the alloys cool slowly through the pressure-depressed transformation temperatures, just as the 34 per cent Ni alloy at 1 atm cools without change below 460°C". Iron–nickel meteorites containing between 13 and 27 per cent nickel consist of finely divided mixtures of kamacite and taenite and are known as the nickel-rich ataxites. UHLIG tries to account for this by high pressures. However, the composition of the octahedrite kamacite and taenite is consistent with crystallization at ~450°C and low pressure (PERRY, 1944) or at ~250°C and high pressure, i.e. about 10^5 atm, but not at 700°K (423°C) and 7×10^4 atm pressure, as LOVERING assumes. Diffusion times would be very long if the temperature were 250–300°C. It may be that the nickel-rich ataxites were formed at high pressures and that the octahedrites were formed at low pressures. The possible effect of impurities on these processes is not completely determined. An attempt to decide between 10^5 atm and 7×10^4 atm pressure is most unrealistic in regard to the present state of the problem.

LOVERING refers only to the dates of Thompson and Mayne for the Brenham pallasite

* JANDER and ROCHSCHILD do not state whether their temperatures are on the Kelvin or centigrade scales, but since they studied liquid equilibria and $FeSiO_3$ melts at 1455°C, I conclude that the temperatures are on the centigrade scale. The extrapolated value for K was secured by plotting apparent values of K against the nickel concentration in the sulphide phase.

† ZUR STRASSEN's discussion of this equilibrium is very brief and obscure to me. In a footnote he says, "Auf eine Anfrage wegen elticher Unstimmigkeiten, auf die hier nicht eingegangen werden kann, war Herr Priv.–Doz. Dr. JANDER so freundlich uns mitzuteilen, dass die Arbeit einen mehr orientierenden Charakter trage and nur einen Überblick über die Verhältnisse bei Sulfid–Silikatgleichgewichten geben sollte. Deshalb sind aus den Zahlen keine weitergehenden Schlüsse zu ziehen."

and neglects other data in the literature. These dates of Thompson and Mayne are doubtful. Since this work was done, Turkevich, Reed and Hamaguchi have shown that there is very little uranium in the metal of meteorites, as must be expected on thermodynamic grounds. Hence their helium age is doubtful. Their potassium argon age is highly uncertain because of the difficulty of analysing for potassium. They give 0·019 per cent; Edwards (1955) found 0·01 per cent. (A repetition of this work by Geiss (unpublished) using different samples resulted in no check on either the argon or potassium analyses.) Any history proposed on the basis of this data is uncertain.

(5) *Graphite–diamond phase transformation in iron meteorites*

The conclusions in regard to this problem are identical with those reached previously by Urey (1956), except for slight differences in pressures and temperatures proposed.

Lovering credits Urey with reporting the presence of pseudomorphs of diamonds in iron meteorites. This is incorrect. It is unfortunate if an incorrect impression was given. The observations were made in the 1880's, as could easily have been verified by a study of the literature. (This is summarized with detailed references by Farrington (1915), a reference indicated by Urey.)

In discussing high pressures in connection with the meteorites, the writer did not refer to the work of Brown and Patterson, because it seemed pretty well understood that their conclusions were not valid, as Lovering agrees. I believe that Lovering's revised figures are inconclusive and that the best evidence for high pressures is given by the presence of diamonds. No other high-pressure minerals are reported. Since diamonds are partly converted to graphite, even this record has been partially lost. It may be that only this most durable mineral, namely diamond, has survived and that all other records, such as the equilibria discussed by Lovering, have been destroyed.

Lovering assumes in another paper (Lovering, 1957a) that the parent of the meteorites was a large object with an iron–nickel core, presumably some 500 km in diameter. He ignores arguments that have been advanced against this. For example, the number of stony irons observed to fall is about 0·3 as many as the observed falls of irons. Since the stony irons are characteristic of the boundaries between the silicate and iron phases, this indicates that the parent bodies were small, perhaps some metres or tens of metres in dimensions. If the stony-iron layer were even a kilometre thick on the surface of a sphere of 500 km radius, only 1/160 of the volume would consist of this material and even small gravitational fields would prevent a mixture of melted iron and solid silicate remaining intact, so that the layer cannot have been so thick. Some specimens of Brenham are partly pallasite and partly quite typical octahedrites, so that a surface region has been observed, which is most improbable if the parent object was large. Also, many iron meteorites have holes and pits which Henderson regards as primordial surfaces. These holes have smaller openings than their interior dimensions and they could not have been produced as the broken surfaces from a large iron body. Again, the iron meteorites are comparatively free of gross distortions. Yet any process which would disrupt an object some hundreds of kilometres in diameter would probably produce many pieces of distorted metal! So far as can be seen, Lovering's discussion of the crystallization of an iron–nickel melt could be applied to a comparatively small mass. In addition, much evidence exists for chemical fractionation of the iron–nickel in meteorites (Urey and Craig, 1953). It is most unlikely that the entire variation in nickel content is due to fractional crystallization of an iron–nickel melt containing 11 per cent nickel.

References

Brown H. S. and Patterson C. (1948) *J. Geol.* **56,** 85.

Edwards G. (1955) *Geochim. et Cosmochim. Acta* **8,** 285.
Farrington O. C. *Meteorites.* Lakeside Press, Chicago.
Jander W. and Rothschild K. (1928) *Z. Anorg. Chem.* **172,** 129.
Lovering J. F. (1957a) *Geochim. et Cosmochim. Acta* **12,** 238.
Lovering J. F. (1957b) *Geochim. et Cosmochim. Acta* **12,** 253.
Perry S. H. (1944) *U. S. Nat. Mus. Bull.* **184,**
Uhlig H. H. (1954) *Geochim. et Cosmochim. Acta* **6,** 282.
Urey H. C. and Craig H. (1953) *Geochim. et Cosmochim. Acta* **4,** 36.
Urey H. C. (1956) *Astrophys. J.* **124,** 623.
Zur Strassen H. (1930) *Z. Anorg. Chem.* **191,** 209.

Geochimica et Cosmochimica Acta, 1958, Vol. 13, pp. 339 to 340. Pergamon Press Ltd., London

GEOCHEMICAL NOTE

G-1–*W*-1 values—spectrochemical determination using an internal standard

(*Received* 28 *October* 1957)

This brief note merely adds another list of independently determined values to the growing number of analyses of the two rocks *G*-1–*W*-1 (Fairbairn *et al.*, 1951), but does not attempt to review and assess previous values. The opportunity to analyse *G*-1 and *W*-1 for V, Ti, Zr, Ni, Co, Sc, Cr and La, which belong to the involatile group of elements, arose during the course of graduate work at MIT during 1952. Synthetic standards of the above-mentioned elements were made using a synthetic base of 55 per cent SiO_2, 30 per cent Al_2O_3 and 15 per cent Na_2CO_3. Pd was chosen as the internal standard, following a method by Ahrens (1950) and his co-workers. A recent clay with ordinary trace-element content* was arced ten times and from these results the relative deviation (standard deviation expressed as percentage) for each element was calculated. For arcings in duplicate the relative deviations are: V—8 per cent, Ti—5 per cent, Zr—14 per cent, Ni—10 per cent, Co—5 per cent, Sc—9 per cent, Cr—10 per cent and La—8 per cent. These deviations are only measures of precision of the method, and not of accuracy. Furthermore, determinations which are much lower than the clay values given in this note will fall off in precision.

For comparison, recommended values (Ahrens, 1954) of these elements are listed alongside those of the analyst.

	G-1		*W*-1	
	E. J. Young	Recommended value	E. J. Young	Recommended value
V	24 p.p.m.	18	308	240
Ti	1800	1500	6600	6700
Zr	326	200	156	90
Ni	4	3–5†	114	90
Co	5	4	57	36
Sc	4	3	63	37
Cr	21	20	130	130
La	160	160	26	32‡

Edward J. Young

Geochemistry and Petrology Branch
U.S. Geological Survey
Denver Federal Center
Denver, Colorado, U.S.A.

* The grey clay is from the Gulf of Mexico basin, taken at a depth of 4500 feet approximately 100 miles south of the Mississippi River delta. Its trace-element values were determined using *G*-1 and *W*-1 as standards and the values in p.p.m. are: V—150, Ti—4200, Zr—190, Ni—48, Co—10, Sc—17, Cr—81, and La—98. Note that all of these values fall between the *G*-1–*W*-1 values.

† Personal communication from A. T. Myers, U.S. Geological Survey, Denver.

‡ This value is from Dr. R. L. Mitchell (Fairbairn *et al.*, 1951).

References

Ahrens L. H. (1950) *Spectrochemical Analysis*. Addison–Wesley, Cambridge, Mass.

Ahrens L. H. (1954) *Quantitative Spectrochemical Analysis of Silicates*. Pergamon Press, London.

Fairbairn H. W. *et al.* (1951) A co-operative investigation of precision and accuracy in chemical, spectrochemical and modal analysis of silicate rocks. *U.S. Geol. Survey Bull.* 980.

Report of Meeting

Meeting of the Commission on Geochemistry of the International Union of Pure and Applied Chemistry

The Commission on Geochemistry met at Paris on 20 and 21 July 1957. The following titular members were present: Prof. T. F. W. Barth (Vice-President and Acting President for the meeting), Prof. K. Rankama (Secretary), Prof. H. Brown, Prof. C. Burri, Prof. C. W. Correns, Prof. S. Tomkeieff, Prof. L. R. Wager, and Prof. F. E. Wickman.

Inasmuch as Dr. M. Fleischer had announced his wish to resign as President of the Commission, Prof. Barth was elected President for 1957–1959, and Prof. Correns was elected Vice-President for 1957–1960.

The following members were re-appointed: Prof. Brown for 1957–1960, Prof. Correns for 1957–1960, and Prof. H. C. Urey for 1958–1961.

The following observers were elected: Prof. G. Carobbi (Firenze), re-elected for 1958–1959; Dr. K. Sugawara (Nagoya) for 1958–1960 (to replace Prof. K. Kimura who had announced his wish to resign); Prof. L. H. Ahrens (Cape Town) for 1958–1961 (to replace the late Dr. B. Wasserstein); Dr. E. Ingerson (Washington, D. C.), Prof. J. Orcel (Paris), Prof. C. G. Rossby* (Stockholm), Dr. H. Suess (La Jolla), and Prof. A. P. Vinogradov (Moscow), all for 1958–1960; Dr. C. G. du Plessis (Cape Town), Dr. A. B. Edwards (Melbourne), Prof. G. E. Hutchinson (New Haven), Dr. N. W. Rakestraw (La Jolla), Dr. W. W. Rubey (Washington, D.C.), Prof. H. G. Thode (Hamilton), and Prof. S. Tsuboi (Tokyo), all for 1958–1961.

Prof. Burri reported on his Sub-committee on Compilation of Rock Analyses and Prof. Correns on his Sub-committee on Chemistry of the Oceans. Dr. E. Ingerson of the U.S. Geological Survey at Washington, D.C., who was present by invitation, presented a progress report on the revision of F. W. Clarke's *Data of Geochemistry*, written by Dr. M. Fleischer. A new Sub-committee on Abstracting and Relations with Other Geochemical Groups was established with Prof. Tomkeieff as chairman and Prof. Brown as member.

It was decided to request financial support from I.U.P.A.C. for a meeting of the Commission at Oxford, England, in 1958, a meeting of the Commission and a Symposium on Geochemistry in conjunction with the meeting of the Inorganic Chemistry Section at Munich, Germany, in 1959, and a meeting of the Commission in 1960.

The Commission met with official delegates of the Geochemical Society, the Geochemical Society of Japan, and the Société française de Géochimie. Suggestions relative to co-ordination of the activities and co-operation among the Commission and the three societies were presented and discussed, and a Joint Committee consisting of the Presidents of the four groups was appointed to investigate the present situation and the relationships with still other groups.

A Symposium on Geochemistry was organized by the Commission at Paris on 22–24 July inclusive, followed by two geochemical field trips. Approximately 120 persons attended the Symposium, and 52 papers were presented. The abstracts of the papers presented will be printed in a forthcoming issue of *Geochimica et Cosmochimica Acta*.

Kalervo Rankama
Secretary, Commission on Geochemistry

* The Commission very much regrets to report the sudden and untimely death of Prof. Rossby in August, 1957.

Book reviews

KARL PRZIBRAM: **Irradiation Colours and Luminescence. Contribution to Mineral Physics** (Translated and revised in collaboration with the author by JOHN ESPENETT CAFFYN). Pergamon Press Ltd., London, 1956. xiv + 328. 63s.

K. PRZIBRAM's "Verfärbung und Lumineszenz" was published in Vienna in 1953. It has now been translated into English by J. E. CAFFYN, who, with the assistance of the author, has adapted the text to the most recent results. Thus the English edition of 1956 contains 500 additional references amongst its total of 1500.

Since the coloration and luminescence of solids was the main problem underlying this author's well-known researches carried out in Vienna for several decades, the present volume may well be regarded as a standard work. The mineralogist determining the age of minerals as well as the physicist investigating the qualities of crystals, will get a new angle on their special subject from this book. Scientists working in the chemical dosimetry will also be stimulated in many ways.

The first part is mainly concerned with the rich documentation of the coloration of halide crystals and offers a unique compilation of references; the second part deals with coloration phenomena of minerals found in nature. The reader will be astonished by the comprehensiveness of the survey which takes into account even minor papers. The author has made also the recent Russian literature available to the reader. In treating his material, he always gives precedence to the experiments and afterwards deals briefly with the theory of the phenomena. Scientists engaged in research discussed in this book will not be able to dispense with Professor PRZIBRAM's book in its new form.

M. WENZEL

New Research Methods in Hydrology (Proceedings of a conference held at Scripps Institution of Oceanography, La Jolla, California, February 2–3, 1957). Edited by HARMON CRAIG, Committee on Research in Water Resources, University of California. 37 pp., mimeographed. (Copies available on request from Dr. Harmon Craig, Scripps Institution of Oceanography, La Jolla, California).

THE principal object of this report is to draw the attention of hydrologists and geologists to various powerful new tools for hydrologic studies. This is accomplished by summarizing the nine papers which were presented at the conference and the accompanying discussions, covering the following subjects: (1) Induced polarization studies, (2) evaporation and transpiration studies, with special reference to the use and properties of hexadecanol, (3) use of chemical and radioactive tracers, (4) deuterium and oxygen-18 studies, and (5) tritium studies.

For those wishing more details of these subjects a bibliography of nineteen titles is appended.

EARL INGERSON

PIERRE LAFFITTE: **Introduction à l'étude des roches métamorphiques et des gîtes métallifères.** Masson et Cie, Paris, 1957. 343 pp. 4000 fr.

CET ouvrage de PIERRE LAFFITTE apporte une contribution importante au progrès de la Pétrologie.

Soulignons tout de suite que c'est plutôt un ouvrage de doctrine qu'un traité général. Si, depuis longtemps, la pétrologie fait appel aux lois de la physico-chimie, l'application courante de ces lois rencontre bien des difficultés, se heurtant à la pénurie de beaucoup de données physiques essentielles et à l'incertitude de l'évaluation numérique des facteurs définissant les

conditions naturelles. Ces difficultés rebutent souvent les chercheurs: les lois physico-chimiques et leurs applications font souvent au naturaliste l'effet de hors-d'oeuvres fastidieux et inutiles, introduits par principe dans les traités généraux.

Aussi des géologues qui se disent naturalistes répugnent-ils à raisonner sur des données physico-chimiques qu'ils considèrent comme trop loin des faits d'observation courante. D' autres, au cours de leur carrière, ont pour souci de se perfectionner strictement dans leur spécialité centrée sur l'observation des phénomènes naturels à diverses échelles: tandis que les sciences physiques progressent chaque jour avec le magnifique essor qui les caractérise actuellement, ils restent, faute de temps ou de goût, sur des données de base initiales, incomplètes ou périmées.

Le but de l'ouvrage de Pierre Laffitte est de rendre accessible aux uns et aux autres les données physiques, chimiques, thermodynamiques utiles au progrès de la pétrologie. "Ces données, nous les avons présentées, écrit l'auteur, en pensant constamment au public particulier auquel elles étaient destinées. Nous avons cherché, non pas à substituer notre ouvrage aux manuels existants, mais à faciliter le travail du lecteur géologue en rappelant les données élémentaires qui ne sont pas toujours exposées dans les ouvrages spécialisés. Nous voudrions que chaque chapitre suscite des études plus approfondies. Nous espérons que notre livre pourra faciliter même à des géologues confirmés une prise de contact plus intime avec la physico-chimie ou la thermodynamique, car il n'y a aucune raison pour refuser aux observations accumulées dans les domaines de la physique ou de la chimie la valeur que l'on concède bien volontiers à celles issues des sciences naturelles, et la connaissance des unes peut s'allier avec la connaissance des autres."

Pierre Laffitte était particulièrement qualifié pour écrire un tel livre faisant pont entre physique et géologie. Sa formation polytechnicienne, d'une part, à laquelle il doit sa compréhension de la physique, ses études géologiques de roches métamorphiques dans les Alpes et en Bretagne d'autre part, l'y ont préparé. Directeur du Bureau de Recherches Géologiques, Géophysiques et Minières, il est aussi l'animateur d'une brillante équipe et se trouve en contact quotidien de problèmes géologiques.

Le livre comprend quatre parties. Une première partie "Généralités physico-chimiques" étudie les particules élémentaires de la matière et les liaisons entre particules. L'importance prise en géologie générale par les données sur la structure de la matière, à cause des développements remarquables de la géochimie, ne saurait être discutée. Il suffit d'évoquer les paragraphes consacrés à la radioactivité et aux âges géologiques, aux rayons ioniques et aux remplacements dans les cristaux, pour toucher du doigt les incidences fort importantes de ces données dans le domaine géologique.

Une seconde partie "Composition chimique des roches" présente un chapitre de généralités géochimiques, avec une description sommaire du rôle des principaux anions, un chapitre de discussion approfondie sur la précision en matière d'analyses chimiques, et un autre sur les calculs pétrochimiques, les paramètres, diagrammes de variations et représentations géométriques des résultats.

La troisième partie "Thermodynamique" rappelle sommairement la plupart des notions fondamentales, et développe plus longuement des notions telles que phases, concentrations, potentiels chimiques, dont l'utilisation en pétrologie est plus constante. C'est la matière du chapitre "Généralités thermodynamiques." Le suivant "Description de quelques phases" indique les principales propriétés de la phase aqueuse, du quartz, des feldspaths, des grenats et des micas. Viennent ensuite deux importants chapitres "Equilibres entre les phases" et "Cinétique." Ce dernier traite de questions bien souvent agitées en pétrologie, telles que stabilité des assemblages minéraux, vitesse de réaction, diffusion des éléments chimiques.

La quatrième partie "Pétrologie des Roches métamorphiques" évoque quelques-uns des problèmes du métamorphisme, de façon à montrer comment ces problèmes se posent à la lumière des idées et des méthodes développées dans le corps de l'ouvrage.

Tout le long du livre, des graphiques éclairent le texte, des tableaux de valeurs numériques l'appuient, non à titre de répertoires de constantes physiques, mais pour fixer des ordres de grandeur ou des valeurs comparatives. Une bibliographie solide rend le lecteur à même de pousser plus loin s'il le désire.

Nous avons dit que l'ouvrage s'adresse aux géologues naturalistes, et aussi aux théoriciens, qui y trouveront un inventaire des problèmes et une vue d'ensemble des perspectives de la recherche. Mais c'est surtout à l'étudiant que cette "Introduction" devrait servir par ce qu'elle lui apporte: bases théoriques saines et clarification des définitions, méthodes d'étude et mode de raisonnement, critique des opinions courantes et relativité des théories.

En dehors des exposés de principes, les pages d'application et de mises au point sont fort utiles et agréables à lire, qu'il s'agisse des rayons ioniques, des diagrammes chimiques, des exemples d'équilibres ou de la diffusion des éléments. Celles de la quatrième partie, qui ont en outre un cachet d'originalité et de prise de position en matière controversée, le sont également. Les unes et les autres laissent au lecteur un vif regret qu'elles soient trop courtes. Mais, si l'ouvrage était long et exhaustif, il serait contraire à son esprit: évocation des problèmes plutôt qu'arsenal pour les résoudre, impulsion pour l'étude plutôt qu'exposé comparatif des constructions laborieuses érigées par diverses écoles. L'auteur a voulu que son livre soit un instrument de travail. Nous pensons qu'il a réussi et qu'il aidera les chercheurs dans la pétrologie nouvelle qui surgit peu à peu à l'horizon de la science.

E. Raguin